NOTICE

The quality of this microform is heavily dependent upon the quality of the original thesis submitted for microfilming. Every effort has been made to ensure the highest quality of reproduction possible.

If pages are missing, contact the university which granted the degree.

Some pages may have indistinct print especially if the original pages were typed with a poor typewriter ribbon or if the university sent us an inferior photocopy.

Reproduction in full or in part of this microform is governed by the Canadian Copyright Act, R.S.C. 1970, c. C-30, and subsequent amendments.

AVIS

La qualité de cette microforme dépend grandement de la qualité de la thèse soumise au microfilmage. Nous avons tout fait pour assurer une qualité supérieure de reproduction.

S'il manque des pages, veuillez communiquer avec l'université qui a conféré le grade.

La qualité d'impression de certaines pages peut laisser à désirer, surtout si les pages originales ont été dactylographiées à l'aide d'un ruban usé ou si l'université nous a fait parvenir une photocopie de qualité inférieure.

La reproduction, même partielle, de cette microforme est soumise à la Loi canadienne sur le droit d'auteur, SRC 1970, c. C-30, et ses amendements subséquents.

Canada

Peroxide Oxidation and Derivatization of Myoglobin

Stephen Marmor

A Thesis

in

The Department

of

Chemistry and Biochemistry

Presented in Partial Fulfilment of the Requirements
for the Degree of Master of Science at
Concordia University
Montréal, Québec, Canada

November 1992

ISBN 0-315-87276-4

Abstract

Peroxide Oxidation and Derivatization of Myoglobin

Stephen Marmor

Pentaammineruthenium(III) (a_5Ru^{3+}) derivatives of horse heart myoglobin (MbHH) from its reaction with $a_5Ru^{2+}(H_2O)$ were separated using fast protein liquid chromatography (FPLC) cation-exchange chromatography. Spectrophotometric analysis indicated binding of a_5Ru^{3+} to histidines, and amino acid analysis and mass spectrometry of tryptic peptide fragments confirmed a_5Ru^{3+} binding to His48 and His81 in two different derivatives and probable binding of a_5Ru^{3+} to His116 in a third derivative. Peak potentials (Ep) of free (86 mV) and MbHH-bound a_5Ru^{3+}(His) [Ep = 52 mV (His48), 47 (His81), 76 (probably His116)] were measured by differential pulse voltammetry.

Reaction of Fe^{III}-Mb with peroxide yields Cpd I-Mb which contains Fe^{IV}=O-heme and a protein radical. Half-lives for Fe^{IV}=O-heme formation using 20-fold excess peroxide (pH 8.5) were 10.7 and 37.1 s for sperm whale (MbSW) and MbHH, respectively. Unfolding of Fe^{III}-MbHH in 8 M urea increased tryptophan fluorescence 15-fold, but less for Cpd I-MbHH, Cpd II-MbHH (from Fe^{II}-Mb and H_2O_2 reaction),

Fe^{III}-MbSW and Cpd I-MbSW, indicating greater polypeptide unfolding in Fe^{III}-MbHH. Soret absorption also revealed less solvent exposure of Cpd I-Mb hemes in 8 M urea. However, all species showed increased fluorescence (except Fe^{III}-MbHH) and blue-shifted Soret maxima in 6 M guanidine hydrochloride (Gdn-HCl) suggesting greater polypeptide unfolding in Gdn-HCl. Cpd I-MbSW (but not Cpd I-MbHH) was shown to be partially dimerized by SDS-PAGE consistent with intermolecular crosslinking. Extraction of Cpd I-MbHH heme at pH 1.5 with butanone did not occur, revealing possible heme-polypeptide crosslinking.

Acknowledgements

I would foremost like to thank Ann English for her support and her guidance throughout my Masters. I appreciate all her efforts and I am grateful for her understanding and instilling unto me not only knowledge in the field of Biochemistry, but all aspects of life.

I would also like to thank Susan Mikkelsen for being a member of my committee and for accessibility to her electrochemical apparatus. Also, thanks for sitting through those wonderful group meetings and providing valuable suggestions on my research and specifically my electrochemical work.

Thanks also to Mary Baldwin for being on my committee and proposing helpful ideas during my Masters.

A very special thanks to Bernie Gibbs for all his time and effort with amino acid analysis and mass spectrometry. I don't know how you do it Professor Gibbs.

Thanks to Bruce Hill for the opportunity to do my Masters and introducing me to heme enzymes, and to Pierre Ménassa for his encouragement and giving me the first taste of research.

My deepest heartfelt gratitude for the support and friendship from the cast of characters in the English-Mikkelsen group. Those long hours were made much more enjoyable thanks to George Tsaprailis, Yazhen Hu, Craig Fenwick, Kelly Millan, Line D'Astous, Arthur Fernandez, Ted Fox, Antonella Badia, Pina Teoli, Rina Carlini, Beata Kolakowski, Sean Taylor, Karutha P. Govindaraju, Jin Huong, Fernando Battaglini, Hongtao Qi, Safwan Ismail, Zari Sajedi and Nhuan Ha Huy Thai.

Thanks to my friends and relatives; Alan, Brian, Nathan, Jay, Rob, Stephen, Lorne, Willie, Andrew, Adeline, Barbara, and Nathalie for listening and providing endless encouragement.

To my family, Mom and Dad, Eta and Bonnie, thanks for putting up with me and providing your continuous love, support and guidance.

This degree would not have been achieved without the people I have recognized.

To the department of Chemistry and Biochemistry Graduate Students, Faculty and Staff, I thank you for filling my project with much cherished memories.

Table of Contents

List of Figures

List of Tables

List of Reactions

List of Abbreviations

a	NH_3
a_5Ru^{3+}	pentaammineruthenium(III)
$a_5Ru^{2+}(H_2O)$	aquopentaammineruthenium(II)
API	atmospheric pressure ionization
Asn	asparginine
CAPS	3-[cyclohexylamino]-1-propanesulphonic acid
CCP	cytochrome c peroxidase
CN	cyanide
$Co(phen)_3^{3+}$	tris(1,10-phenanthroline)cobalt(III)
Cpd I-Mb	product of Fe^{III}-Mb + H_2O_2 reaction
Cpd II-Mb	product of Fe^{II}-Mb + H_2O_2 reaction
DPV	differential pulse voltammetry
Ep	peak potential
Fe^{II}-Mb	ferrous myoglobin
Fe^{III}-Mb	ferric myoglobin
Fe^{IV}=O	ferryl iron
FPLC	fast protein liquid chromatography
Gdn-HCl	guanidine-hydrochloride
His	histidine
HPLC	high performance liquid chromatography
Leu	leucine
Mb	myoglobin
MbHH	horse heart myoglobin
MbSW	sperm whale myoglobin
NHE	normal hydrogen electrode
$Ru^{3+}(NH_3)_6$	hexaammineruthenium(III)
TPCK	[L-(1-tosylamido-2-phenyl)ethychloromethyl ketone]
Tris	[tris(hydroxymethyl)aminomethane]
SDS-PAGE	sodium dodecyl sulfate polyacrylamide gel electophoresis
Trp	tryptophan
Tyr	tyrosine
X°	protein radical formed by the reaction of Fe^{III}-Mb with H_2O_2
ZnP	zinc protoporphyrin
^{3}ZnP	triplet-excited state of ZnP

1.0 Introduction

Ferryl iron (Fe^{IV}=O) is present in the enzyme intermediates of heme enzymes such as cytochrome c peroxidase (CCP),[1] cytochrome c oxidase[2] and heme peroxidases.[3] Because of its wide biological importance, recent studies[1,4] have focused on the characterization of the electron transfer reactivity of this high oxidation state of iron. In cytochrome c peroxidase (CCP), the most exposed histidine residue (His60) was covalently modified with pentaammineruthenium(III) (a_5Ru^{3+}) to probe the electron transfer reactivity of Fe^{IV}=O centre of Compound I,[1] the two-electron oxidized intermediate of CCP. Electron transfer rates between the a_5Ru^{2+} groups on His and the Fe^{IV} heme centre were ~ 3 s^{-1}, which is slower than expected for electron transfer over 22 Å at a high driving force (ΔE° ~ 1).[1] This raises the possibility that the reorganizational energy associated with the reduction of Fe^{IV}=O to Fe^{III} may be large, or that no efficient electron transfer pathway[5,6] exists between His60 and the heme of CCP.

The original aim of the present work was to examine the electron transfer reactivity of the Fe^{IV}=O heme in myoglobin (Mb). Both the ferric (Fe^{III}-Mb) and ferrous (Fe^{II}-Mb) forms of Mb react with peroxides to produce Fe^{IV}=O heme species. Mb was chosen for this study since electron transfer in this protein has been well characterized.[7,8] Sperm whale myoglobin (MbSW) derivatives with an a_5Ru^{3+} group attached to surface-exposed histidine residues have been studied extensively.[7,8,9] The a_5Ru(His48)MbSW derivative has a heme-edge to Ru distance of 13 Å,[6,10] and the

electron transfer rate from Ru^{II} to the Fe^{III} is 0.041 s^{-1} ($\Delta E°$ = - 20 mV).[7,8] Electron transfer was not observed in the other a_5Ru^{3+}(His) derivatives of MbSW (His12, His81, His116), because of the large separation between the Ru and Fe (19-22 Å) centres.[6,10] However, when the heme of MbSW is replaced with zinc protoporphyrin (ZnP), photoexcitation gives the triplet ^{3}ZnP, which is a strong reductant.[11] ^{3}ZnP rapidly reduces the a_5Ru^{3+} centre, enabling electron transfer rates in the Zn-substituted a_5Ru^{3+}(His) derivatives of MbSW to be determined.

MbSW is no longer commercially available so horse heart myoglobin (MbHH) was chosen for this study. The X-ray structure of MbHH is now known,[12] and since MbHH is cheap and readily available, it is an ideal system to covalently modify for electron transfer studies. Structurally well-defined metalloproteins derivatized with a_5Ru^{3+} at histidine residues have been used extensively in electron transfer studies.[7,8,11,13,14,15] This technology involves the covalent attachment of a_5Ru^{2+} to histidine residues on the surface of the protein. Upon oxidation, a stable a_5Ru^{3+}(His)-protein complex is obtained which can be purified and separated into its derivatives by cation-exchange chromatography. a_5Ru^{3+} is a useful probe to study electron transfer since it is substitution inert, has a reduction potential of ~ 0.1 V, and its hydrophillic nature reduces its affinity for the protein's interior so that it does not appear to structurally perturb proteins upon modification.[7,8,11,13,14,15] In this work, the preparation of a_5Ru^{3+} derivatives of MbHH, was undertaken. In Chapter 2 the preparation and purification of three ruthenium derivatives of MbHH are discussed in detail, while Chapter 3 outlines methods used in the characterization of the singly-

modified a_5Ru(His)MbHH derivatives.

The reaction of Fe^{III}-Mb with H_2O_2 has been linked to oxidative damage in cell membranes.[16] Fe^{III}-Mb will bind peroxide at its iron atom resulting in the formation of a ferryl iron and an unstable protein radical (X°):[17,18]

$$Fe^{III}\text{-heme} + H_2O_2 + 2H^+ \rightarrow X°Fe^{IV}=O\text{-}\dot{h}eme + 2H_2O \qquad (1.1)$$

Fe^{II}-Mb will also bind peroxide to form a ferryl iron but no X°:

$$Fe^{II}\text{-heme} + H_2O_2 + 2H^+ \rightarrow Fe^{IV}=O\text{-heme} + 2H_2O \qquad (1.2)$$

It is important to determine if X° formation alters the polypeptide before electron transfer studies are carried out on the ferryl form of Mb. Studies have shown that MbHH is modified upon binding of peroxide, resulting in the covalent attachment of a fraction of the prosthetic heme to the protein (~ 18% at pH 7.4).[19] The residue which is crosslinked to the heme has been identified as Tyr103 using peptide-mapping by HPLC and amino acid analysis.[19] SDS-PAGE experiments have shown that H_2O_2-induced dimerization in MbSW, but not in MbHH,[20] indicating that intermolecular crosslinking occurs in MbSW. The residues involved in dimerization of the protein were identified by chymotryptic digestion and peptide sequencing to be Tyr103 of one MbSW molecule and Tyr151 of another MbSW molecule. Tyr151 has been identified by studies of MbSW mutants to be essential for formation of protein dimers.[21] The

physical properties of the products from Reaction 1.1 for MbSW and MbHH will be looked at in detail in Chapter 4 to probe the effects of X° generation on the polypeptide. The reaction of Fe^{II}-MbHH with peroxide (Reaction 1.2) will reveal the effects, if any, of formation of Fe^{IV}=O in the absence of X° on the polypeptide. Chapter 5 will give a general discussion of results presented in Chapters 2, 3 and 4, and discuss future experiments which should be carried out.

1.1 References

1) Fox, T.; Hazzard, J. T.; Edwards, S. L.; English, A. M.; Poulos, T. L.; Tollin, G. *J. Am. Chem. Soc.* **1990**, *112*, 7426.

2) Varotsis, C. & Babcock, G. T. *Biochem.* **1990**, *29*, 7357.

3) Reczek, C. M.; Sitter, A. J.; Terner, J. *J. Mol. Struct.* **1989**, *214*, 27.

4) Babcock G. T. & Wikström, M. *Nature* **1992**, *356*, 301.

5) Beratan, D. N.; Onuchic, J. N.; Betts, J. N.; Bowler, B. E.; Gray, H. B. *J. Am. Chem. Soc.* **1990**, *112*, 7915.

6) Cowan, J. A.; Upmacis, R. K.; Beratan, D. N.; Onuchic, J. N.; Gray, H. B. *Ann. New York Acad. Sci.* **1988**, *550*, 68.

7) Crutchley, R. J.; Ellis, W.R.; Gray, H. B. *Frontiers in Bioinorganic Chemistry*; Xavier, A. V., Ed.; VCH, **1968**, 679.

8) Crutchley, R. J.; Ellis, W.R.; Gray, H. B. *J. Am. Chem. Soc.* **1985**, *107*, 5002.

9) Karas, J. L. "Long-Range Electron Transfer in Ruthenium-Labelled Myoglobin", Ph.D. Thesis, California Institute of Technology, **1989**.

10) Mayo, S. L.; Ellis, W.R., Jr.; Crutchley, R. J.; Gray, H. B. *Science* **1986**, *233*, 948.

11) Axup, A. W.; Albin, M.; Mayo, S. L.; Crutchley, R. J.; Gray, H. B. *J. Am. Chem. Soc.* **1988**, *110*, 435.

12) Evans, S. V. & Brayer, G. D. *J. Mol. Biol.* **1990**, *213*, 885.

13) Margalit, R.; Kostić, N. M.; Che, C-M.; Blair, D. F.; Chaing, H-J.; Pecht, I.; Shelton, J. B.; Shelton, J. R.; Schroeder, W. A.; Gray, H. B. *Proc. Natl. Acad. Sci. USA* **1984**, *81*, 6554.

14) Yocom, K. M.; Shelton, J. B.; Shelton, J. R.; Schroeder, W. A.; Worosila, G.; Isied, S. S.; Bordignon, E.; Gray, H. B. *Proc. Natl. Acad. Sci. USA* **1982**, *79*, 7052.

15) Recchia, J.; Matthews, C. R.; Rhee, M.; Horrocks, W. D. *Biochim. Biophys. Acta.* **1982**, *702*, 105.

16) Bruckdorfer, K. R.; Jacobs, G. D.; Rice-Evans, C. A. *Biochem. Soc. Trans.* **1990**, *18*, 285.

17) George, P. & Irving, D. H. *Biochem. J.* **1952**, *52*, 511.

18) Yonetani, T. & Schleyer, H. *J. Biol. Chem.* **1967**, *242*, 1974.

19) Catalano, C. E.; Choe, Y. S.; Ortiz de Montellano, P. R. *J. Biol. Chem.* **1989**, *264*, 10534.

20) Tew, D. & Ortiz de Montellano, P. R. *J. Biol. Chem.* **1988**, *263*, 17880.

21) Wilks, A. & Ortiz de Montellano, P. R. *J. Biol. Chem.* **1992**, *267*, 8827.

2.0 Preparation and Purification of a_5Ru(His)MbHH Derivatives

2.1 Introduction

A redox centre may be attached to histidine residues in proteins by a simple substitution reaction using the reagent aquopentaammineruthenium(II) [$a_5Ru^{2+}(H_2O)$]:

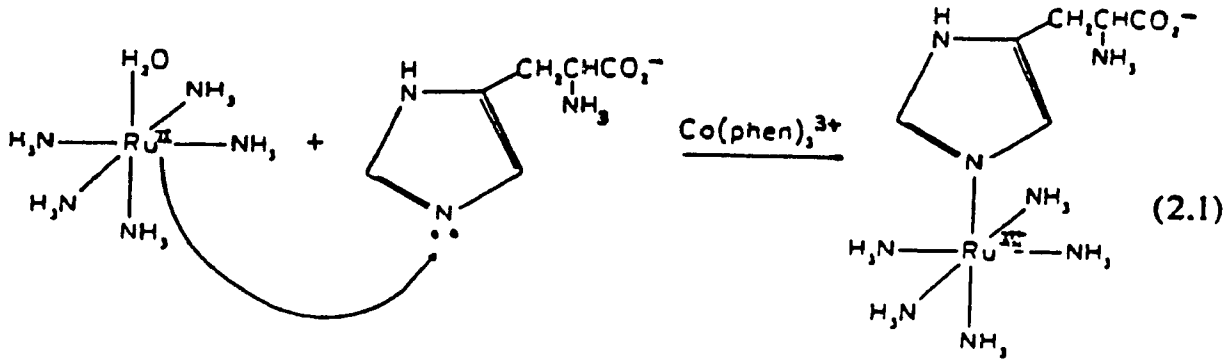

(2.1)

Reaction 2.1: Reaction of $a_5Ru^{2+}(H_2O)$ with histidine[1]

The Ru(II) product is labile but can be readily oxidized by reagents such as tris(1,10-phenanthroline)cobalt(III) [($Co(phen)_3^{3+}$)] to the Ru(III) product which is stable.[2] The number of a_5Ru(His) derivatives formed will depend on the number and accessibility of the protein's histidine residues. Horse heart cytochrome c has only one buried histidine residue available for modification, so reaction times of 1-3 days are required.[3,4] Cytochrome c peroxidase (CCP), on the other hand, has three surface histidine residues which are modified in 3 hours.[5]

Horse heart myoglobin (MbHH) has eleven histidines [Figure 2.1(a)], three of which are surface exposed and the most likely candidates for modification [Figure 2.1(b)]. Two of the remaining histidines are buried in the heme pocket; His93 is

(a)

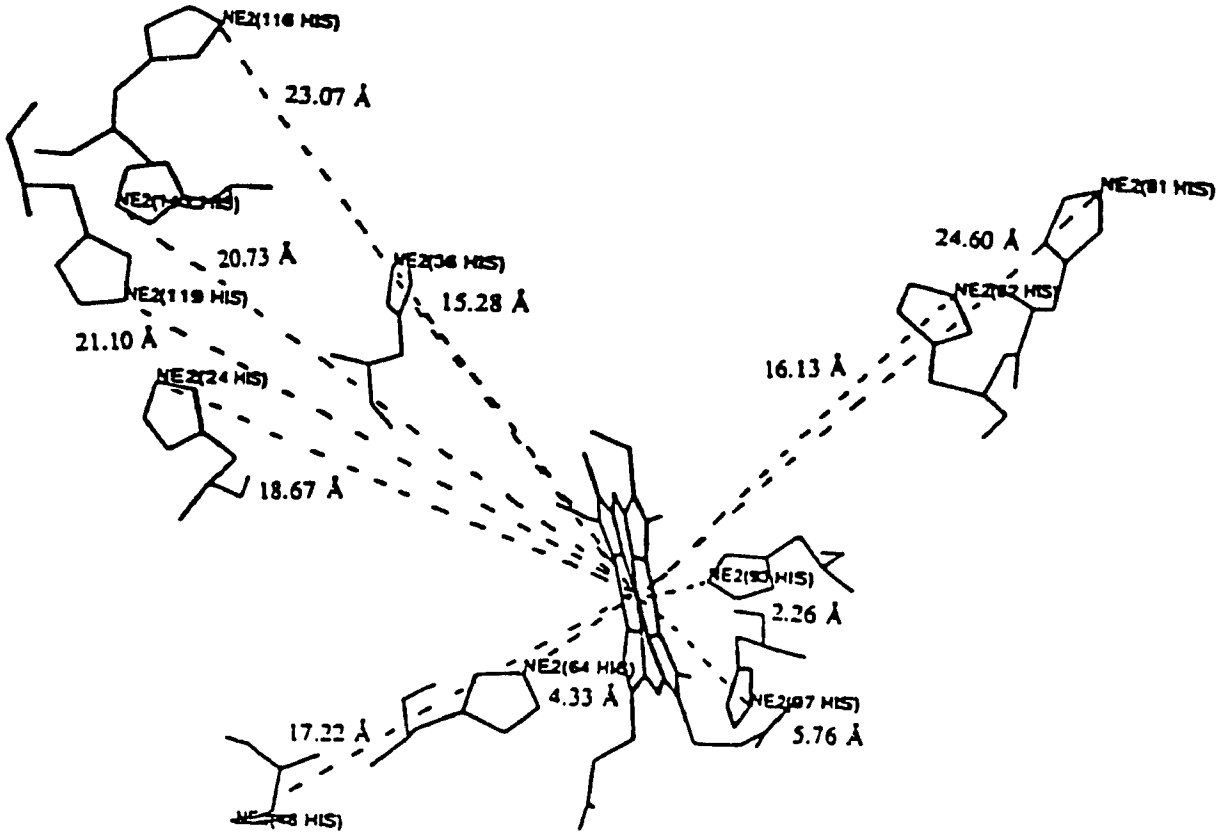

Figure 2.1: (a) (this page) Location of histidine residues in MbHH and their distances from the iron centre, from the crystal structure at 1.9 Å resolution.[9] (b) (next page) Computer graphics display of the C_α backbone of MbHH indicating the location of the heme and the three surface histidine residues (His48, His81 and His116).[10] Molecular graphics images were produced using the MidasPlus software system from the Computer Graphics Laboratory, University of California, San Francisco (UCSF).

(b)

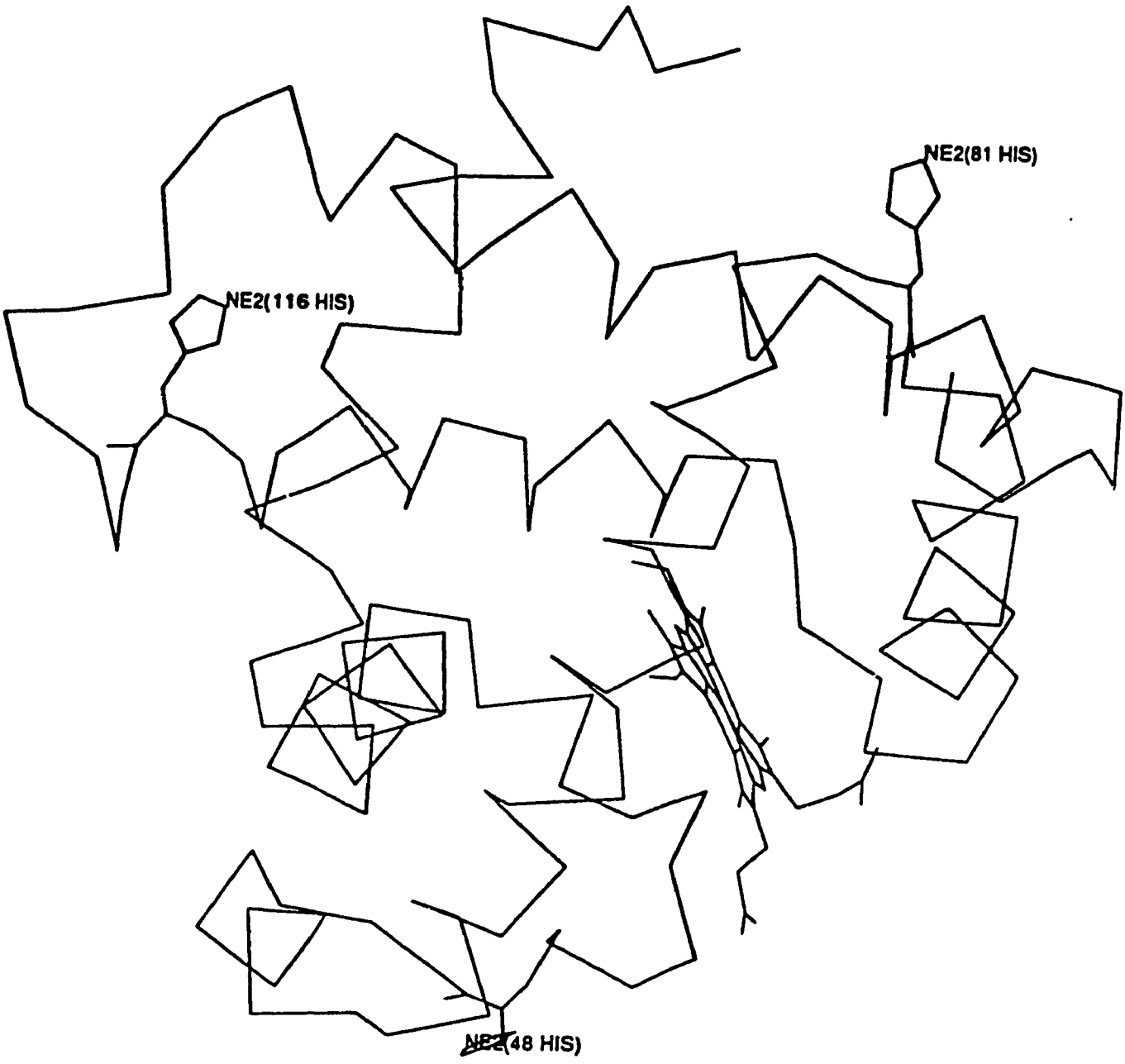

coordinated to the heme Fe and His64 lines the distal pocket. The remaining six histidines are not solvent exposed. The three surface histidines (His48, 81 and 116) are expected to show different reactivities with the a_5Ru^{3+} complex since computer graphics revealed that His116 is less exposed than both His48 and His81 (Figure 2.2).

Conditions similar to the ruthenation of sperm whale myoglobin (MbSW)[6] were chosen for MbHH, since MbSW has four surface histidines, three at the same position as MbHH, that can be easily modified. Thus, the protein is expected to be derivatized at one or more of the reactive histidine residues. After modification, the a_5Ru^{3+}(His)MbHH derivatives were separated by cation-exchange chromatography using fast protein liquid chromatography (FPLC). Methods previously used to determine the number of histidines derivatized by a_5Ru^{3+} include atomic absorption analysis,[4] inductively coupled plasma atomic emission analysis,[7] and diethyl pyrocarbonate reactivity.[7,8] In this work, a_5Ru(His)/heme ratios in modified MbHH were determined by uv-vis absorption spectroscopy.[3] The a_5Ru^{3+}(His) complex has a near UV absorption band with an absorption maximum that depends on the protonation state of the histidine pyrrole nitrogen. Upon protonation of the pyrrole nitrogen, absorption maxima are seen at 303 nm and 450 nm, and deprotonation shifts the absorption maxima to 370 nm and 600 nm. The derivatives with a_5Ru(His)/heme ratios close to 1:1 were characterized by HPLC analysis of the tryptic digests and mass spectrometry in order to identify the sites of a_5Ru^{3+} attachment. Electrochemistry (specifically, differential pulse voltammetry) was used to measure the reduction potentials of the derivatives. This chapter will describe the modification and

Figure 2.2: Space filling models of MbHH generated by computer graphics displaying in red (a) His48 and (b) His116.[10] His81 is not shown, but its solvent exposure is similar to His48. MbHH coordinates were obtained from the crystal structure.[9] Molecular graphics images were produced using the MidasPlus software system from the Computer Graphics Laboratory, UCSF.

(a)

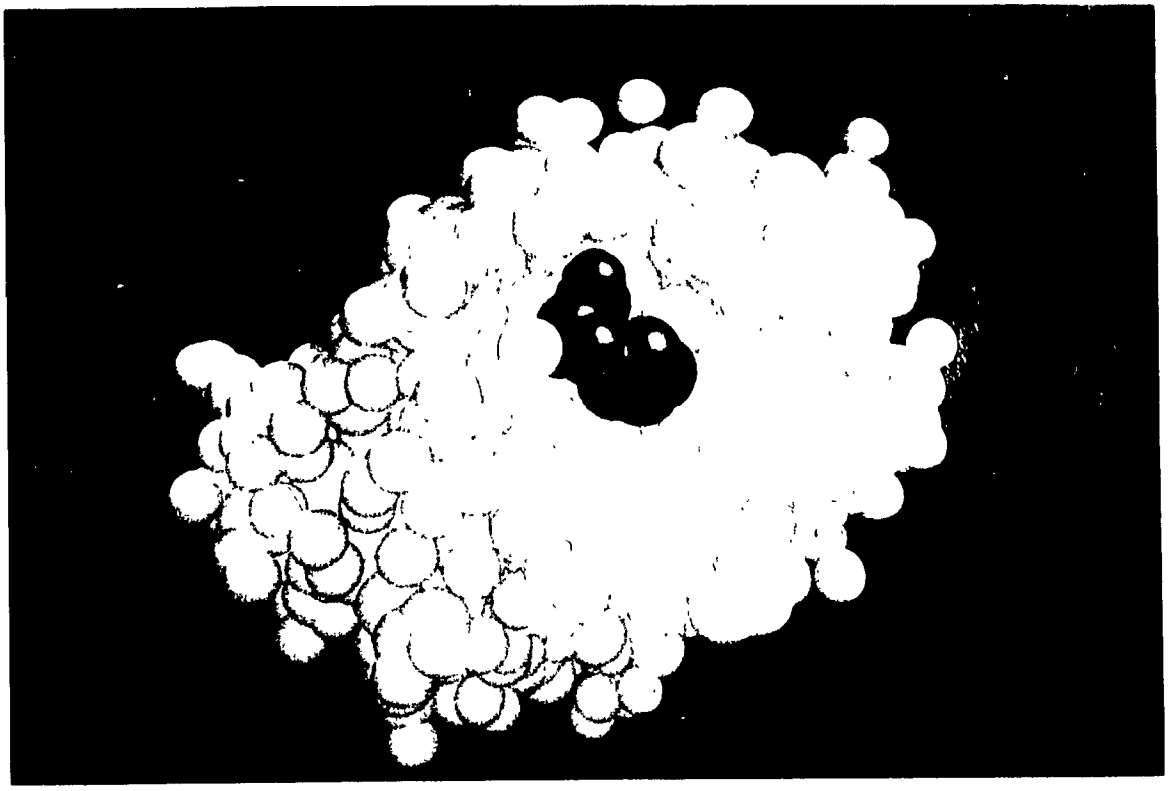

(b)

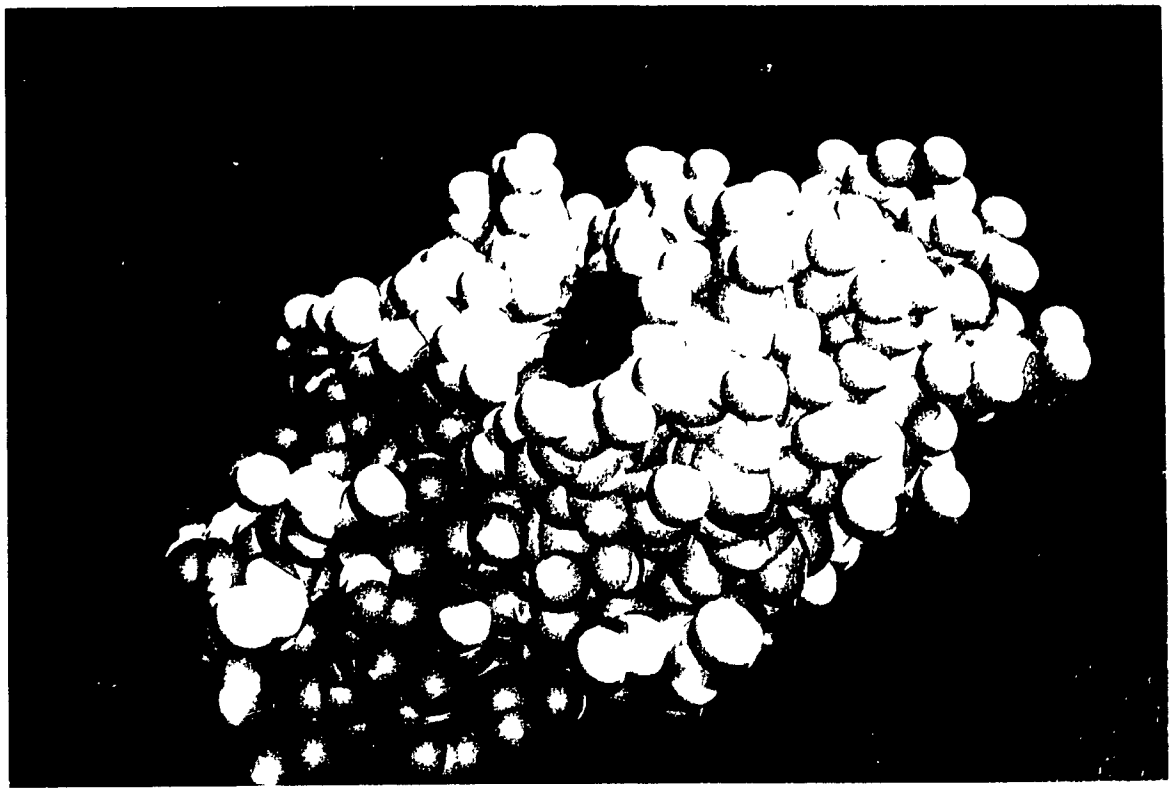

purification procedures utilized to isolate three singly-modified a_5Ru^{3+}(His)MbHH derivatives. In Chapter 3, the procedures used to determine the sites of a_5Ru^{3+} attachment will be discussed in detail.

2.2 Experimental

2.2.1 Materials

Horse heart myoglobin was purchased from Sigma and used without further purification. Sodium monophosphate and zinc metal (technical) were purchased from Fisher. KCN, chloropentaammineruthenium(III) chloride [$(a_5RuCl)Cl_2$] and DL-histidine were purchased from BDH Chemicals, Strem and Winthrop-Stears, Inc., respectively. All other chemicals used were reagent grade. Sephadex G-25 fine grade, a molecular exclusion gel, was purchased from Pharmacia. Pharmacia also provided the FPLC system which was controlled by a LC-500 control unit connected to two P-500 pumps, a UV-M monitor and an MV-7 motorized valve for sample injection. FPLC buffers were filtered through 0.45 μm membranes (Gelman Science) and all buffers were degassed by sonication or under vacuum prior to use. The buffers were prepared with nanopure water (specific resistance 18 MΩcm) from a Barnstead Nanopure system. Proteins were concentrated on an Amicon ultrafiltration cell using a YM 5 filter, also purchased from Amicon. Gas-tight syringes were from Hamilton, prepurified argon gas was purchased from Linde, Union Carbide.

2.2.2 Methods

Preparation of Pentaammineruthenium(III) Histidine [a_5Ru^{3+}(His)]: a_5Ru^{3+}(His) was prepared by the published procedure.[1] DL-His (0.6 g) was dissolved in 0.1 N HCl (40 ml), and purged with argon for 1 h. A few pieces of Zn/Hg amalgam were added to the solution followed by 0.3 g of $(a_5Ru^{3+}Cl)Cl_2$, and the reaction was allowed to proceed under argon for 3 h. The reaction was terminated by diluting the mixture to 100 ml with nanopure H_2O and subjected to a vigourous bubbling with air for 1 h. The dark red solution obtained following exposure to air was adjusted to pH 1.0 with 5.0 N HCl, and passed through a Dowex 50W-X2 (Bio-Rad) cation-exchange column. a_5Ru^{3+}(His) was eluted by 3.0 N HCl as an orange band. The solution was evaporated to dryness using a rotary evaporator, followed by a vacuum oven. A residual solid was obtained from an acetone - water mixture (1:1) and shown to have the reduction potential (Chapter 3) and spectral properties characteristic of the a_5Ru^{3+}(His) complex.

Preparation of Ruthenium-Modified MbHH: a_5Ru^{3+}(His)MbHH was prepared by the published procedure[11] in which excess $a_5Ru^{2+}(H_2O)$ was reacted with Mb. A solution containing Fe^{III}-MbHH (600 mg in 25 ml) in 0.05 M Tris buffer, pH 7.2, in a septum-stoppered bottle was deaerated using argon. A second solution containing $(a_5Ru^{3+}Cl)Cl_2$ (130 mg in 15 ml) in the same buffer was also deaerated for 1 h and a few pieces of Zn/Hg amalgam (used as a reductant) were added to the solution. Both solutions were kept under argon for another 1.5 h and the solution of aquopentaammineruthenium(II) $a_5Ru^{2+}(H_2O)$ was then transferred under argon to the

solution of Fe^{III}-MbHH. This immediately caused a color change from brown to deep red due to the reduction of Fe^{III}-MbHH $\rightarrow$ Fe^{II}-MbHH. The solution was left standing at room temperature without agitation for 1 h and then added to a G-25 fine Sephadex (1.5 cm x 40 cm) column that was equilibrated with of 0.05 M Tris buffer, pH 7.2 (4 °C). The protein fraction was collected and oxidized with a saturated solution of $Co(phen)_3^{3+}$. The mixture of ruthenated Mb derivatives was desalted with five washings of nanopure water on an Amicon concentrator using a YM 5 filter and concentrated to ~ 6 ml in 0.05 M phosphate buffer, pH 6.0. An absorption spectrum was recorded after this step to assure that Mb was in the ferric state (ε_{409} = 188 mM^{-1} cm^{-1}).[12]

Separation of Ruthenium-Modified MbHH Derivatives by FPLC: The mixture of modified MbHH species was separated into its derivatives on a cation-exchange Mono S HR 10/10 FPLC column equilibrated with 50 mM phosphate buffer, pH 6.0. The sample size loaded was between 5-20 mg in 1.0 ml of the starting buffer and elution was with 0-1 M NaCl in 50 mM phosphate buffer, pH 7.0. The absorbance was followed at 280 nm and the flow rate was 0.5 ml/min.

a_5Ru^{3+}(His) to Heme Ratios of Modified MbHH: Following the procedure reported by T. Fox,[8] 10 μM native and ruthenium-modified MbHH samples were prepared in 0.1 M CAPS buffer (pH 11.0) containing 10 mM KCN. The absorption maximum of a_5Ru^{3+}(His) (ε_{370} = 3400 M^{-1} cm^{-1})[13] at high pH (> 10) is easier to detect than that at low pH (ε_{303} = 2100 M^{-1} cm^{-1}).[1] The spectral shift at high pH is due to deprotonation of the pyrrole nitrogen of the histidine, and the Soret of MbHH is red-

shifted on forming its cyanide complex; this prevented overlap of the heme and a_5Ru^{3+}(His) absorbances. A concentration of 10 μM was chosen for the cyanide complexes of native and ruthenium-modified MbHH (ε_{422} = 116 mM^{-1} cm^{-1})[14] since this allowed measurement of the absorbance of the a_5Ru^{3+}(His) complex at 370 nm while using a minimum amount of protein. The difference spectra of the cyanide complexes of the derivatives separated by FPLC and native MbHH-CN were examined to determine if the protein had indeed been modified with a_5Ru^{3+}. A difference spectrum showing a broad band at 370 nm indicates that MbHH had been modified at a histidine residue by a_5Ru^{3+}; the difference spectrum of two different native MbHH-CN samples displayed a flat baseline. All spectrophotometric measurements were carried out on a Hewlett Packard 8451A diode array spectrophotometer which has a resolution of ± 2 nm.

Computer Graphics: The x-ray structure coordinates of MbHH[9] were obtained through a personal communication with Gary Brayer (U.B.C.). The coordinates were used in the molecular graphics program MidasPlus[10] and viewed on a Silicon Graphics 4D Personal IRIS system.

2.3 Results

FPLC Cation-Exchange Chromatography: Native MbHH has a pI of 6.9 and therefore does not bind to the FPLC Mono S HR 10/10 cation-exchange column.[15] Native MbHH should therefore elute in the void volume, while ruthenium-modified MbHH should bind to the cation-exchange column due to the positive charge

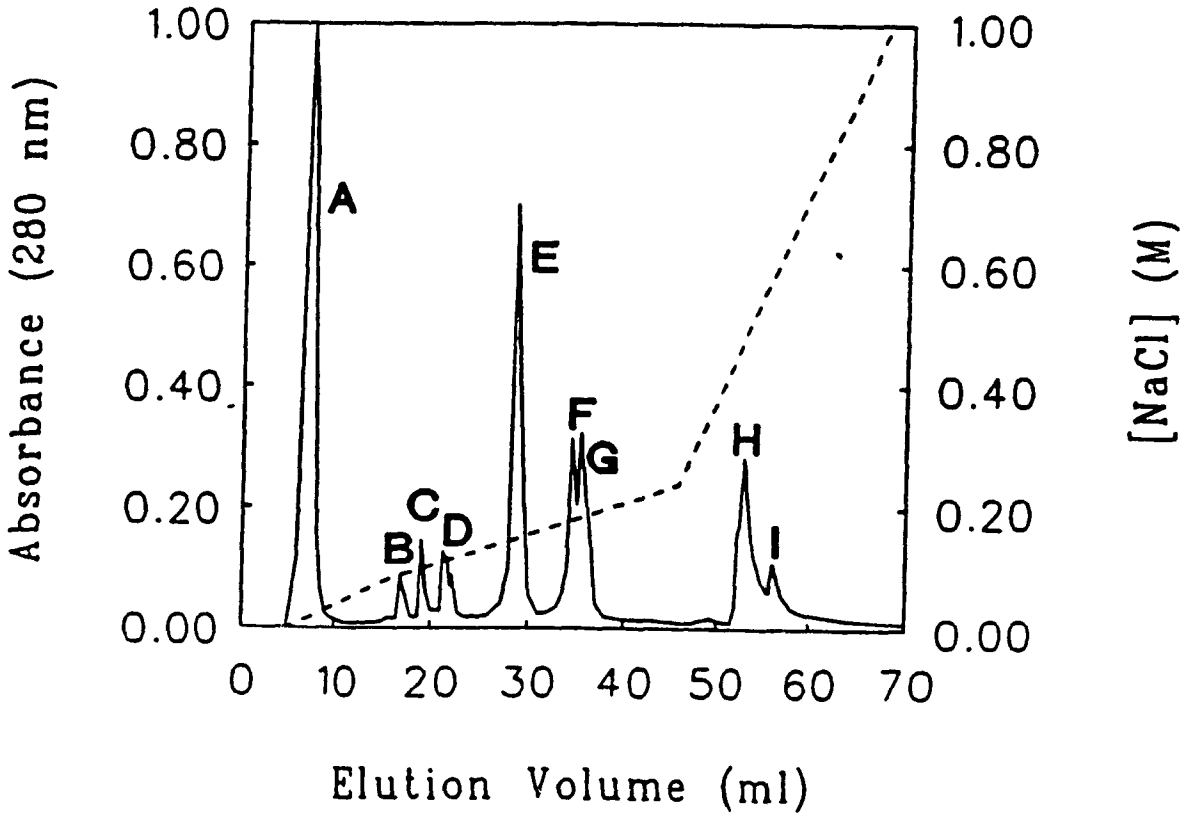

Figure 2.3: FPLC cation-exchange chromatography (Mono S, HR 10/10) of 17.35 mg of the mixture of products from the reaction of $a_5Ru(H_20)^{2+}$ with horse heart myoglobin. The column was equilibrated with 50 mM phosphate buffer (pH 6.0) and elution was with 0-1.0 M NaCl gradient (dashed line) in 50 mM phosphate buffer (pH 7.0). Flow rate: 0.5 ml/min. Fraction size: 4.0 ml.

(a)

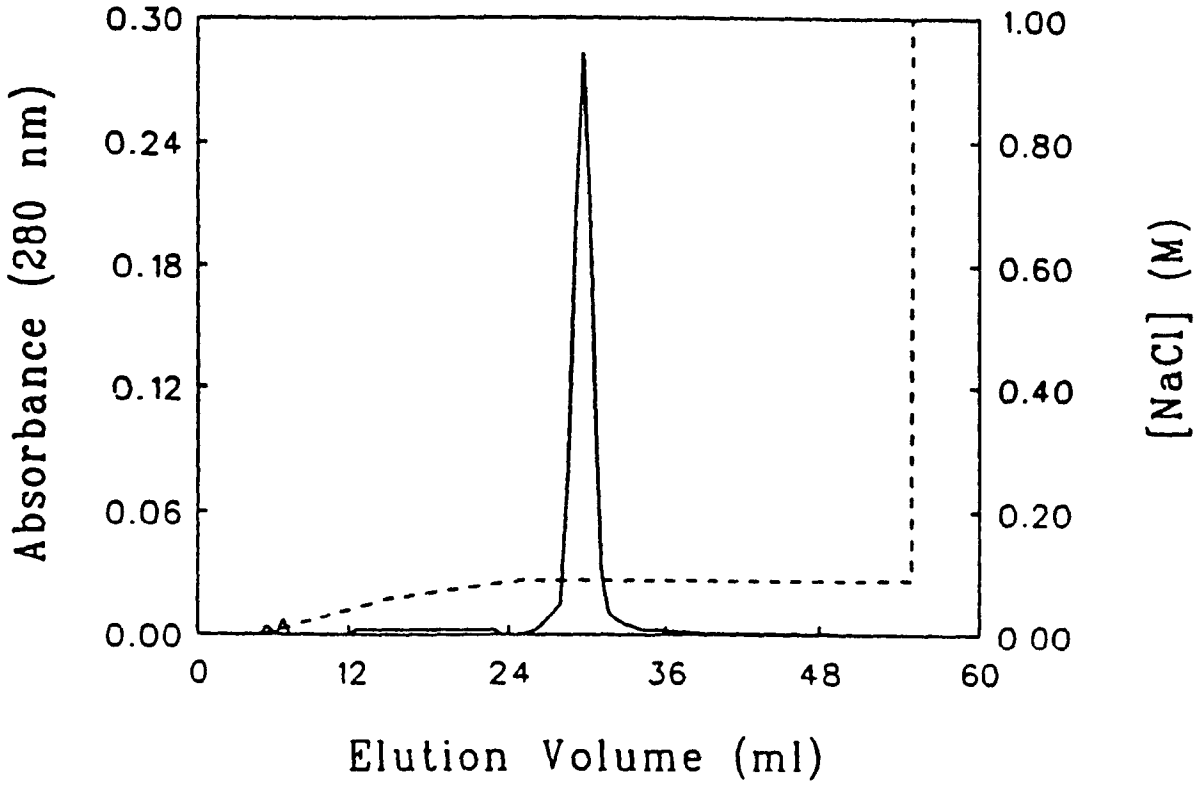

Figure 2.4: FPLC cation-exchange (Mono S, HR 10/10 column equilibrated in 50 mM phosphate buffer, pH 6.0) rechromatography of (a) 5.0 mg Peak E, (b) 2.0 mg Peak F and (c) 4.5 mg Peak G (Figure 2.3) in 1.0 ml of equilibrated buffer. Elution of the rechromatographed peaks occurred at 90 mM NaCl in 50 mM phosphate buffer (pH 7.0). Flow rate: 0.5 ml/min. Fraction size: 4.0 ml.

(b)

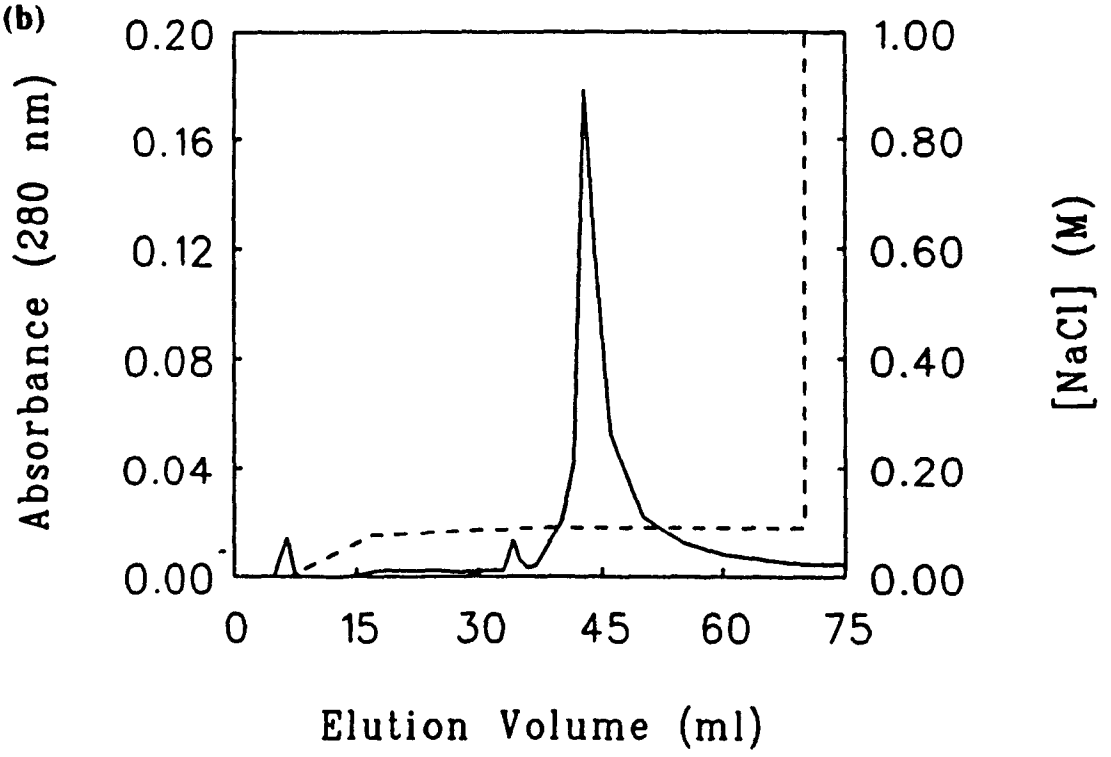
0.20
0.16
0.12
0.08
0.04
0.00
Absorbance (280 nm)
1.00
0.80
0.60
0.40
0.20
0.00
[NaCl] (M)
0
15
30
45
60
75
Elution Volume (ml)

(c)

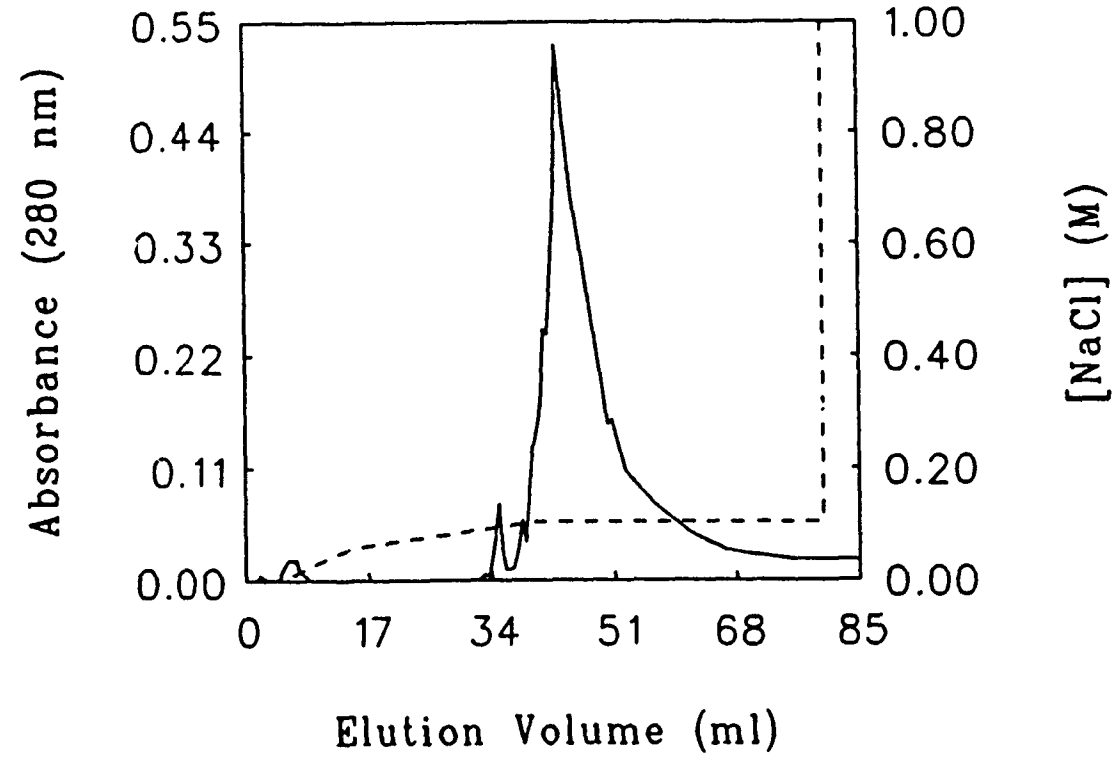
0.55
0.44
0.33
0.22
0.11
0.00
Absorbance (280 nm)
1.00
0.80
0.60
0.40
0.20
0.00
[NaCl] (M)
0
17
34
51
68
85
Elution Volume (ml)

incorporated on a_5Ru^{3+}-complexation. In the published FPLC elution profile of a_4(pyridine)Ru^{3+}MbSW,[6] the initial elution band was shown to be native Mb, while bands which were eluted at high salt concentrations (1.0 M NaCl) were shown to be multiply-modified Mb. The FPLC Mono S elution profile (Figure 2.3) of the products from ruthenium-modified MbHH displays nine distinct peaks (A-I). Peak A was eluted in the void volume, and Peaks B, C and D yielded small amounts of protein. Peaks E, F and G were the most abundant after Peak A, and were eluted at 90 mM NaCl, whereas Peaks H and I were eluted on increasing the NaCl gradient. Peaks A-G in Figure 2.3 were collected and rechromatographed on the same column using shallow NaCl gradients [Figure 2.4(a), (b) & (c)]. The reaction of $a_5Ru^{2+}(H_2O)$ with MbHH was repeated 6 times and the FPLC profiles of the products were reproducible.

a_5Ru^{3+}(His) to Heme Ratios of Modified MbHH: The uv-vis absorption spectra in Figure 2.5 show the spectral shift from the 303 nm to 370 nm of the absorption maxima of a_5Ru^{3+}(His) complex at high pH due to the deprotonation of the pyrrole nitrogen of the histidine side chain. Figure 2.6 shows the uv-vis absorption spectra in the Soret region of native MbHH (pH 7.0) and its cyanide-bound form, MbHH-CN at pH 11.0. Figure 2.7(a), (b) & (c) are difference spectra obtained by subtracting the spectra of MbHH-CN from the spectra of the cyanide complexes of Peak E, F and G, respectively. Subtracting the spectra of two different MbHH-CN samples gives a difference spectrum with a flat baseline (not shown), whereas the difference spectra of Peaks E, F and G yielded the spectrum of a_5Ru^{3+}(His).

The ruthenium content determined by absorption spectroscopy for each peak

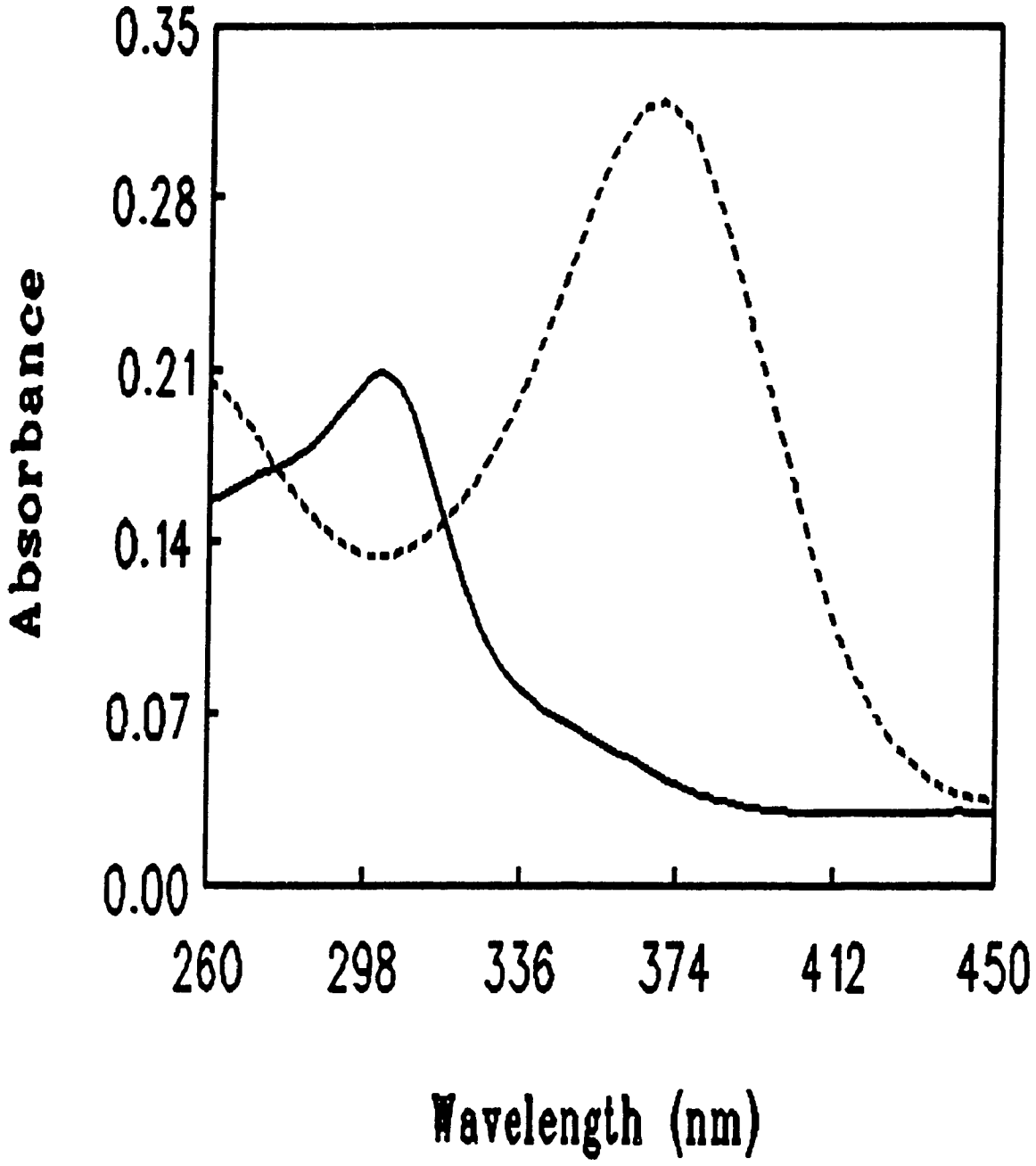

Figure 2.5: Absorption spectra of 100 μM a_3Ru^{3+}(His) in 0.1 M phosphate buffer, pH 7.0 (solid line) and in 0.1 M CAPS buffer, pH 11.7 (dashed line).

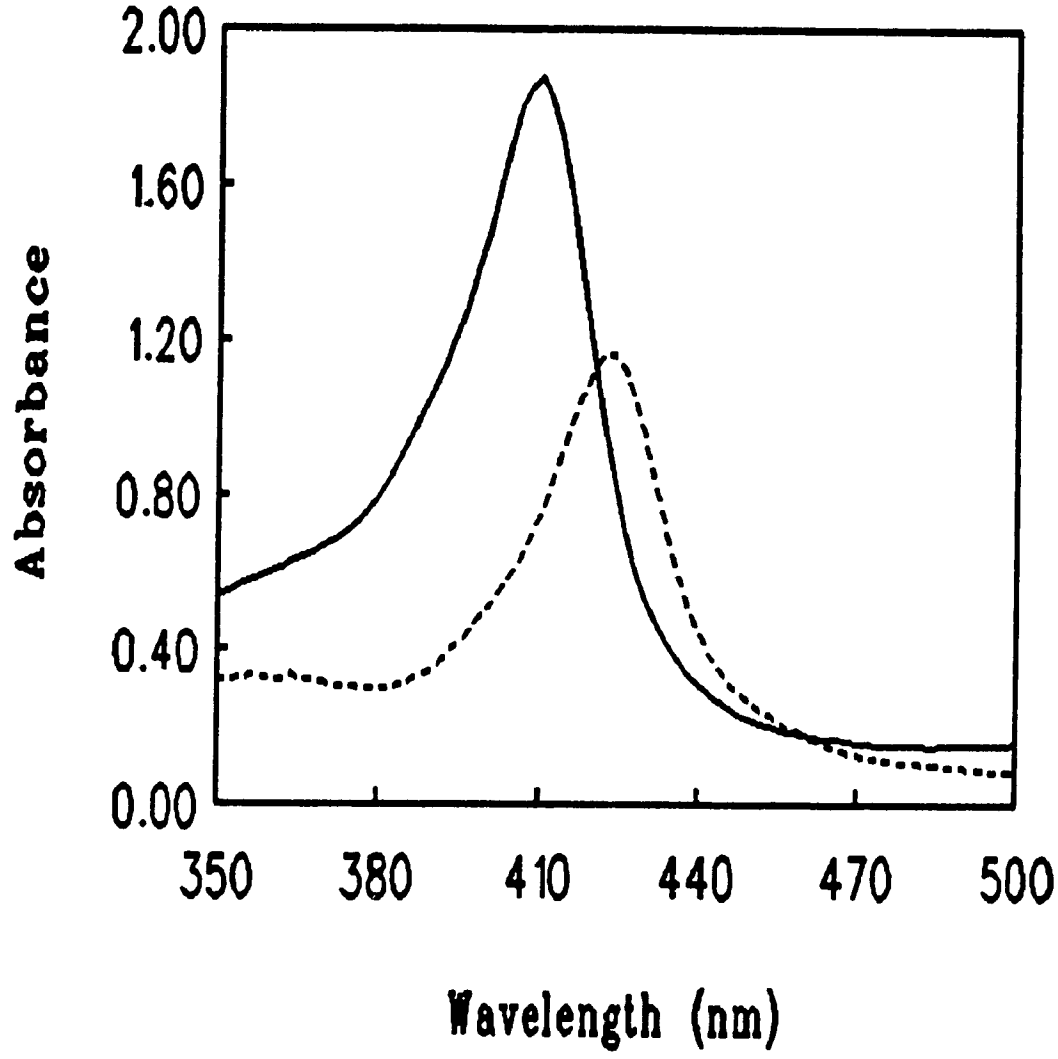

Figure 2.6: Absorption spectra of 10.0 μM native MbHH in 0.1 M phosphate buffer, pH 7.0 (solid line) and its cyanide complex in 0.1 M CAPS buffer at pH 11.0 with 10 mM KCN (dashed line).

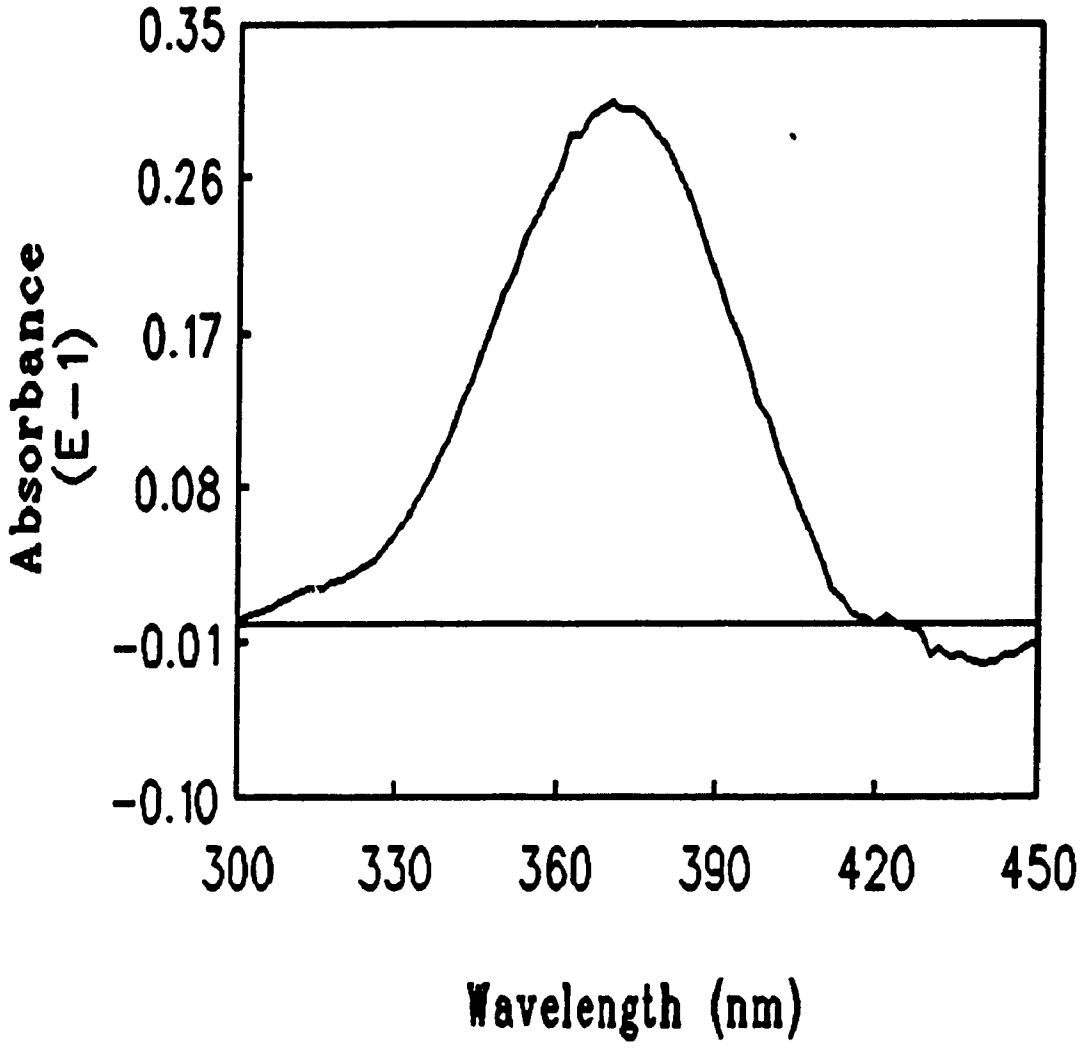

Figure 2.7: Difference spectra obtained by subtracting the spectrum of MbHH-CN from the spectra of the cyanide complexes of (**a**) Peak E, and (next page) (**b**) Peak F and (**c**) Peak G. All samples contained 10 μM protein with 10 mM KCN in 0.1 M CAPS buffer, pH 11.0.

(b)

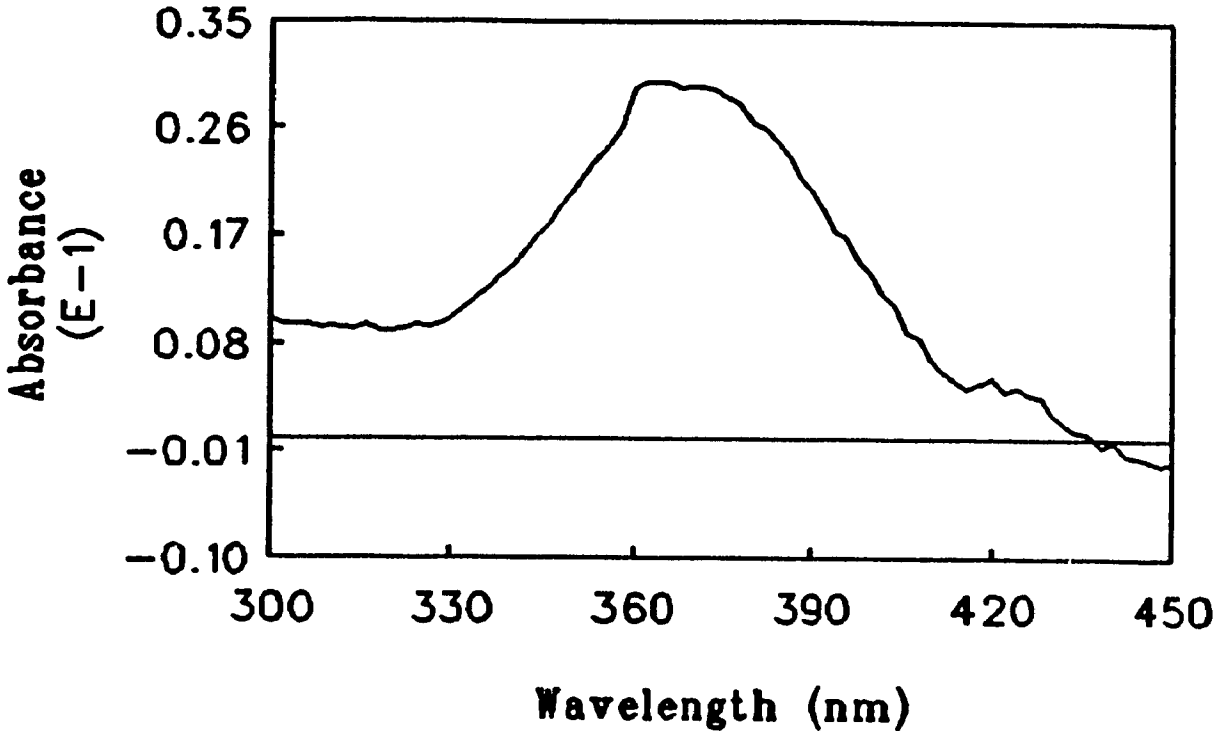
0.35
0.26
0.17
0.08
−0.01
−0.10
Absorbance (E−1)
300
330
360
390
420
450
Wavelength (nm)

(c)

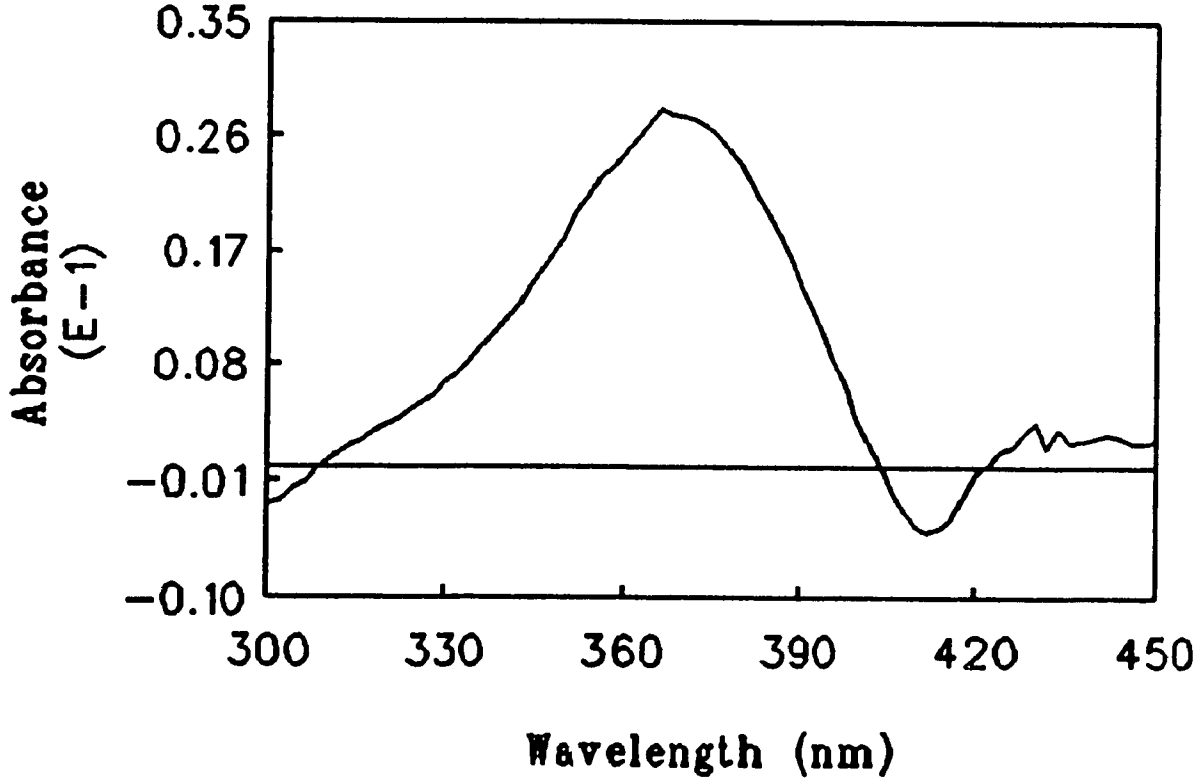
0.35
0.26
0.17
0.08
−0.01
−0.10
Absorbance (E−1)
300
330
360
390
420
450
Wavelength (nm)

of the FPLC elution profile is given in Table 2.1. The difference spectrum of Peak A did not contain a a_5Ru^{3+}(His) band and since it was eluted in the void volume, this indicates that Peak A is probably native MbHH. There was not a sufficient amount of Peak B to determine its a_5Ru^{3+}(His) content. Peak C and D possessed a_5Ru^{3+}(His)/heme ratios of 0.52:1 and 0.68:1, respectively. Peaks E, F and G gave a_5Ru^{3+}(His)/heme ratios close to 1:1, indicating that these derivatives of MbHH were likely modified with a single ruthenium complex. Peak H and I, which were eluted at high salt concentrations, are believed to be multiply-labelled MbHH. Peak H gave an a_5Ru^{3+}(His)/heme of ratio 3.2:1, the ratio for Peak I was not determined, but it is assumed to contain multiply-labelled MbHH species since it was eluted after Peak H.

2.4 Discussion

The mixture of products from the reaction of $a_5Ru^{2+}(H_2O)$ with MbHH for 1 hour at pH 7.2 yielded nine distinct peaks with different chromatographic properties upon separation by FPLC cation-exchange chromatography. A 3+ charge is introduced for each a_5Ru^{3+} redox centre attached, which increases the affinity of MbHH for the cation-exchange matrix. Evidence for the attachment of a_5Ru^{3+} to histidine residues in MbHH is shown by the difference spectrum of a_5Ru^{3+}(His)MbHH-CN and MbHH-CN which has a peak at 370 nm at pH > 10, similar to the peak observed for the model complex, a_5Ru^{3+}(His). Ruthenium determination by this method is specific for a_5Ru^{3+} bound to histidine residues, since binding to other residues in the protein is not expected to give the same characteristic absorption maximum at 370 nm.

Table 2.1: Determination of a_5Ru^{3+}(His)/Heme Ratios for MbHH Derivatives Separated by FPLC Cation-Exchange Chromatography[a]

Species	a_5Ru^{3+}(His)/Heme[b]
Peak A	0
Peak C	0.52
Peak D	0.68
Peak E	0.89
Peak F	0.86
Peak G	0.81
Peak H	3.2

[a]See Figure 2.3 for labelling of peaks.

[b]Ratios determined using difference absorption spectra of the samples as outlined in the Results section.

Peak A which was eluted in the void volume and was not ruthenated (Table 2.1), is most probably native MbHH. Peaks H and I, which were eluted at high salt concentration are most probably multiply-modified MbHH derivatives. The difference spectra of Peaks B, C and D did not give the characteristic 370 nm absorption band but showed broad low intensity peaks between 300-420 nm (not shown). Thus these derivatives possibly have a_5Ru^{3+} bound to other residues in the protein (eg., methionine) or bound to buried histidine[8] residues causing a conformational change in the protein. Peaks E, F and G, appear to contain singly-modified a_5Ru(His)MbHH. The difference spectra of Peaks F and G, shows some perturbation which could possibly be due to small conformational changes occurring in the protein due to modification.[8]

In summary, it was seen that the reaction of $a_5Ru^{2+}(H_2O)$ with MbHH for 1 hour at pH 7.2 yielded three singly-modified a_5Ru(His)MbHH derivatives. These results are in agreement with predictions from the computer graphics analysis of MbHH [Figure 2.1(b)] and the results obtained for MbSW.[16] Further characterization of the a_5Ru(His)MbHH derivatives is the focus of the following chapter.

2.5 References

1) Sundberg, R. J.; Gupta, G. *Bioinorg. Chem.* **1973**, *3*, 39.

2) Yocom, K. "The Synthesis and Characterization of Inorganic Redox Reagent-Modified Cytochrome *c*", Ph.D. Thesis, California Institute of Technology, **1982**.

3) Yocom, K. M.; Shelton, J. B.; Shelton, J. R.; Schroeder, W. A.; Worosila, G.; Isied,

S. S.; Bordignon, E.; Gray, H. B. *Proc. Natl. Acad. Sci. USA* **1982**, *79*, 7052.

4) Yocom, K. M.; Winkler, J. R.; Nocera, D. G.; Gray, H. B. *Chemica Scripta* **1983**, *21*, 29.

5) Bosshard, H. R.; Banziger, J.; Hasler, T.; Poulos, T. L. *J. Biol. Chem.* **1984**, *259*, 5683.

6) Karas, J. L. "Long-Range Electron Transfer in Ruthenium-Labelled Myoglobin", Ph.D. Thesis, California Institute of Technology, **1989**.

7) Osvath, P.; Salmon, G. A.; Sykes, A. G. *J. Am. Chem. Soc.* **1988**, *110*, 714.

8) Fox, T. "Studies on Enzyme Intermediates of Yeast Cytochrome *c* Peroxidase", Ph.D. Thesis, Concordia University, **1991**.

9) Evans, S. V.; Brayer, G. D. *J. Mol. Biol.* **1990**, *213*, 885.

10) Ferrin, T. E.; Huang, C. C.; Jarvis, L. E.; Langridge, R. *J. Mol. Graphics* **1988**, *6*, 13.

11) Axup, A. W.; Albin, M.; Mayo, S. L.; Crutchley, R. J.; Gray, H. B. *J. Am. Chem. Soc.* **1988**, *110*, 435.

12) Tsukahara, K. *Inorg. Chim. Acta* **1986**, *124*, 199.

13) Recchia, J.; Matthews, C. R.; Rhee, M.; Horrocks, W. D. *Biochim. Biophys. Acta.* **1982**, *702*, 105.

14) Scheler, W.; Schaffa, G.; Junge, F. *Biochem. Z.* **1957**, *317*, 232.

15) Johansson, B-L; Gustavsson, J. *J. Chromatogr.* **1988**, *457*, 205.

16) Crutchley, R. J.; Ellis, W. R.; Gray, H. B. *Frontiers in Bioinorganic Chemistry* Xavier, A. V., VCH, Weinham, FRG, **1986**.

3.0 Characterization of a_5Ru(His)MbHH Derivatives

3.1 Introduction

Determining the site of derivatization and ensuring that the structure has not been perturbed is required after modification of a protein. UV-vis absorption spectroscopy,[1,2] circular dichroism (CD),[3] electronic paramagnetic resonance (EPR)[4] and resonance Raman spectroscopy[4] have demonstrated that proteins such as cytochrome c,[2] sperm whale myoglobin[5,6] and azurin[4] are not structurally perturbed by the attachment of a_5Ru^{3+} to surface histidines. The reduction potentials of the metal centres in these modified proteins have also been measured using differential pulse polarography (DPP),[5] cyclic voltammetry (CV)[2,7,8] and spectroelectrochemistry[4,5,8]. In this work, the reduction potentials of the singly-modified a_5Ru(His)MbHH derivatives will be evaluated by differential pulse voltammetry.

The site of modification can be found by a number of techniques including nuclear magnetic resonance (NMR) spectroscopy[3,6,9] and peptide mapping.[2,4,5,6,8,9] The attachment of the a_5Ru^{3+} group to a histidine residue causes paramagnetic shifting and broadening of the C-2 and C-4 protons in the ^1H NMR spectrum of the protein.[6] The ^1H NMR resonances of histidine residues in MbHH and MbSW have been assigned,[6,10] but a high field NMR instrument was unavailable for the present work, so peptide mapping was used to determine the site of modification.

Peptide mapping involves the cleavage of the protein with a protease, such as trypsin, which cleaves at lysine and arginine residues as shown in Figure 3.1 for

MbHH. The peptide fragments obtained from the cleavage can be separated by high performance liquid chromatography (HPLC). A change in mobility of a peptide fragment, along with the appearance of a new peak in the chromatogram monitored at 300 nm, indicates that a peptide fragment contains a_5Ru^{3+}(His). The presence of the metal complex can be confirmed by absorption spectroscopy and the peptide fragment can then be identified by amino acid analysis and/or mass spectrometry. This chapter outlines the characterization of the singly-modified a_5Ru(His)MbHH derivatives discussed in Chapter 2.

|| Gly-Leu-Ser-Asp-Gly-Glu-Trp^{7}-Gln-Gln-Val^{10}-Leu-Asn-Val-Trp^{14}-Gly-Lys ||

|| Val-Glu-Ala-Asp^{20}-Ile-Ala-Gly-His-Gly-Gln-Glu-Val-Leu-Ile^{30}-Arg ||

|| Leu-Phe-Thr-Gly-His-Pro-Glu-Thr-Leu^{40}-Glu-Lys || Phe-Asp-Lys || Phe-Lys ||

|| His^{*48}-Leu-Lys^{50} || Thr-Glu-Ala-Glu-Met-Lys || Ala-Ser-Glu-Asp^{60}-Leu-Lys || Lys ||

|| His-Gly-Thr-Val-Val-Leu-Thr^{70}-Ala-Leu-Gly-Gly-Ile-Leu-Lys || Lys || Lys ||

|| Gly^{80}-His^{*81}-His-Glu-Ala-Glu-Leu-Lys-Pro-Leu-Ala^{90}-Gln-Ser-His-Ala-Thr-Lys ||

|| His-Lys || Ile-Pro^{100}-Ile-Lys ||

|| Tyr-Leu-Glu-Phe-Ile-Ser-Asp-Ala^{110}-Ile-Ile-His-Val-Leu-His^{*116}-Ser-Lys ||

|| His-Pro^{120}-Gly-Asn-Phe-Gly-Ala-Asp-Ala-Gln-Gly-Ala^{130}-Met-Thr-Lys ||

|| Ala-Leu-Glu-Leu-Phe-Arg || Asn^{140}-Asp-Ile-Ala-Ala-Lys || Tyr-Lys ||

|| Glu-Leu-Gly^{150}-Phe-Gln-Gly ||

Figure 3.1: Tryptic peptide map of horse heart myoglobin. Exposed histidine residues are noted by *.

3.2 Experimental

3.2.1 Materials

Trypsin (TPCK-treated; TPCK, [L-(1-tosylamido-2-phenyl)ethylchloromethyl ketone]) was obtained from Sigma. 4,4'-dipyridyl was purchased from G.Frederick Smith Company. HPLC grade acetonitrile and trifluoroacetic acid (TFA) were purchased from Fisher. An LKB-HPLC system was purchased from Pharmacia. The HPLC system consisted of an LKB Variable Wavelength Monitor 2141, a Gradient Pump 2249, and samples were injected through a PV-7 valve (maximum pressure = 35 MPa). The column used to separate the peptide fragments was a 0.5 x 27.5 cm Vydac C_{18} reverse phase column. Results were viewed on chart recorders from Mandel Scientific and Kipp & Zonen. HPLC buffers were prepared with nanopure water (specific resistance 18 MΩcm) from a Barnstead Nanopure system. The buffers were filtered through 0.2 μm nylon membranes purchased from Gelman Science and all buffers were degassed by sonication or vacuum prior to use.

3.2.2 Methods

Tryptic Digest of Native and Singly-Modified a_5Ru(His) MbHH: Native and singly-modified a_5Ru(His)MbHH (Peaks E and G in Figure 2.3) were digested by trypsin and the resulting peptides were separated by reverse phase HPLC. Peptide mapping of Peak F, the other singly-modified a_5Ru(His)MbHH, was not performed in this work. Native MbHH (4 mg) was added to 2 ml of 0.2 M NH_4HCO_3 (pH 8.0) followed by the addition of 20 μl trypsin (10 mg/ml in 0.001 N HCl) to give a ratio

of 20:1 (w/w) for native and singly-modified a_5Ru(His)MbHH to trypsin. The digest was incubated at 37 °C for 16 h, and upon completion of the incubation, the pH of the solution was lowered to 2.0. Between 0.2 and 0.5 mg of the tryptic digests (20 µl - 100 µl) were injected on the C_{18} column. The peptides were eluted in 120 min with a linear gradient from 0 to 55% acetonitrile in 0.1% TFA at pH 2.85. TFA was used to form ion pairs with the peptides to improve their separation. The eluent was monitored at 210 nm [1.0 Absorbance Unit Full Scale (AUFS)] to view the backbone separation and at 300 nm (0.1 AUFS) to view tryptophan and heme containing peptides. The attachment of a_5Ru^{3+} to a histidine residue generates a chromophore that has a detectable maximum at 303 nm which facilitates identification of the modified peptides. Peptides visualized at 210 nm were collected and sent to the Biotechnological Research Institute (BRI) for amino acid analysis and mass spectrometry.

Amino Acid Analysis of Tryptic Peptides: Amino acid analysis was carried out at BRI by Bernard Gibbs. The collected tryptic peptides (~ 3 µg/tube) were placed in culture tubes from Corning which were previously muffled at 450 °C overnight. The tubes were placed in reaction vials from Waters and the samples were dried in the Waters Pico-Tag Work Station. Boiling HCl (200 µl) containing 1% phenol was added to the vials and then purged with dried N_2 and evacuated. Following three purges, the vials were heated at 150 °C for 4 h under vacuum. The values obtained from the amino acid analyser for the ten amino acids (histidine, proline, leucine, lysine, glycine, alanine, arginine, phenylalanine, aspartate, glutamine) stable to acid

hydrolysis were not corrected.[11] Values obtained for serine, threonine and tyrosine were extrapolated to zero time, and isoleucine and valine were extrapolated to infinity. The analysis was performed on a Beckman System 7300 High Performance Analyser.

Mass Spectrometry: Atmospheric pressure ionization (API) mass spectrometry was carried out at BRI by Bernard Gibbs. Mass spectra were obtained in the positive mode of a triple stage mass spectrometer (Model API-111, Sciex, Toronto, Canada). Samples (0.1 - 1.0 μg/μl) of MbHH and peptide fragments were dissolved in 10% acetic acid and infused through a stainless steel capillary (ID = 1 x 10^{-4} m). A stream of air was introduced to assist in the formation of the submicron droplets (pneumatic nebulization). These droplets were evaporated at the interface by N_2 gas producing highly charged ions which were detected by the analyzer.

Differential Pulse Voltammetry (DPV) of Native and Singly-Modified a_5Ru(His)MbHH: DPV was used to measure the reduction potentials of the a_5Ru(His)MbHH derivatives. The electrochemical cell (Figure 3.2) was composed of a gold working electrode, a platinum wire counter electrode and a silver-silver chloride (3 M KCl, E = 0.194 V vs. NHE) reference electrode. The protein samples (50.0 μM) were in 0.1 M phosphate buffer, pH 7.0, with 10 mM 4,4'-dipyridyl, which was used as an electron transfer promoter. Solutions were purged with nitrogen for 15 min before measurements and blanketed with nitrogen during measurements. The gold electrode was polished with fine alumina in a water suspension prior to immersion in the electrochemical cell. A BAS 100A Electrochemical Analyzer was used for electrochemical measurements.

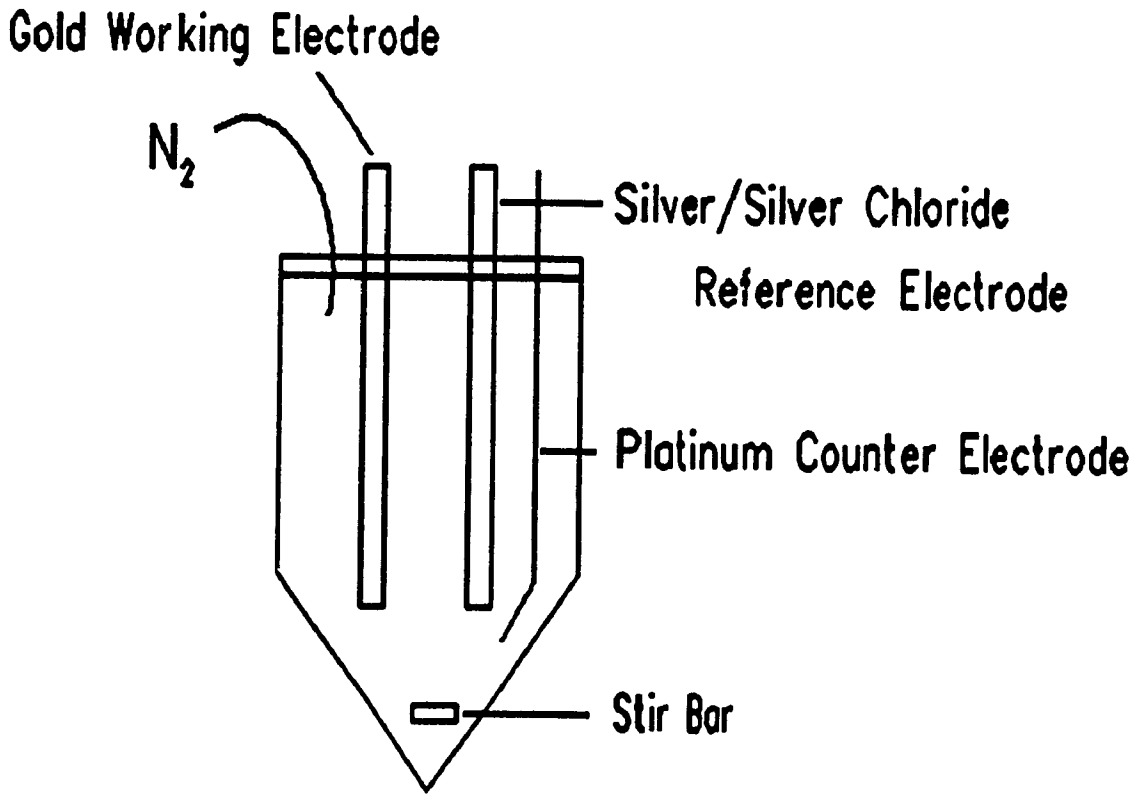

Figure 3.2: Schematic diagram of the electrochemical cell used to measure reduction potentials

3.3 Results

Mass Spectrometry of Native and Singly-Modified a_5Ru(His)MbHH: The API mass spectra of native MbHH, Peak E and Peak F are shown in Figures 3.3 and 3.4. Native MbHH was found to have a molecular weight of 16,950 which is in excellent agreement with the most recent literature value (16,951)[12] for this protein.

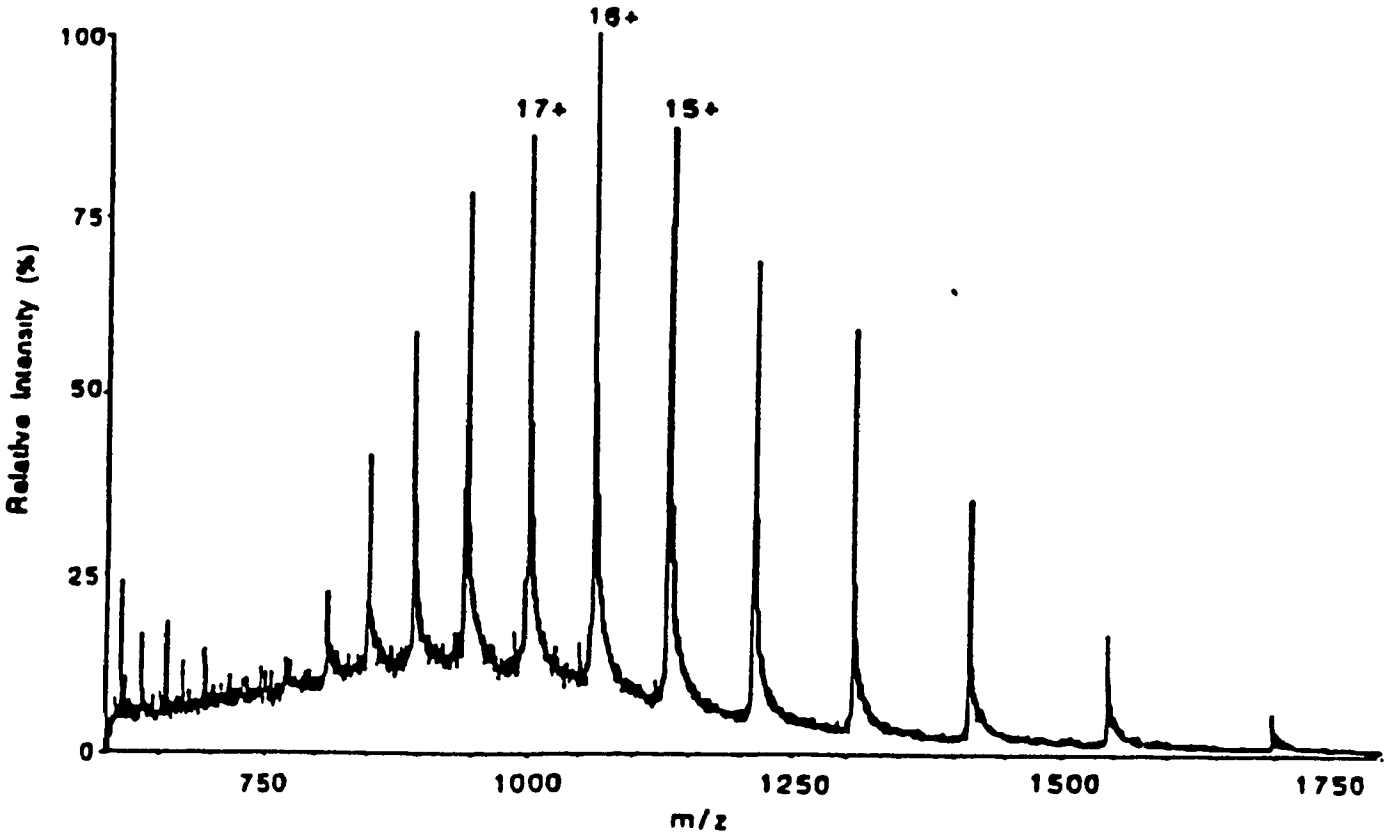

Figure 3.3: Atmospheric pressure ionization (API) mass spectrum of native horse heart myoglobin (1.0 µg/µl) in 10 % CH_3COOH. A molecular weight of 16,950 was obtained for the protein.

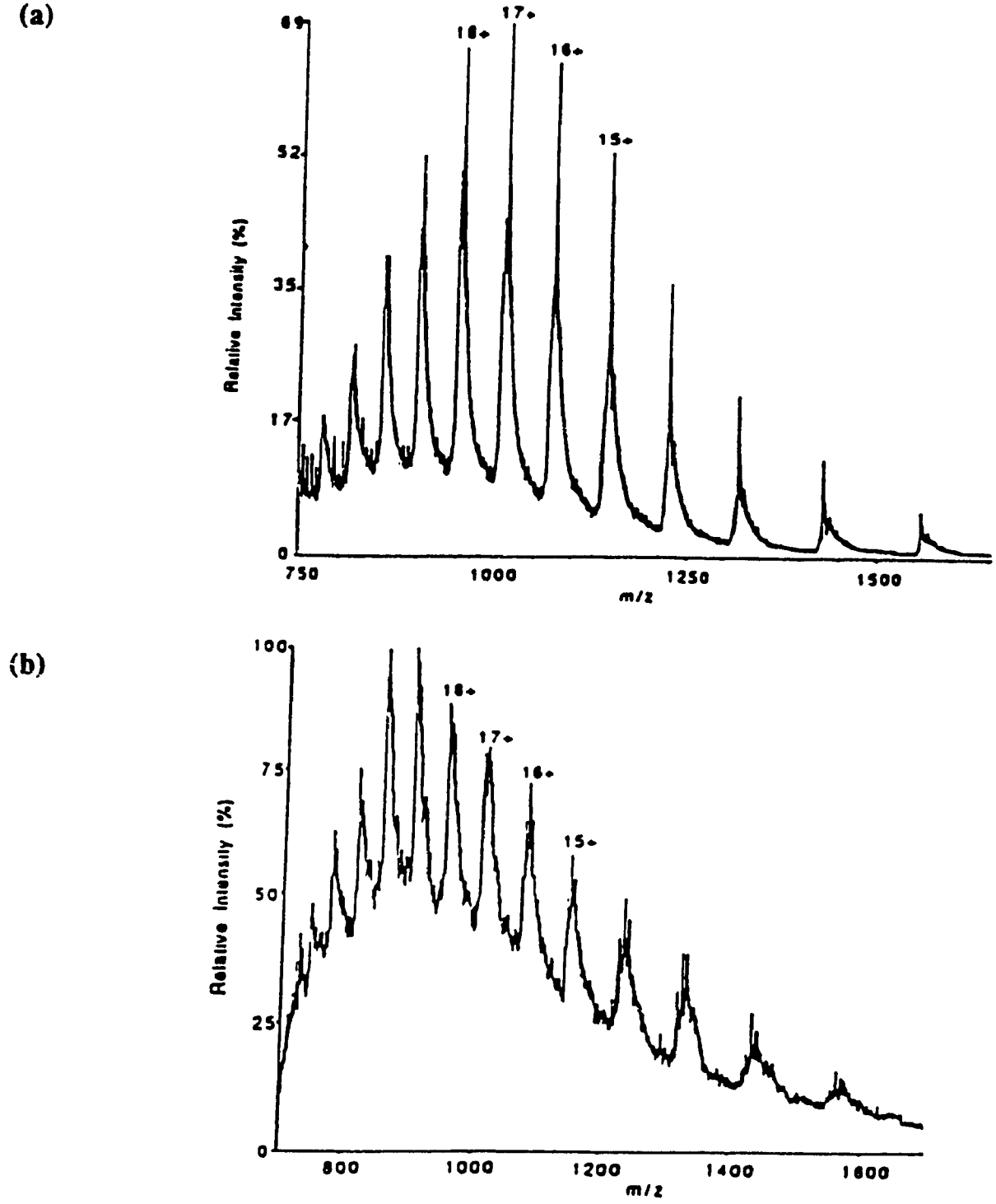

Figure 3.4: API mass spectra of the ruthenium-modified horse heart myoglobin derivatives (1.0 µg/µl) found in (a) Peak E and (b) Peak F in 10 % CH_3COOH. A molecular weight of 17,133 was obtained for both samples.

The molecular weight of Peaks E and F was determined by API to be 17,133. Subtracting the molecular weight of native MbHH (taking into account the loss of a proton upon binding of a_5Ru^{3+} to histidine) from this value gave a mass of 184. The additional mass of 184 of these derivatives is close to the mass of 186 expected for RuN_5H_{15}; thus, the mass spectrometry results are consistent with those found by uv-vis absorption spectroscopy in Chapter 2 since both techniques indicate that Peaks E and F are singly-modified a_5Ru^{3+} derivatives of MbHH.

Peptide Mapping by HPLC: The native and singly-modified MbHH in Peaks E and G were digested with trypsin and the resulting peptide fragments were separated by HPLC reverse phase chromatography. Figures 3.5 and 3.6 show the HPLC chromatograms, monitored at 210 nm to view the backbone separation, of the peptide fragments of native MbHH and Peaks E and G. The chromatograms monitored at 210 nm were similar in all cases. The peptide map of MbHH monitored at 300 nm (Figure 3.7) has three major bands. Peptide fragment 1 was eluted at 34.3 ml, while peptide fragment 2 was eluted at 64.3 ml. The third band at 109.0 ml was found to be composed of undigested protein and free heme. From amino acid analysis, peptide fragment 1 was found to be amino acid residues 12-16, while peptide fragment 2 was found to be residues 1-11; thus, it appears that MbHH was cleaved between Leu11 and Asn12 (Figure 3.1).

Figure 3.8(a) is the peptide map of Peak E monitored at 300 nm and four major bands are observed. Peptide fragments 1 and 2, and the third band composed of undigested protein and free heme, were all eluted at similar positions as in the map

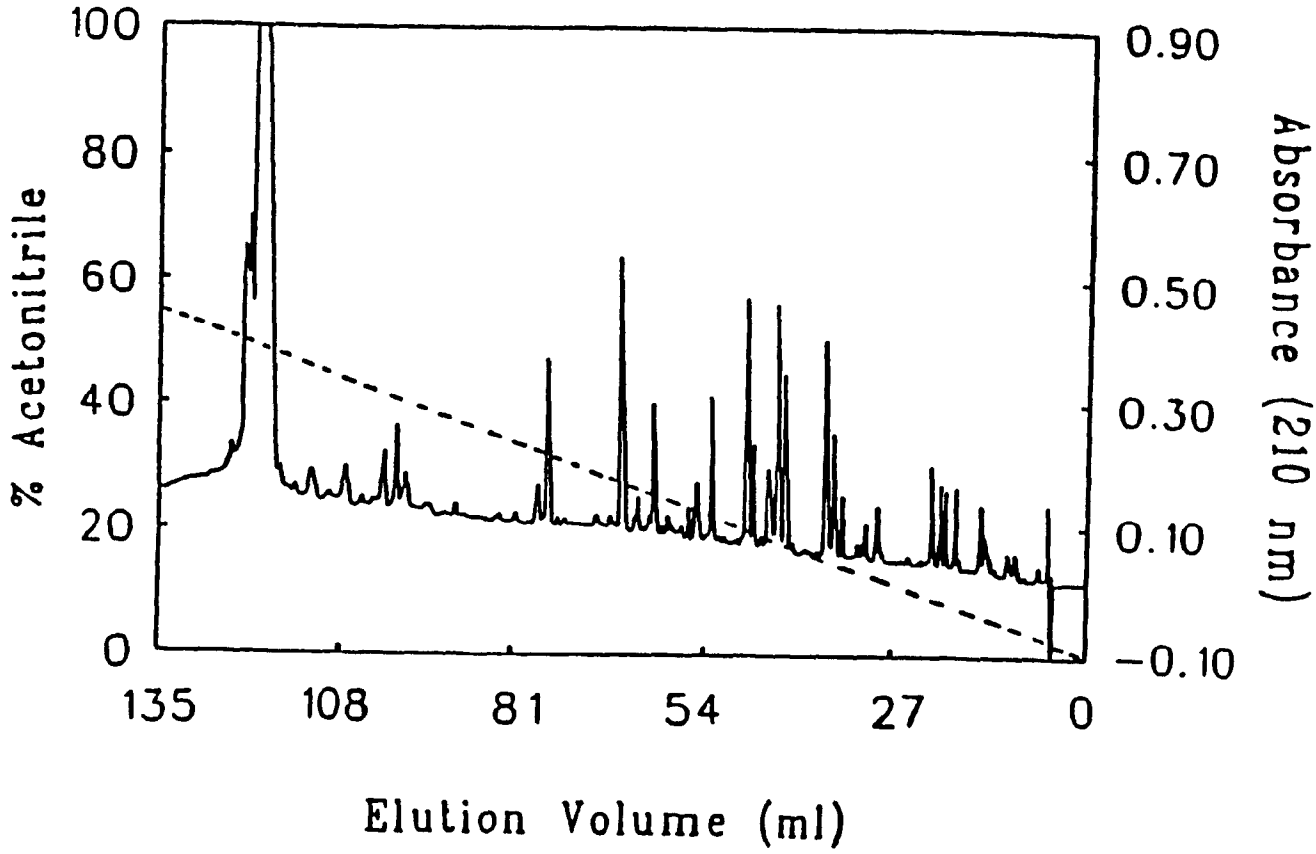

Figure 3.5: HPLC reverse phase chromatography of the tryptic digest of native horse heart myoglobin monitored at 210 nm. The ratio of protein to trypsin for the digest was 20:1 (w/w). Separation of the resulting peptide fragments was by a linear gradient of 0-55 % acetonitrile containing 0.1 % trifluoroacetic acid at a pH of 2.85 (dashed line). Sample concentration was 5 mg/ml and the injection volume was 100 µl. Flow rate was 1 ml/min.

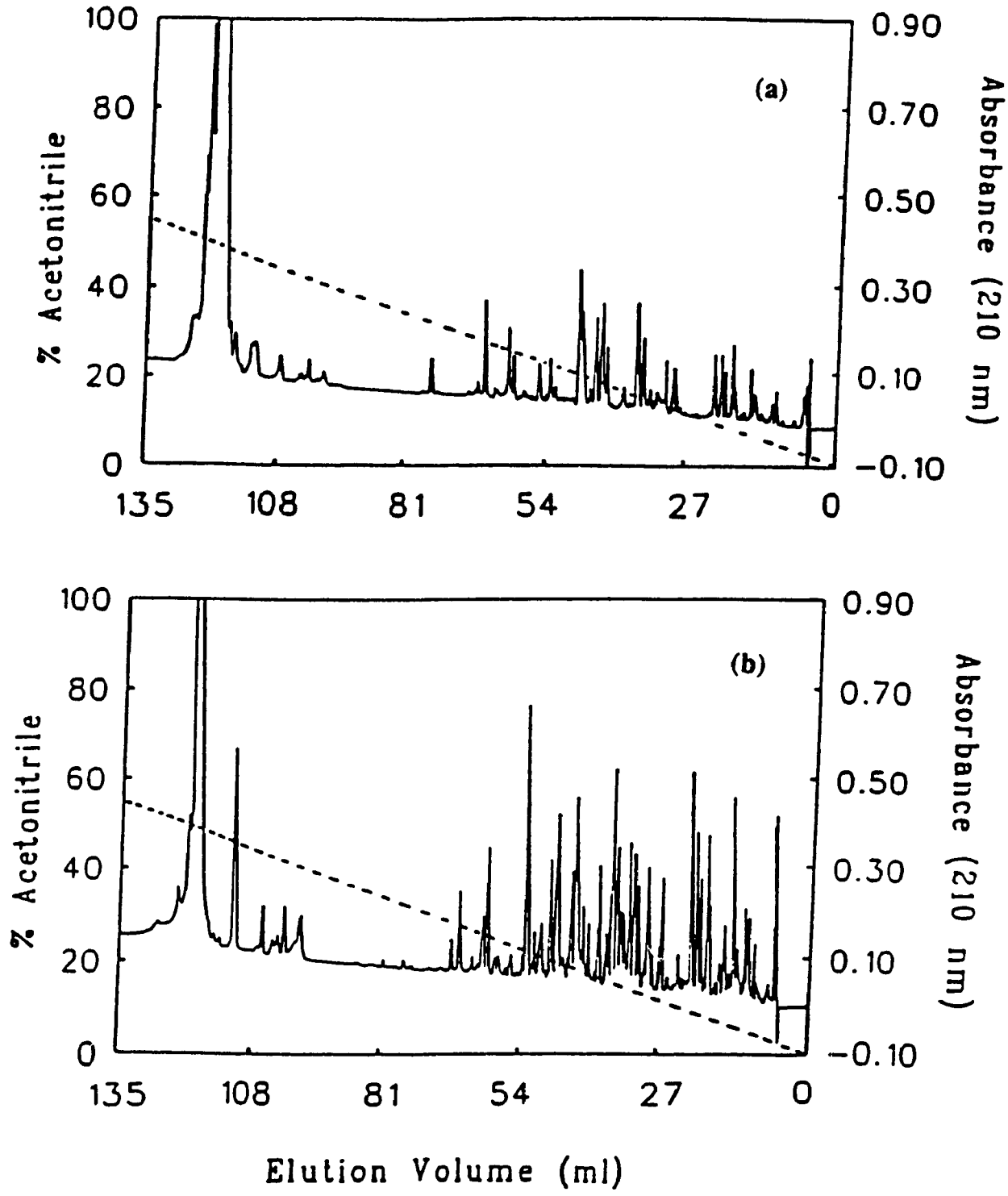

Figure 3.6: HPLC reverse phase chromatography of the tryptic digests of (a) Peak E and (b) Peak G. The experimental conditions were the same as those given in Figure 3.5.

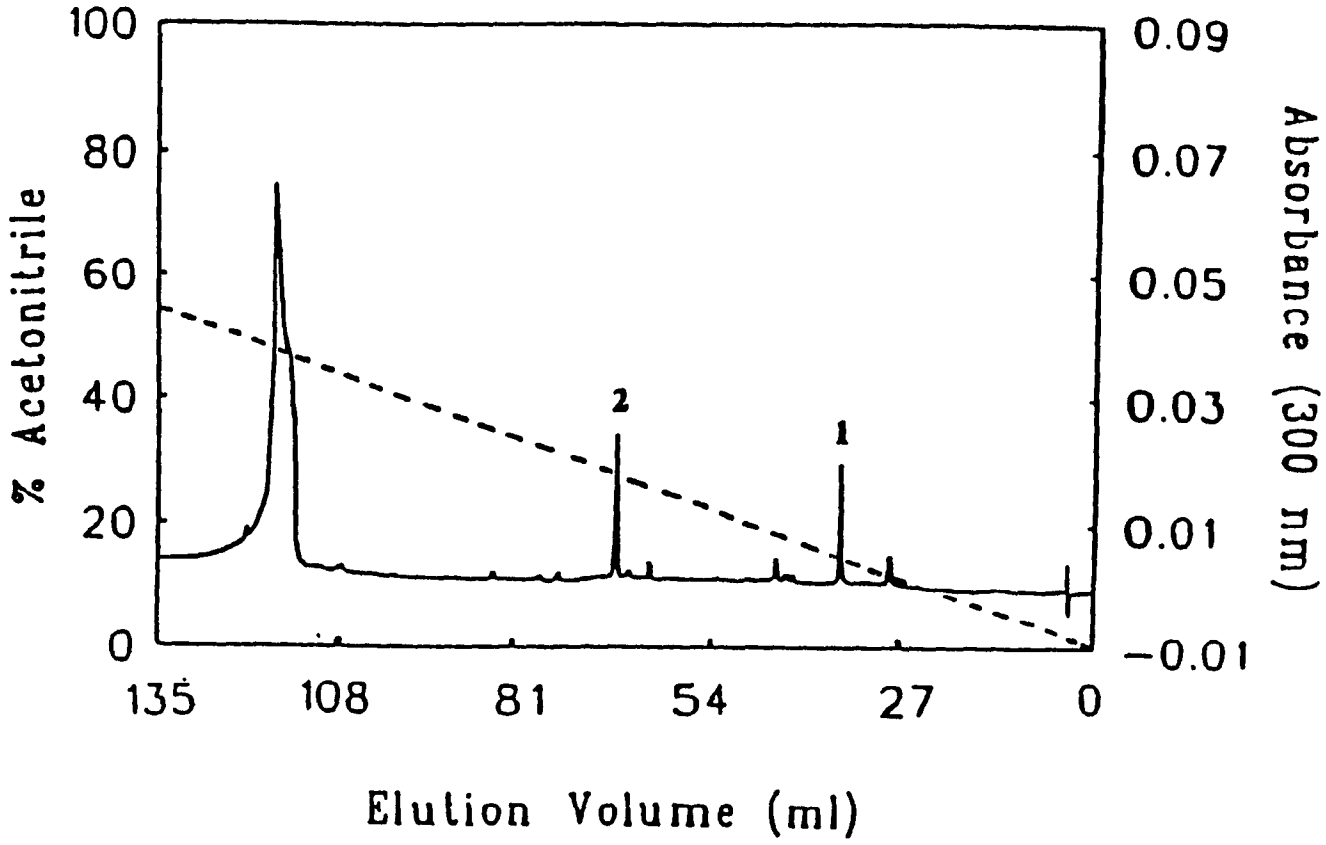

Figure 3.7: HPLC reverse phase chromatography of the tryptic digest of native horse heart myoglobin monitored at 300 nm. The conditions for the digestion of the protein and the separation of its peptide fragments are the same as those listed in Figure 3.5.

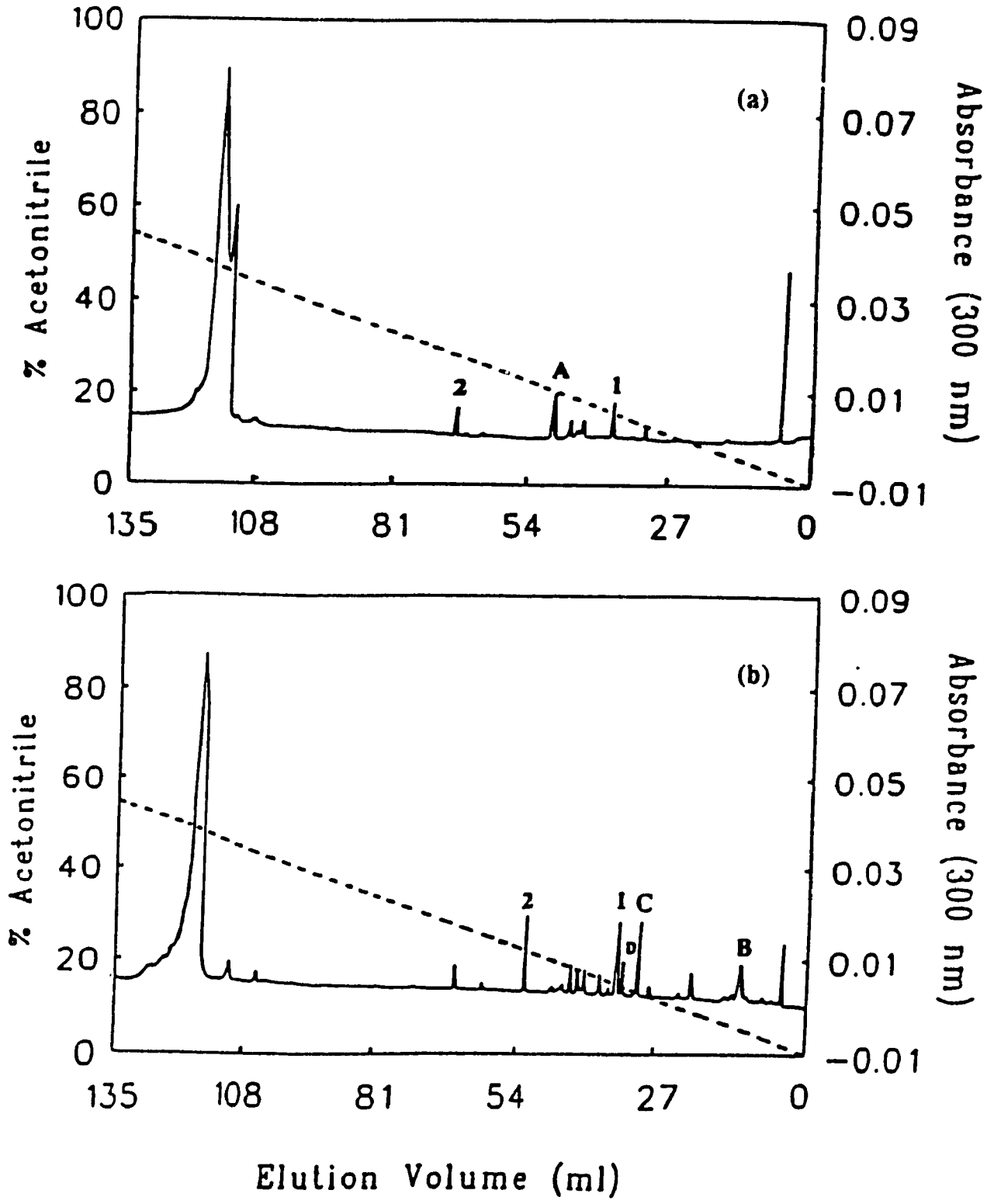

Figure 3.8: HPLC reverse phase chromatography of the tryptic digest of (a) Peak E and (b) Peak G. The experimental conditions are the same as those given in Figure 3.5.

Table 3.1: Amino Acid Analysis of Peptide Fragments Obtained from Tryptic Digests of Horse Heart Myoglobin, Peak E and Peak G

MbHH[a]	Peptide Fragments[b]	Amino Acid Residues[c]
Native MbHH	1	12-16
	2	1-11
Peak E	1	12-16
	2	1-11
	A	80-89
Peak G	1	12-16
	2	1-11
	B	48-50
	C	46-50 & 105-115
	D	46-49

[a]Peaks E and G from Figure 2.3.

[b]Peptide Fragments from Figures 3.7 and 3.8(a) & (b).

[c]See Figure 3.1 for sequence of MbHH.

of native protein (Figure 3.7). Amino acid analysis of peptide fragments 1 and 2 confirmed that these were the same fragments obtained for the digested native protein. A fourth peptide fragment, labelled A was eluted at 44.2 ml, and amino acid analysis showed that this fragment was residues 80-89. Peptide fragments 1 and 2 were also observed in the peptide map of Peak G [Figure 3.8(b)], but peptide fragment 2, which was confirmed by amino acid analysis to be residues 1-11, was eluted sooner (52.0 ml) than previously observed (64.3 ml). Additional peptide fragments, labelled B, C and D appeared in this chromatogram. Amino acid analysis determined that peptide fragment B was residues 48-50. Band C was found to consist of two peptide fragments, residues 46-50 and 105-115, and peptide fragment D was found to contain residues 46-49. A summary of the amino acid content of the peptide fragments labelled in Figures 3.7 and 3.8 is given in Table 3.1.

Mass Spectrometry of Peptide Fragments: API mass spectra were obtained for peptide fragments A and C from the tryptic digests of Peaks E [Figure 3.8(a)] and G [Figure 3.8(b)], respectively. The mass of peptide fragment A was found to be 1313.8 [Figure 3.9(a)]. Subtracting the mass of amino acid residues 80-89, gives a mass of 185.2 which corresponds to the mass change expected on binding a_5Ru, taking into consideration the loss of the histidine proton. The mass of peptide fragment C was 856.6 [Figure 3.9(b)]. Subtracting the mass of amino acid residues 46-50, also gives a mass of 185.2. Therefore, both peptide fragments A and C contain bound a_5Ru.

Differential Pulse Voltammetry (DPV): DPV was used to measure the

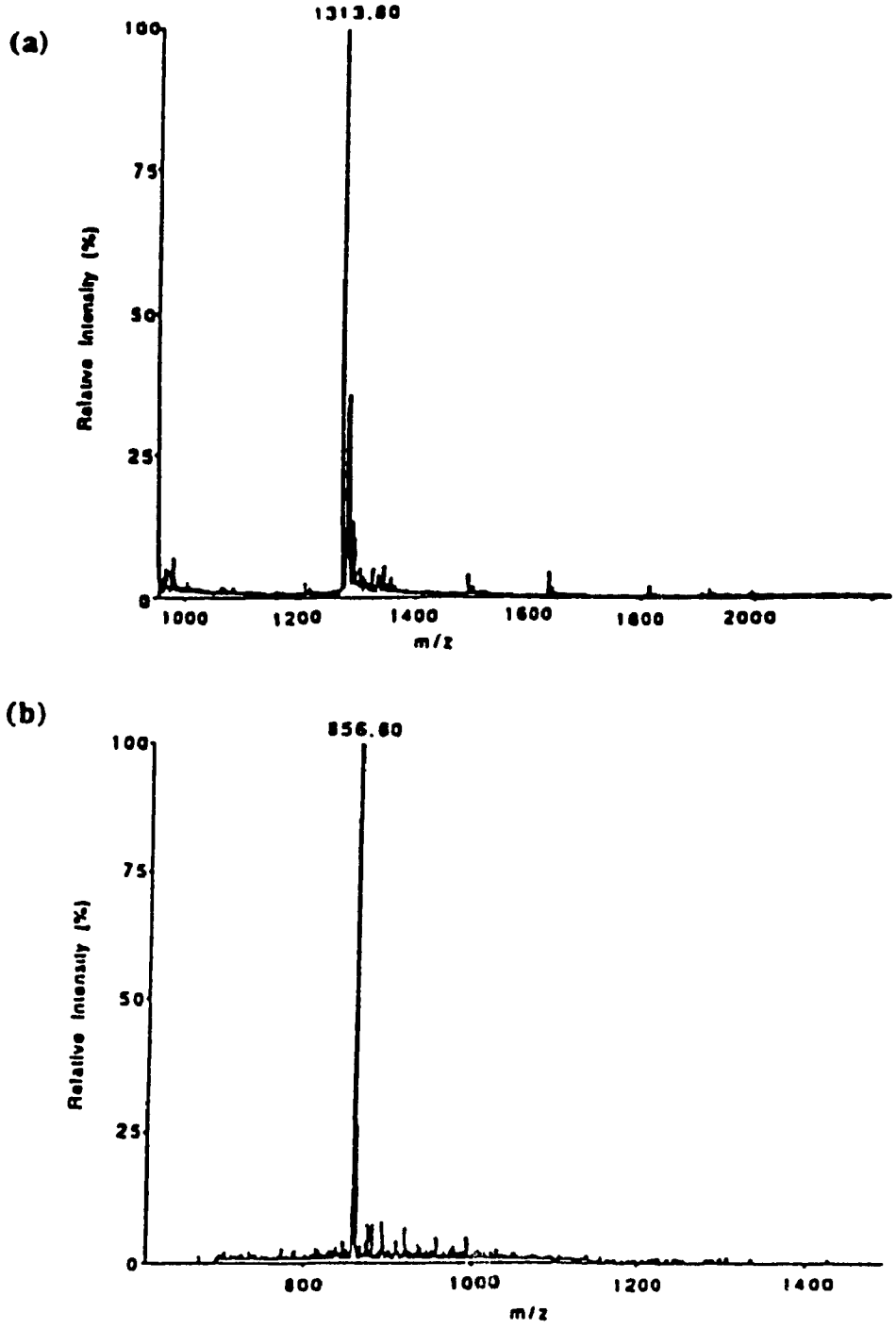

Figure 3.9: API mass spectra of (a) peptide fragment A from tryptic digest of Peak E and (b) peptide fragment C of the tryptic digest of Peak G (0.1 µg/µl) in 10 % CH_3COOH.

reduction potentials of free and MbHH-bound a_5Ru^{3+}(His) groups. The peak potentials (Ep) reported here can be converted to $E_{1/2}$ values by subtracting half the pulse amplitude (ie., 50 mV) from Ep. Voltammagrams of native MbHH (Figure 3.10) and of the redox promoter, 4,4'-dipyridyl (Figure 3.11) show no peaks indicating that these species are not electroactive under the present experimental conditions. Figure 3.12(a), (b) & (c) display the voltammagrams observed for Peaks E, F and G, respectively, and their Ep and peak currents are summarized in Table 3.2. Table 3.2 also gives the Ep of free a_5Ru^{3+}(His) and $Ru^{3+}(NH_3)_6$. The Ep of free a_5Ru^{3+}(His) is in good agreement with the reported value[5], but that of $Ru^{3+}(NH_3)_6$ is slightly lower than reported which is probably due to the different experimental conditions used here.[13] It can be seen that a_5Ru^{3+}(His), $Ru^{3+}(NH_3)_6$, and Peak E display more anodic peak potentials in the presence of the promoter.

3.4 Discussion

Characterization of the singly-modified ruthenium MbHH derivatives obtained from the reaction of $a_5Ru^{2+}(H_2O)$ with MbHH was carried out using peptide-mapping by HPLC, amino acid analysis, mass spectrometry and DPV. The sites of attachment of a_5Ru^{3+} on peaks E and G were identified by isolating and locating the ruthenium-containing peptide fragments. The binding of a_5Ru^{3+} to a histidine residue allows for the ready detection at ~ 300 nm of the derivatized peptide fragments. Amino acid analysis and mass spectrometry confirmed that peptide fragment A of Peak E [Figure 3.8(a)] was residues 80-89, while peptide fragments B, C and D of Peak G were

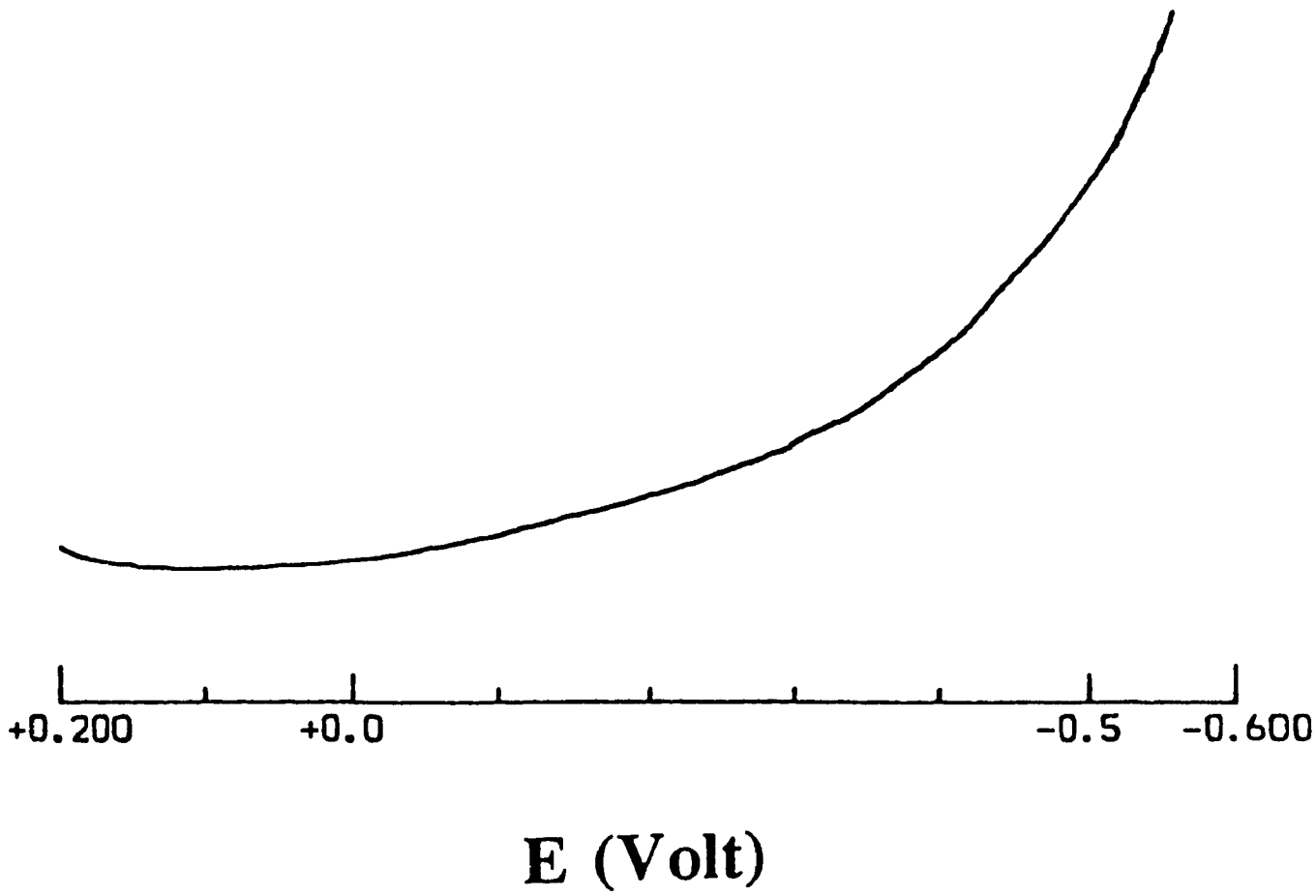

Figure 3.10: DPV of 10 mM 4,4'-dipyridyl in 0.1 M sodium phosphate buffer, pH 7.0. Experimental conditions: initial potential, 200 mV; final potential, -600 mV; scan speed, 2 mV/sec; pulse amplitude, 100 mV; sample width, 17 msec; pulse width, 57 msec; pulse period, 500 msec. These conditions were used for all DPV experiments.

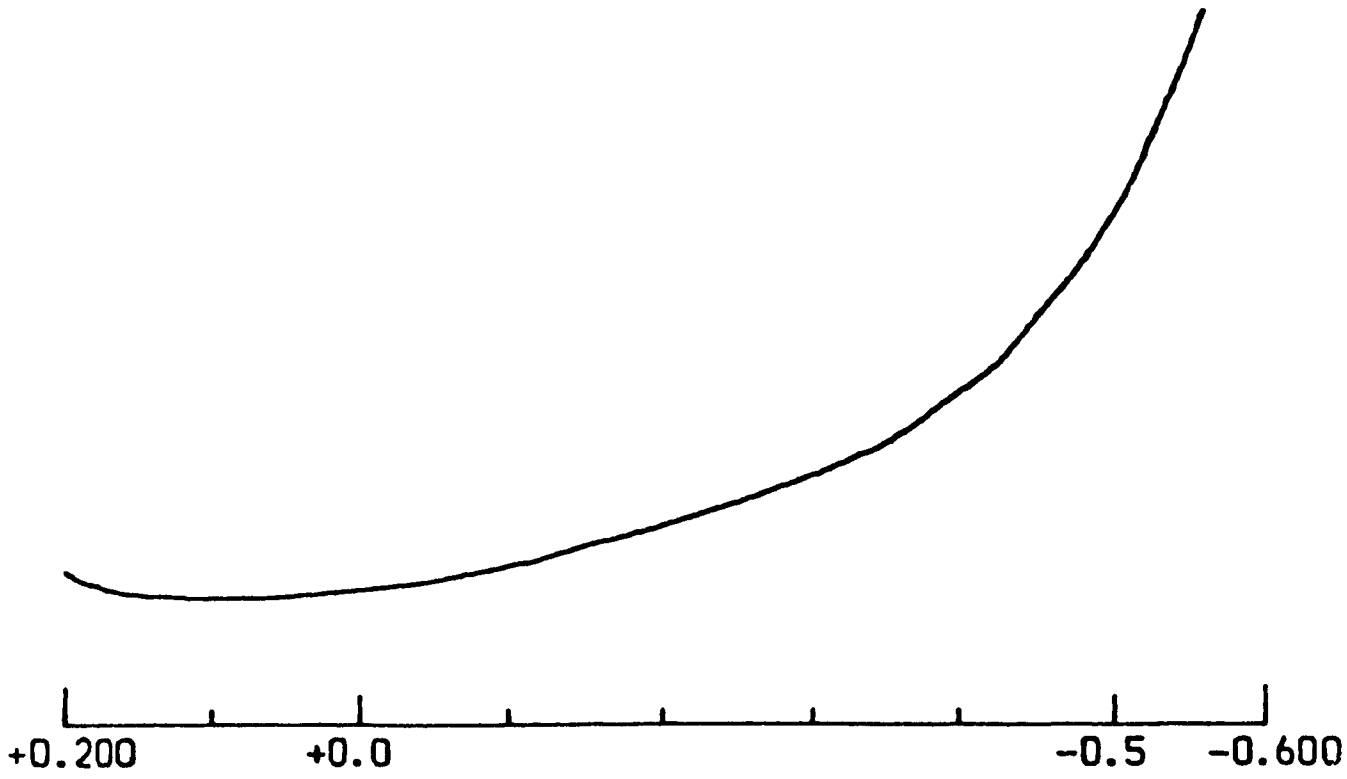

Figure 3.11: DPV of 100 μM of horse heart myoglobin in 0.1 M sodium phosphate buffer, pH 7.0, with 10 mM 4,4'-dipyridyl. The experimental conditions are given in Figure 3.10.

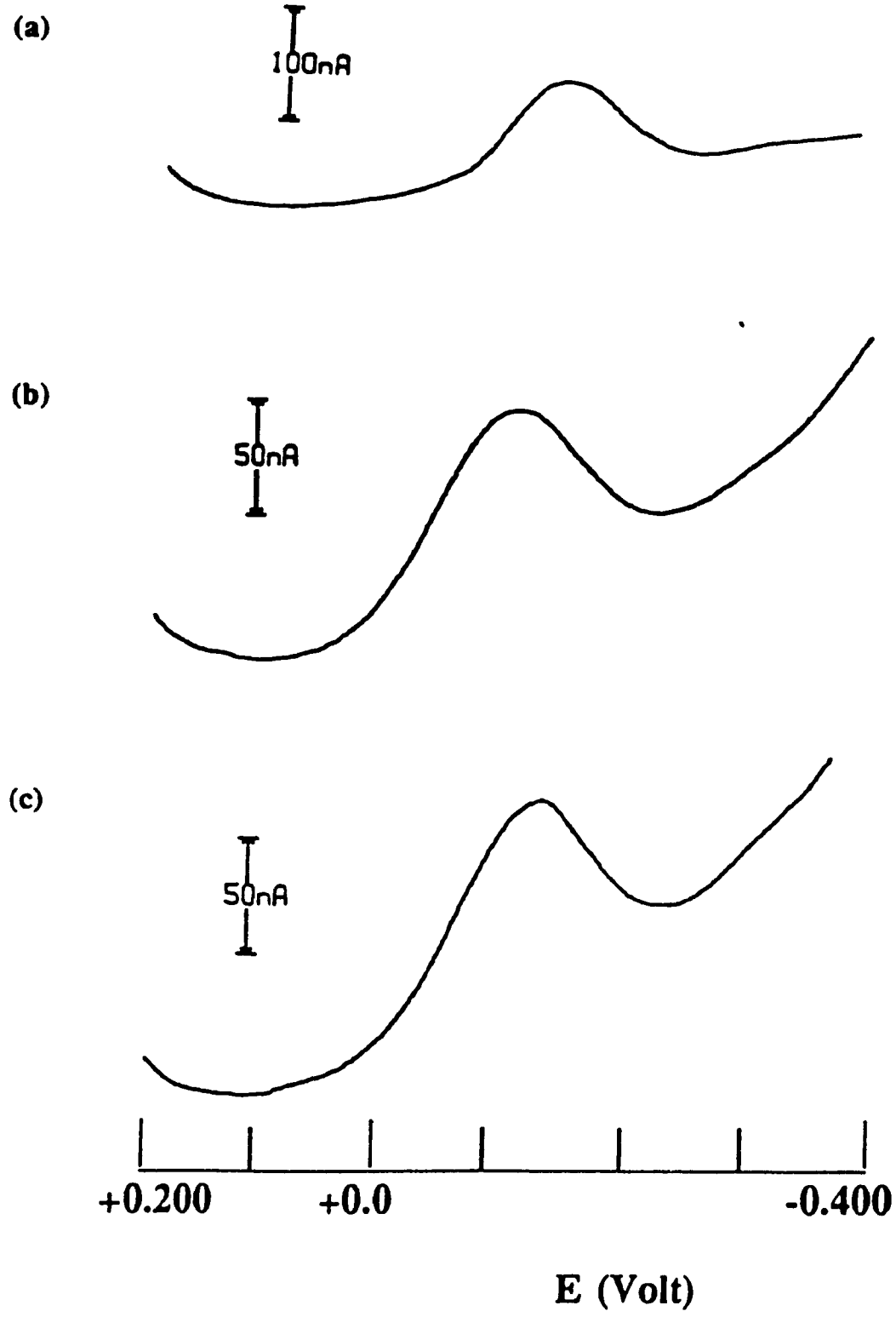

Figure 3.12: DPV of 50 μM (a) Peak E, (b) Peak F and (c) Peak G in 0.1 M sodium phosphate buffer, pH 7.0 containing 10 mM 4,4'-dipyridyl.

Table 3.2: Peak Potentials (Ep) and Peak Currents of a_5Ru^{3+}(His), $Ru^{3+}(NH_3)_6$ and the Singly-modified a_5Ru(His)MbHH Derivatives

Sample[a]	Ep (mV)[b]	Peak Current (A)[b]
a_5Ru^{3+}(His)	86 ± 0.5[d]	3.81×10^{-7}
	79 ± 2.0[c]	4.47×10^{-7}[c]
$Ru^{3+}(NH_3)_6$	34 ± 0.25	2.49×10^{-7}
	23 ± 3.0[c,e]	1.94×10^{-7}[c]
Peak E	47 ± 3	8.04×10^{-8}
	43 ± 11[c]	1.65×10^{-7}[c]
Peak F	76 ± 6	6.88×10^{-8}
Peak G	52 ± 4	7.22×10^{-8}

[a]Peaks E, G are MbHH derivatives modified at His81 and His48, respectively; Peak F is probably a_5Ru(His116)MbHH but this was not confirmed here.

[b]Ep (vs. NHE) and peak currents are averages of 4-8 measurements using 50 μM sample in 0.1 M sodium phosphate, pH 7.0, with 10 mM 4,4'-dipyridyl.

[c]Ep and peak currents measured in the absence of 4,4'-dipyridyl.

[d]Ep = 85.8 ± 2 mV (vs. NHE) was reported for a_5Ru^{3+}(His) in 0.1 M sodium phosphate, pH 7.0 with 10 mM 4,4'-dipyridyl (Ref. 5).

[e]Ep = 50 mV (vs. NHE) was reported for $Ru^{3+}(NH_3)_6$ in 0.1 M p-toluenesulfonic acid/ 0.1 M potassium p-toluenesulfonate (Ref. 13).

residues 48-50, 46-50 and 46-49 [Figure 3.8(b)]. Thus, the peptide mapping results reveal that Peak E has a_5Ru^{3+} attached to His81, and Peak G has a_5Ru^{3+} attached to His48. Since there are three surface exposed histidine residues in MbHH, and it is known from mass spectrometry (Figure 3.4) that Peak F has the same mass as Peak E, we predict that Peak F is a_5Ru(His116)MbHH. Support for this comes from uv-vis absorption spectra reported in Chapter 2, and future peptide mapping shou'd confirm this prediction. Attachment of a_5Ru^{3+} to His48, His81 and His116 in MbHH is consistent with published results for MbSW,[5,6] and is also consistent with the location and exposure of these histidines in MbHH observed by computer graphics [Figure 2.1(b) and 2.2].

Peptide fragments are eluted from a reverse phase column in order of increasing size and hyrophobicity.[14] Consistent with this expectation, the peptide map of native MbHH (Figure 3.7) shows that peptide fragment 1 (residues 12-16) is eluted before peptide fragment 2 (residues 1-10). However, contrary to expectation, trypsin, although TPCK-treated, showed chymotrypsin-like activity since it cleaved native MbHH after Leu11 (Figure 3.1) yielding peptide fragments 1 and 2.[14] Autoproteolysis of trypsin, which could be due to the high trypsin content used for digestion (20:1 ratio of MbHH to trypsin), gives ψ trypsin which has chymotrypsin-like activity.[15] Appearance of peptide fragments A and D is also consistent with ψ trypsin activity. Since Peak G was modified at His48, which should inhibit tryptic cleavage at Lys47 more than at Lys50, peptide fragment C had the highest relative intensity of the a_5Ru-labelled peptide fragments of Peak G.

DPV was used to measure the reduction potentials of free and MbHH-bound a_5Ru^{3+}(His) complexes. DPV was chosen over other electrochemical methods, such as cyclic voltammetry, because it is more sensitive and has lower detection limits. Ruthenium complexes bound to proteins undergo reversible electron transfer[7] in the presence or absence of redox promoters. The redox promoter presumably acts by adsorbing to the gold electrode surface and thereby forming a monolayer of 4,4'-dipyridyl,[7] which provides a suitable interface for interaction with the modified MbHH. An illustration of the proposed electrode-promoter-protein interaction can be seen in Figure 3.13. For cytochrome c, it has been proposed that hydrogen bonding occurs between lysine residues of the protein and the pyridyl nitrogens at the modified electrode surface.[16] This is believed to orient the protein to facilitate rapid electron transfer to and from the heme group, while preventing irreversible adsorption and denaturation of the protein on the electrode surface. However, native MbHH, which has an Ep = 58 mV,[5] was not electroactive in the presence of the promoter (Figure 3.11) indicating that MbHH may not be suitably oriented for electron transfer between the heme and the electrode under these conditions. Table 3.2 summarizes the Ep and peak currents obtained for free and MbHH-bound a_5Ru^{3+}(His) complexes and $Ru^{3+}(NH_3)_6$. The potentials are increased and have smaller standard deviations in the presence of the promoter, suggesting that hydrogen bonding may be occurring between the ammine groups of a_5Ru^{3+} and $Ru^{3+}(NH_3)_6$, and the pyridyl nitrogens of the promoter.

The Ep values obtained for ruthenated MbHH and MbSW are compared in

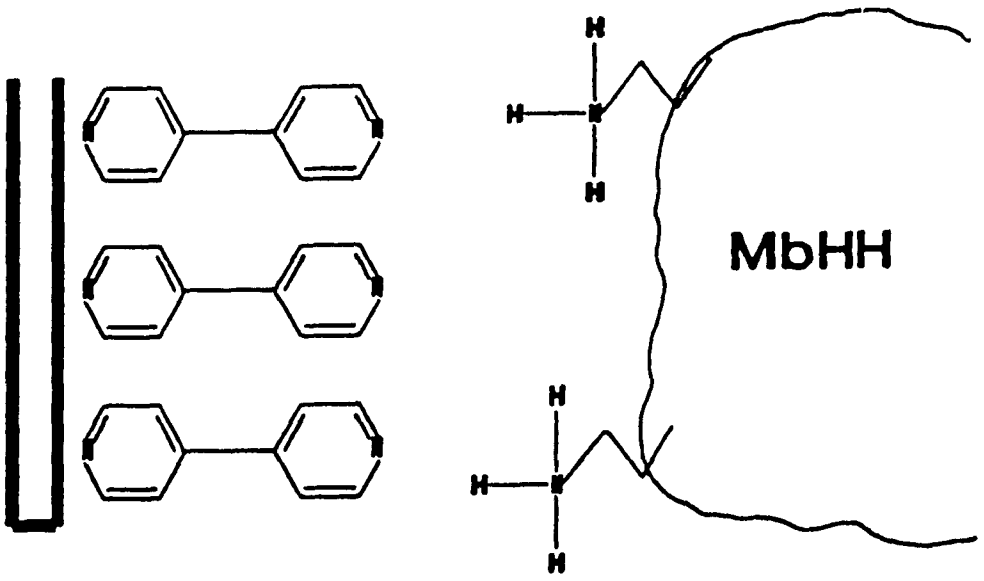

Figure 3.13: Illustration of the protein-promoter-electrode complex of horse heart myoglobin, 4,4'-dipyridyl and the gold electrode.

Table 3.3: Comparison of Eps of Ru^{3+}/Ru^{2+} for a_5Ru(His)MbSW and MbHH Derivatives

Mb Species	MbSW[a] Ep (mV vs. NHE)	MbHH[b] Ep (mV vs. NHE)	Δ Ep (MbSW - MbHH)
a_5Ru(His48)	85	52 ± 4	33
a_5Ru(His81)	61	47 ± 3 43 ± 11[c]	14
a_5Ru(His116)	70	76 ± 6[d]	-6
a_5Ru(His12)	75	-	-

[a]Data for MbSW from Ref. 17.

[b]Data from Table 3.2.

[c]Ep in absence of 10 mM 4,4'-dipyridyl.

[d]Modification of His116 was not confirmed here (see text).

Table 3.3. The variations in Ep could be due to different microenvironments surrounding each of the histidines. The ΔEp value (Ep MbSW - Ep MbHH) is relatively small for His116, while the large ΔEp for His48 (Table 3.2) suggests that this residue is more exposed in MbSW than in MbHH since Ep for a_5Ru(His48)MbSW is identical to that obtained for free a_5Ru^{3+}(His) (Table 3.2).

This chapter has presented results of the full characterization of the a_5Ru(His48)MbHH and a_5Ru(His81)MbHH derivatives. These species can now be used in future electron transfer studies.

3.5 References:

1) Fox, T. "Studies on Enzyme Intermediates of Yeast Cytochrome *c* Peroxidase" Ph.D. Thesis, Concordia University, **1991**.

2) Yocom, K. M.; Shelton, J. B.; Shelton, J. R.; Schroeder, W. A.; Worosila, G.; Isied, S. S.; Bordignon, E.; Gray, H. B. *Proc. Natl. Acad. Sci. USA* **1982**, *79*, 7052.

3) Osvath, P.; Salmon, G. A.; Sykes, A. G. *J. Am. Chem. Soc.* **1988**, *110*, 7114.

4) Margalit, R.; Kostić, N. M.; Che, C-M.; Blair, D. F.; Chaing, H-J.; Pecht, I.; Shelton, J. B.; Shelton, J. R.; Schroeder, W. A.; Gray, H. B. *Proc. Natl. Acad. Sci. USA* **1984**, *81*, 6554.

5) Crutchley, R. J.; Ellis, W. R.; Gray, H. B. *Frontiers in Bioinorganic Chemistry*; Xavier, A. V., Ed.; VCH, **1968**, 679.

6) Karas, J. L." Long-Range Electron Transfer in Ruthenium-Labelled Myoglobin" Ph.D. Thesis, California Institute of Technology, **1989**.

7) Armstrong, F. A.; Hill, H. A. O.; Walton, N. *J. Acc. Chem. Res.* **1988**, *21*, 407.

8) Yocom, K. M.; Winkler, J. R.; Nocera, D. G.; Gray, H. B. *Chemica Scripta* **1983**, *21*, 29.

9) Bechtold, R.; Gardineer, M. B.; Kazmi, A.; van Hemelryck, B.; Isied, S. S. *J. Phys. Chem.* **1986**, *90*, 3800.

10) Carver, J. A. & Bradbury, J. H. *Biochem.* **1984**, *23*, 4890.

11) Glazer, A. N.; DeLange, R. J.; Sigman, D. S. *Chemical modification of proteins. Selected methods and analytical procedures* Elsevier, New York, **1975**.

12) Zaia, J.; Annan, R. S.; Biemann, K. *Rapid Commun. Mass Spectrom.* **1992**, *6*, 32.

13) Matsubara, T. & Ford, P. C. *Inorg. Chem.* **1976**, *15*, 1107.

14) Darbre, A. Practical Protein Chemistry: A Handbook John Wiley & Sons, Great Britain, **1986**.

15) Keil-Dlouhà, V.; Zylba, N.; Imhoff, J.-M.; Tong, N.-T.; Keil, B. *FEBS Lett.* **1971**, *16*, 291.

16) Eddowes, M. J. & Hill, H. A. O. *J. Chem. Soc.* **1979**, *101*, 7113.

17) Cowan, J. A.; Upmacis, R. K.; Beratan, D. N.; Onuchic, J. N.; Gray, H. B. *Ann. New York Acad. Sci.* **1988**, *550*, 68.

4.0 Physical Properties of Peroxide-Oxidized Myoglobins

4.1 Introduction

As discussed in Chapter 1, myoglobin, whose main role is as an oxygen storage protein,[1] will also react with peroxides.[2] The ferric form of myoglobin (Fe^{III}-Mb) will bind peroxide at the iron atom resulting in the formation of ferryl iron and an unstable radical (X°) on the Mb polypeptide:[3]

$$Fe^{III}\text{-heme} + H_2O_2 + 2H^+ \rightarrow X°Fe^{IV}\text{-heme} + 2H_2O \qquad (4.1)$$

The ferrous form (Fe^{II}-Mb) will also bind peroxide to form a ferryl iron:

$$Fe^{II}\text{-heme} + H_2O_2 + 2H^+ \rightarrow Fe^{IV}\text{-heme} + 2H_2O \qquad (4.2)$$

These two-electron reductions of peroxide by Mb are similar to the reactions of peroxide with the Fe^{III} and Fe^{II} forms of CCP.[4] Since Compound I and Compound II of CCP contain $X°Fe^{IV}$-heme and Fe^{IV}-heme species, respectively, these forms of Mb will therefore be given the same designation, Cpd I-Mb and Cpd II-Mb.

Cpd I-Mb acts as a potent oxidant and has been linked to oxidative degradation in tissues.[5] Electron paramagnetic resonance (EPR) studies provide evidence for radical formation following the reaction of both sperm whale myoglobin (MbSW) and horse heart myoglobin (MbHH) with peroxide.[3,6] An EPR instrument was unavailable

for the present work, so kinetics of formation and decay of the radical species in Cpd I-Mb could not be monitored. However, for electron transfer studies, it is important to determine if formation, migration and quenching of the protein radical (X°) formed in Reaction 4.1, alters the polypeptide.

There are three tyrosine residues (Tyr103, Tyr146, Tyr151) in MbSW [Figure 4.1(a)], while only two (Tyr103, Tyr146) are present in MbHH [Figure 4.1(b)]. A peptide with covalently-bound heme was isolated from the tryptic digest of Cpd I-MbHH formed by Reaction 4.1 at pH 7.4, and amino acid analysis indicated loss of one tyrosine residue.[10] The close proximity of Tyr103 to the heme (3 Å) would permit intramolecular crosslinking of these groups on tyrosyl radical formation; thus, Tyr103 is a proposed site of X° formation in MbHH.

SDS-PAGE experiments have shown H_2O_2-induced dimerization in MbSW, but not in MbHH.[11] Intermolecular crosslinking of Tyr103 and Tyr151 has been identified by chymotryptic digestion and peptide sequencing of the protein.[11] Crosslinking is purportedly between Tyr103 of one MbSW molecule and Tyr151 of another MbSW molecule,[11] and studies of MbSW mutants have shown that Tyr151 is an essential residue for formation of protein dimers.[12]

Aromatic residues fluoresce when excited by ultraviolet light, but it has been observed that tyrosine and phenylalanine fluorescence is efficiently quenched by excited-state energy transfer to tryptophan, such that protein emission is dominated by tryptophan fluorescence.[13] It has been well documented that heme is a highly efficient quencher of protein fluorescence.[14,15] Protein unfolding relieves heme quenching of

Figure 4.1: Computer graphics display of the spatial relationships between the Tyr residues and the heme moiety in **(a)** MbSW[7] and **(b)** MbHH[8] obtained from their crystal structure. The closest ring carbon of Tyr103 is ≈ 3 Å from the heme vinyl group in both cases. Molecular graphics images were produced using the MidasPlus software system from the Computer Graphics Laboratory, UCSF.[9]

(a)

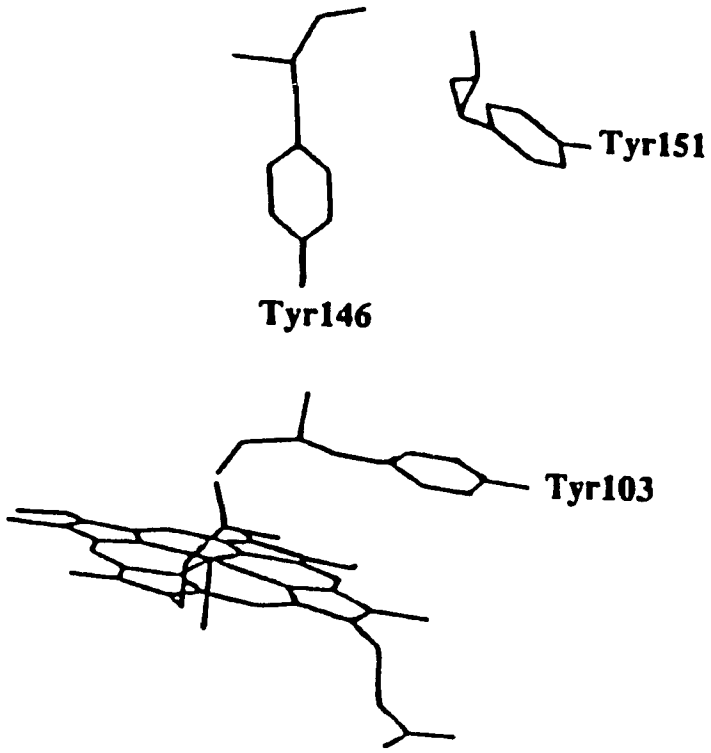

(b)

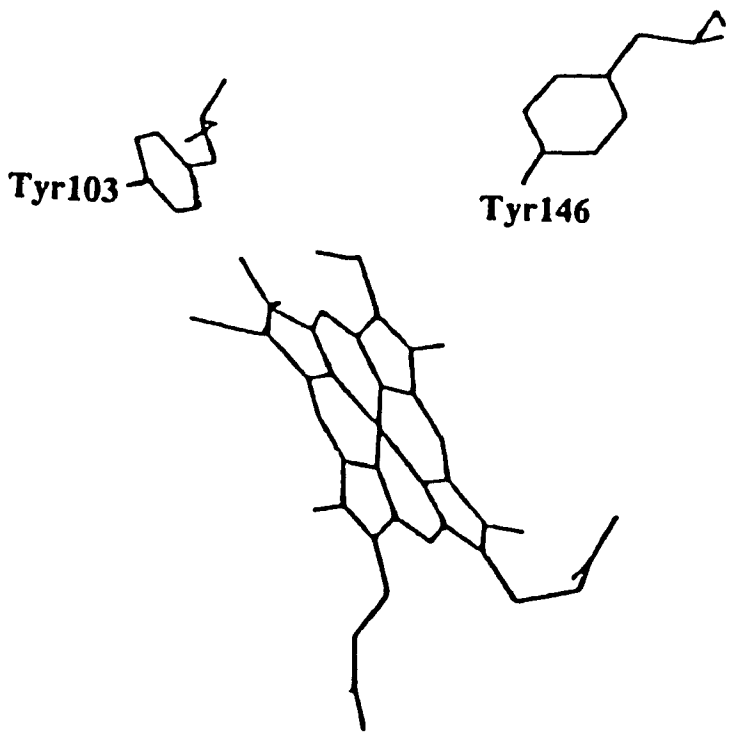

tryptophan fluorescence, and exposes these residues to the solvent. There are two tryptophan residues in both MbHH[8] and MbSW[7] with Trp14 being 13 Å and Trp7 being 19 Å from the centre of the heme. Consequently, a fluorescence quantum yield of < 1% relative to free Trp has been reported for Mb.[14] Monitoring Trp fluorescence intensity under denaturing conditions should indicate if H_2O_2-induced loss of Trp occurs in Mb or if internal crosslinking exists between the heme and adjacent residues in Cpd I-Mb. There has been no reported H_2O_2-induced loss of Trp in Mb, presumably because of the larger distances (13-20 Å) between these residues and the heme. However, intramolecular crosslinking should inhibit unfolding of the polypeptide and prevent relief of fluorescence quenching by the heme. Steady-state protein fluorescence in the presence and absence of 8 M urea and 6 M guanidine-hydrochloride (both strong denaturants) is used here to probe modification of the polypeptide.[16] Investigation of the unfolding of Cpd II-MbHH, which lacks the X°, should reveal the effects of radical formation, if any, on the polypeptide.

This chapter reports the kinetics of formation and decay of the ferryl centres in Cpd I-Mb which were followed spectrophotometrically.[2] Formation of Cpd I-Mb was carried out in 50 mM sodium borate buffer at pH 8.5, because at this pH the formation of Cpd I-MbHH was unattended by oxidative side reactions affecting the porphyrin ring[2] and also the ferryl heme is stable, which is required for electron transfer studies. The results of steady-state Trp fluorescence and Soret absorption measurements on Fe^{III}-Mb, Cpd I-Mb and Cpd II-MbHH in the presence and absence of 8 M urea and 6 M guanidine-hydrochloride are also reported. Monitoring the Soret

maxima of Fe^{III}-Mb, Cpd I-Mb and Cpd II-MbHH under denaturing conditions provides information on the coordination state of the heme iron and the nature of the heme environment. SDS-PAGE was used to assess Cpd I-MbSW dimerization and the acidic butanone method was used to determine if the heme moiety can be removed from Cpd I-MbHH.

4.2 Experimental

4.2.1 Materials

Horse heart myoglobin and guanidine-hydrochloride (Gdn-HCl) were obtained from Sigma and used without further purification. Sperm whale myoglobin (originally from Sigma) was a generous gift from Professor H. B. Gray at Caltech. Analytical grade urea, analytical grade hydrogen peroxide (30% w/v), 2-butanone and boric acid were purchased from Anachemia, ACP, Aldrich and Shawinigan, respectively. Buffers were prepared with nanopure, glass distilled water. Sodium dodecyl sulfate polyacrylamide gel electrophoresis (SDS-PAGE) was performed on precast 12% single percentage Tris-HCl gels using a Mini Protean II Electrophoresis Dual Slab Cell purchased from Bio-Rad. Proteins on gels were visualized using a Bio-Rad silver staining system. Fluorescence measurements were carried out on a Shimadzu Model RF 5000 spectrofluorometer. All absorbance measurements were performed on a Hewlett Packard 8451A diode array spectrophotometer.

4.2.2 Methods

Formation of Cpd I-Mb: Stock solutions of 5 μM ferric MbHH (ε_{408} = 188 $mM^{-1}cm^{-1}$)[17] and ferric MbSW (ε_{409} = 157 $mM^{-1}cm^{-1}$)[18] were prepared in 50 mM sodium borate buffer at pH 8.5. A 20 mM stock H_2O_2 solution was prepared from 30% (w/v) H_2O_2 in the same buffer. Loss of Fe^{III}-Mb was monitored at 410 nm following rapid manual mixing of 5.0 μl stock peroxide and 1.0 ml stock Mb in a semi-micro cuvette. This gave a molar ratio of peroxide to protein of 20:1. Formation of Cpd I-Mb was monitored simultaneously at 422 nm.

Formation of Cpd II-MbHH: Solutions of Fe^{III}-MbHH and dithionite were purged for 1 h under argon prior to use. A 5 μM stock solution of ferrous MbHH was prepared by titrating a solution of Fe^{III}-MbHH with a freshly-prepared solution of 0.1 M dithionite ($Na_2S_2O_4$) under argon. Careful titration allowed Fe^{II}-MbHH to be prepared with no excess dithionite. Absorption spectroscopy was used to monitor the shift in the Soret band from 410 nm to 434 nm upon Mb reduction with dithionite, and the concentration of Fe^{II}-MbHH was determined spectrophotometrically (ε_{435} = 121 $mM^{-1}cm^{-1}$).[19] The stock peroxide solution was purged under argon for 30 min prior to use, and a 20:1 ratio of peroxide to protein was used to form Cpd II-MbHH. The addition of peroxide to Fe^{II}-MbHH was done under argon and monitored by absorption spectroscopy. Cpd II-MbHH has a Soret maximum at 422 nm.

Steady-State Protein Fluorescence: Following excitation at 280 nm, the fluorescence emission of 1 μM Fe^{III}-Mb, Cpd I-Mb and Cpd II-MbHH was monitored in the range of 300-450 nm in the presence and absence of 8 M urea and 6 M Gdn-

HCl at pH 8.5. Solutions of 1 μM Cpd I-MbSW, Cpd I-MbHH and Cpd II-MbHH were added to the denaturants 3 min after their mixing with 20-fold excess peroxide. Excitation and emission slits were 5 nm and the Raman peak of water was subtracted from all emission spectra. Inner-filter effects were corrected using the formula:[13]

$$F_c = F \text{ Antilog}[(A_{ex} + A_{em})/2]$$

where F_c is the corrected fluorescence intensity, F the measured intensity, A_{ex} the absorbance of the solution at the excitation wavelength, and A_{em} the absorbance at the emission wavelength.

Spectral Shifts of the Soret Bands: The Soret bands of Fe^{III}-Mb, Cpd I-Mb and Cpd II-MbHH were monitored after 40 min in the presence and absence of the denaturants at pH 8.5 to observe shifts in the Soret maxima.

SDS-PAGE of Fe^{III}-Mb and Cpd I-Mb: Crosslinking of Cpd I-Mb, formed on the addition of 20-fold molar excess of H_2O_2 to 5 μM Fe^{III}-Mb in 50 mM sodium borate buffer (pH 8.5), was investigated by SDS-PAGE. At various time intervals (3 min, 60 min and 24 h), following addition of H_2O_2, 10 μl of Mb were added to 40 μl of 10% (w/v) SDS. The samples were allowed to stand for 30 min in SDS and boiled for 5 min prior to loading on the gel.[20] The total amount of protein loaded onto the gel was 0.85 μg in 25 μl.

Removal of MbHH Heme by the Acidic Butanone Method:[10] A stock solution of 10 μM Fe^{III}-MbHH was prepared in 50 mM sodium borate buffer, pH 8.5 and cooled to 0 °C. The solution was acidified to pH 1.5 with 5 N HCl and four volumes of cold (-10 °C) 2-butanone were rapidly added to the solution. The mixture

was shaken and the organic layer was removed. This extraction step was repeated twice. The same procedure was carried out on Cpd I-MbHH 3 min after mixing with 20-fold peroxide.

4.3 Results

Kinetics of Cpd I-Mb Formation: Distinctive Soret maxima appear at 410 nm for Fe^{III}-Mb and 422 nm for Cpd I-Mb (Figure 4.2); thus, the formation of the ferryl heme of Cpd I-MbSW and Cpd I-MbHH can be followed spectrophotometrically. Both myoglobins display pseudo-first-order kinetics for the formation of Cpd I in the presence of 20-fold excess peroxide at room temperature in 50 mM sodium borate buffer, pH 8.5. Under these conditions, half-lives of formation of Cpd I were 9.8 s for MbSW and 34.1 s for MbHH, while half-lives of decay of Fe^{III}-Mb were 11.5 s for MbSW and 40.2 s for MbHH; thus MbSW forms the ferryl species, more readily than MbHH (Figure 4.3).

Unfolding of Fe^{III}-Mb, Cpd I-Mb and Cpd II-MbHH: Fluorescence was used to monitor the extent of unfolding of Fe^{III}-Mb, Cpd I-Mb and Cpd II-MbHH after 40 min exposure to 8 M urea and 6 M Gdn-HCl (Table 4.1). Absorption spectra were taken of the myoglobins after 40 min exposure to the denaturants in order to monitor shifts in the Soret maxima.

Fe^{III}-MbHH: A 15-fold increase in fluorescence intensity was observed for Fe^{III}-MbHH in 8 M urea and 6 M Gdn-HCl relative to that in buffer (Table 4.1); thus quenching of steady-state Trp fluorescence by the heme is significantly reduced in the

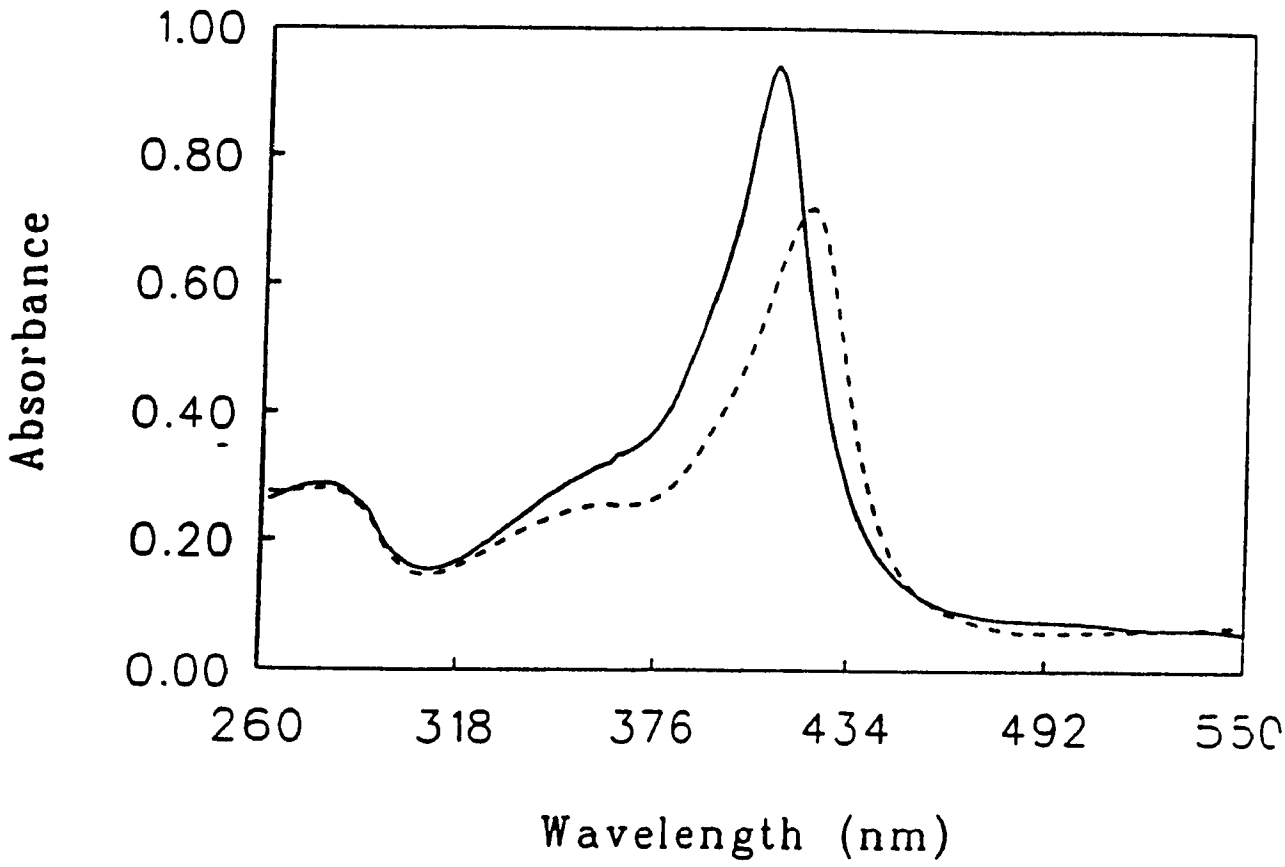

Figure 4.2: Absorption spectra of 5.0 μM Fe^{III}-MbHH (solid line) and Cpd I-MbHH (dashed line) in 50 mM sodium borate buffer, pH 8.5. The Soret maxima of Fe^{III}-Mb is at 410 nm, while that of Cpd I-Mb is at 422 nm. The ratio of peroxide to Mb was 20:1.

Figure 4.3: Semi-log plot of the ratio (ΔA) of the absorbance change at time, t ($\Delta A_t = A_t - A_\infty$) to the total absorbance change ($\Delta A_0 = A_0 - A_\infty$) vs. time for **(a)** MbHH and **(b)** MbSW. A_∞ was calculated by the Guggenheim method. The absorbance decrease due to decay of Fe^{III}-Mb was monitored at 410 nm (open circles), and the absorbance increase due to formation of Cpd I-Mb was monitored at 422 nm (closed circles). From these plots, half-lives of 9.8 and 34.1 s were obtained for Cpd I-MbSW and Cpd I-MbHH formation; and 11.5 and 40.2 s for Fe^{III}-MbSW and Fe^{III}-MbHH decay.

(a)

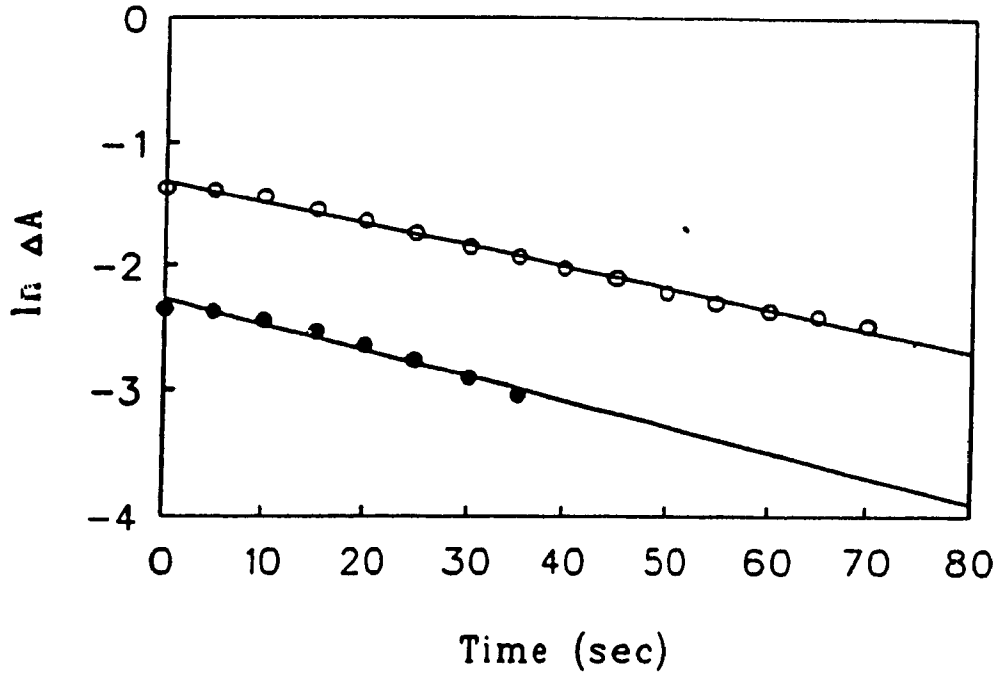
0
−1
−2
−3
−4
ln ΔA
0
10
20
30
40
50
60
70
80
Time (sec)

(b)

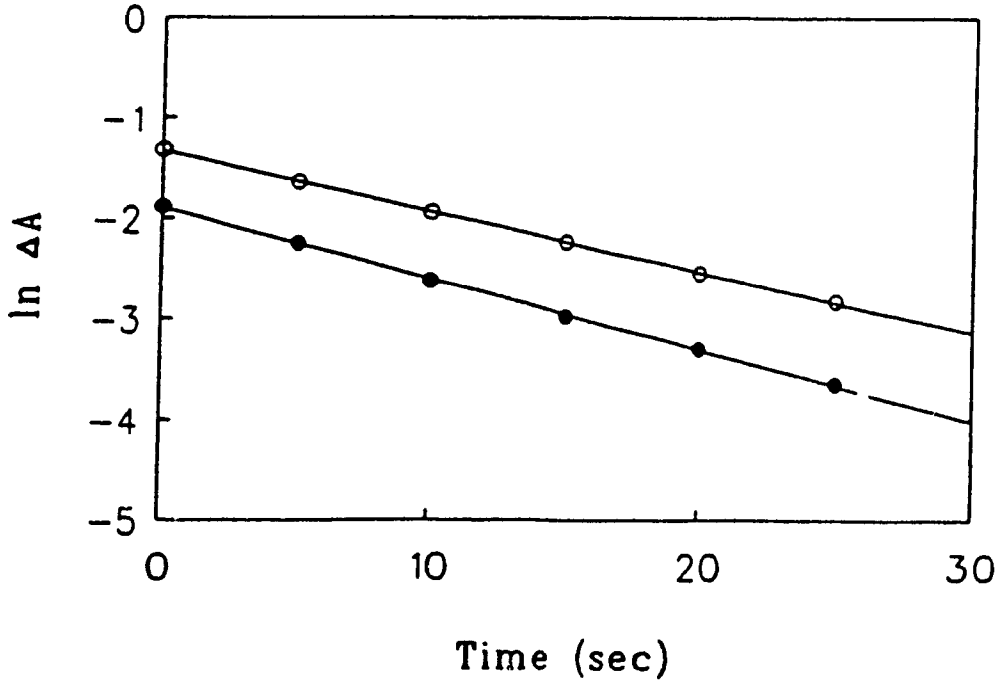
0
−1
−2
−3
−4
−5
ln ΔA
0
10
20
30
Time (sec)

Table 4.1: Relative Fluorescence Intensities at 350 nm of Fe^{III}-Mb, Cpd I-Mb and Cpd II-MbHH in 8 M Urea and 6 M Gdn-HCl[a,b]

Mb	8 M Urea	6 M Gdn-HCl	Buffer[c]
Fe^{III}-MbHH	100	97.5	6.5
Cpd I-MbHH	33.1	90.2	7.2
Cpd II-MbHH	37.6	71.1	7.6
Fe^{III}-MbSW	32.6	77.1	2.8
Cpd I-MbSW	25.6	78.9	3.6

[a]Intensities relative Fe^{III}-MbHH in 8 M urea.

[b]Experimental conditions: excitation wavelength, 280 nm; excitation and emission slits, 5 nm. Samples were exposed to the denaturants for 40 min prior to the recording of their fluorescence intensities.

[c]Samples in 50 mM sodium borate buffer, pH 8.5.

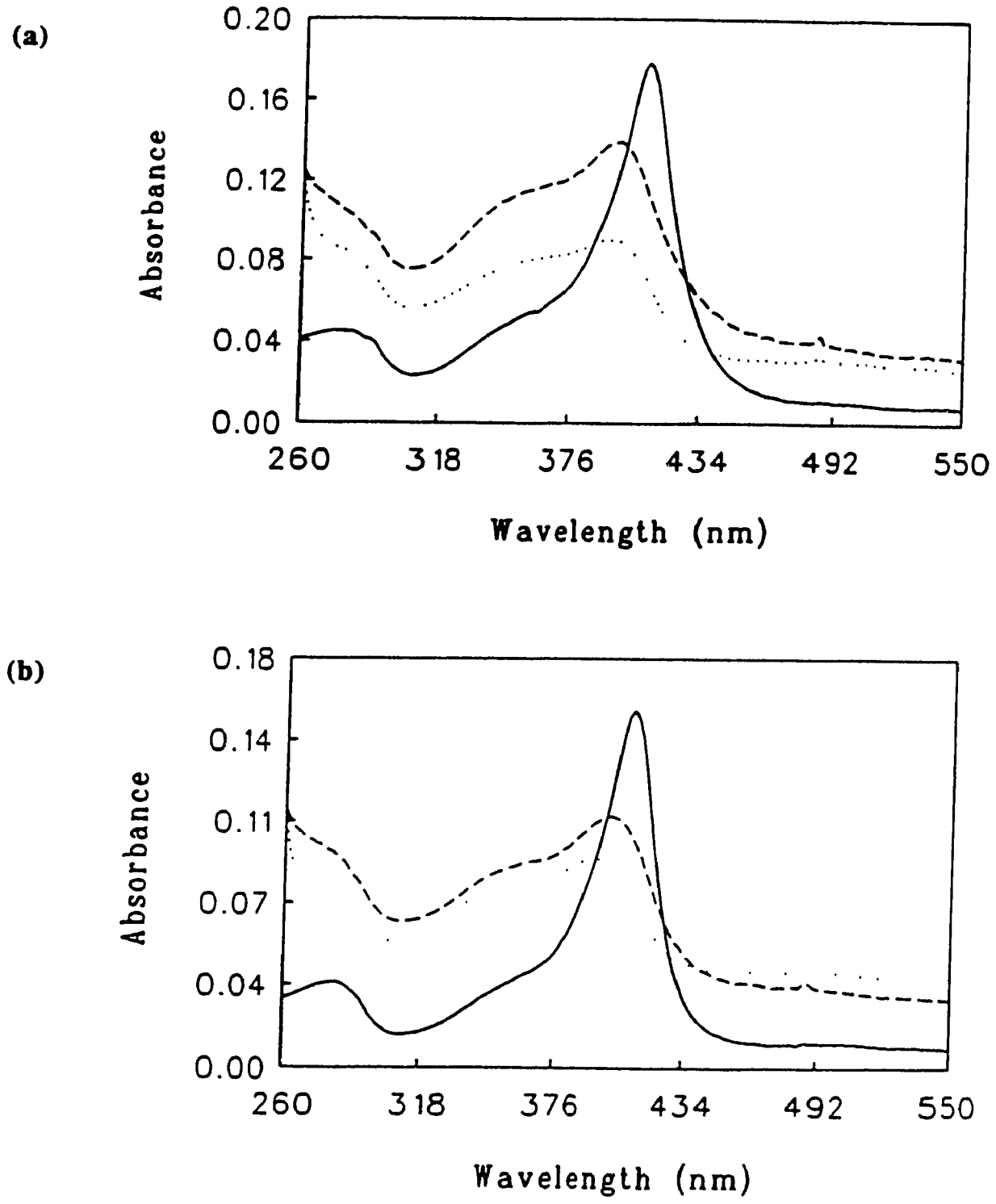

Figure 4.4: Absorption spectra of 1.0 μM (a) Fe^{III}-MbHH and (b) Fe^{III}-MbSW in 50 mM sodium borate buffer, pH 8.5 (solid line) and after 40 min exposure to 8 M urea (dashed line) and 6 M Gdn-HCl (dotted line).

presence of the denaturants. The emission maximum shifted from 326 ± 2 nm in buffer to 350 ± 2 nm in the denaturants after 40 min, indicating exposure of Trp residues to the aqueous solvent. The absorption spectra in Figure 4.4(a) show that the Soret band of Fe^{III}-MbHH, which is a sharp band with a λ_{max} at 410 nm in buffer at pH 8.5, appears broadened and blue-shifted in both of the denaturants after 40 min, which is indicative of free or solvent-exposed heme.[21]

Cpd I-MbHH: A 4.6-fold increase in fluorescence intensity was observed for Cpd I-MbHH in 8 M urea compared to in buffer. Although the relative fluorescence intensities of Fe^{III}-MbHH and Cpd I-MbHH are similar in buffer, after 40 min in 8 M urea Cpd I-MbHH has only 33% the fluorescence intensity of Fe^{III}-MbHH (Table 4.1). Cpd I-MbHH also displayed a shift in emission maximum from 328 ± 2 nm in buffer to 350 ± 2 nm in the denaturants after 40 min. Figure 4.5(a) shows the absorption spectra of Cpd I-MbHH in different solutions, and reveals the presence of a sharp maximum at 422 nm in both buffer and 8 M urea, while a broad band is observed after 40 min in 6 M Gdn-HCl. These results show that the heme cavity of Cpd I-MbHH remains partially intact after 40 min in 8 M urea, although quenching by the heme is reduced (Table 4.1) and the Trp residues are exposed to the aqueous environment. In 6 M Gdn-HCl, the fluorescence intensity of Cpd I-MbHH is similar to that for Fe^{III}-MbHH (Table 4.1) suggesting greater unfolding of Cpd I-MbHH in 6 M Gdn-HCl than in 8 M urea. This is not surprising given that 6 M Gdn-HCl is a stronger denaturant than 8 M urea.[22]

Cpd II-MbHH: Cpd II-MbHH displays a 5-fold increase in fluorescence

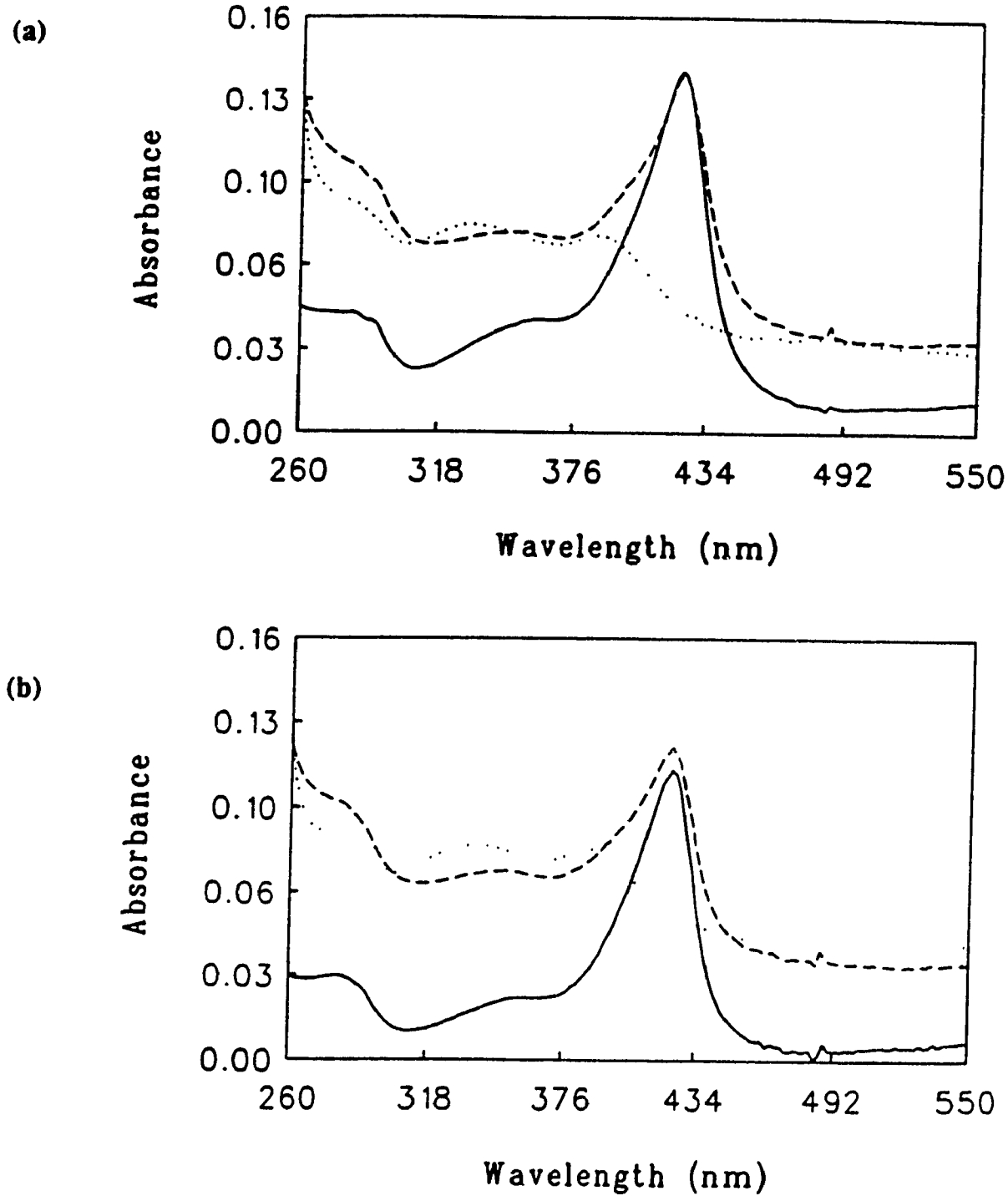

Figure 4.5: Absorption spectra of 1.0 μM (a) Cpd I-MbHH and (b) Cpd I-MbSW in 50 mM sodium borate buffer, pH 8.5 (solid line) and after 40 min exposure to 8 M urea (dashed line) and 6 M Gdn-HCl (dotted line). The ratio of peroxide to Mb was 20:1.

intensity in 8 M urea compared to in buffer (Table 4.1). A fluorescence emission maximum at 350 nm, consistent with solvent exposure of Trp residues, was once again observed. Although fluorescence intensities of Cpd I-MbHH and Cpd II-MbHH are similar in 8 M urea, their absorption spectra under the same conditions are significantly different (Figures 4.5 & 4.6). The broad, blue-shifted Soret band of Cpd II-MbHH in 8 M urea suggests that the heme is partially solvent exposed. In 6 M Gdn-HCl, the fluorescence intensity of Cpd II-MbHH increases ~ 9-fold compared to in buffer, but its fluorescence is still 26% less than that of Fe^{III}-MbHH in 6 M Gdn-HCl. This decrease in fluorescence intensity indicates that Cpd II-MbHH may be more stable to denaturation by Gdn-HCl than both Fe^{III}-MbHH and Cpd I-MbHH. The absorption spectra in Figure 4.6 show that the heme of Cpd II-MbHH is partially solvent exposed after 40 min in 6 M Gdn-HCl. However, a careful examination of Figures 4.5(a) and 4.6 reveals that the spectra of Cpd-I MbHH and Cpd-II MbHH in 6 M Gdn-HCl are not identical, consistent with differences in the extent of solvent exposure.

Fe^{III}-MbSW: The fluorescence intensity of Fe^{III}-MbSW is ~ 3-fold lower than that of Fe^{III}-MbHH after 40 min in 8 M urea (Table 4.1). The emission maximum of Fe^{III}-MbSW red shifts from 326 ± 2 nm to 350 nm ± 2 nm upon exposure of the protein to the denaturants. The absorption spectra in Figure 4.4(b) show that the Soret band of Fe^{III}-MbSW blue shifts and broadens after 40 min in 8 M urea and 6 M Gdn-HCl, indicative of solvent-exposed heme. Approximately 20% less fluorescence relative to Fe^{III}-MbHH was observed for Fe^{III}-MbSW in 6 M Gdn-HCl. Since MbSW

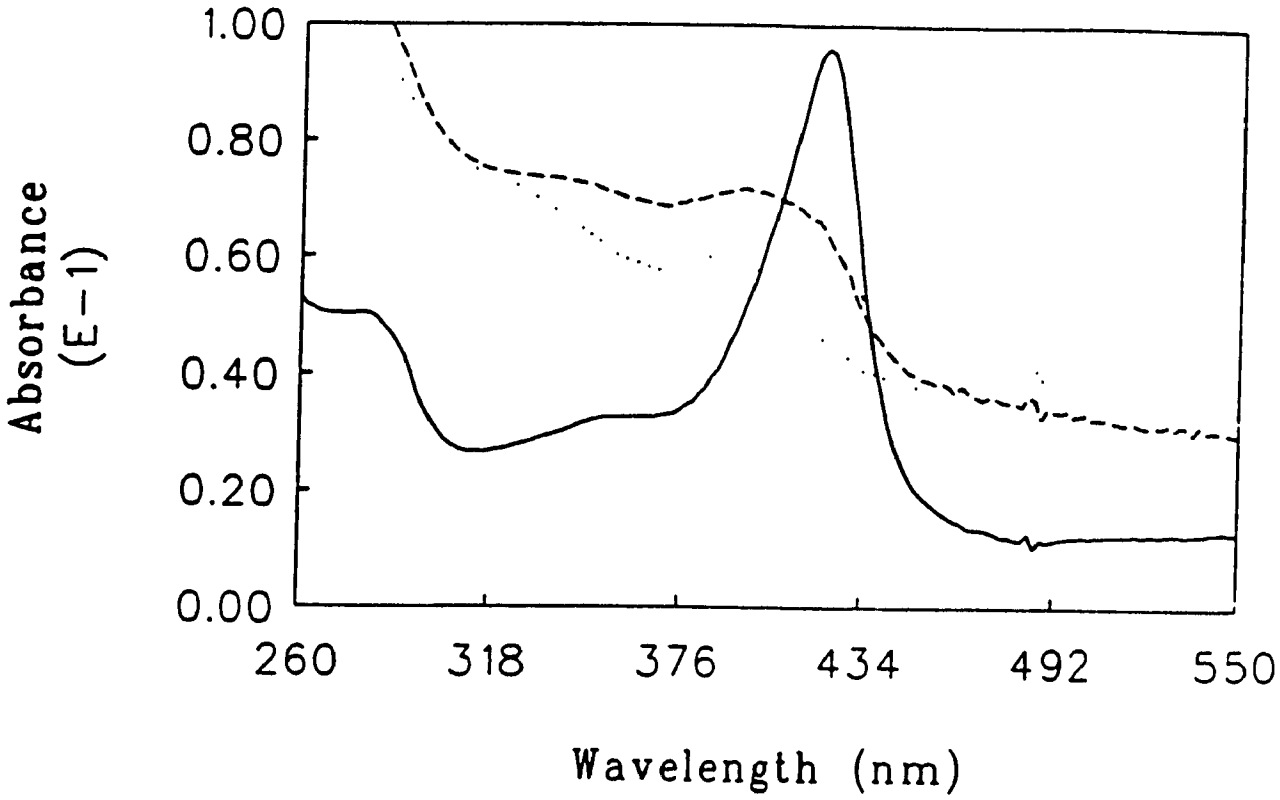

Figure 4.6: Absorption spectra of 1.0 μM Cpd II-MbHH in 50 mM sodium borate buffer, pH 8.5 (solid line) and after 40 min exposure in 8 M urea (dashed line) and 6 M Gdn-HCl (dotted line). The ratio of peroxide to MbHH was 20:1.

has two Trp residues in the same positions as MbHH it was expected that denaturation of both proteins should result in the same Trp fluorescence intensity. This suggests that Fe^{III}-MbSW unfolds to a lesser extent than Fe^{III}-MbHH after 40 min in 6 M Gdn-HCl.

Cpd I-MbSW: The fluorescence intensities of Cpd I-MbSW in buffer and denaturants are similar to those observed for Fe^{III}-MbSW under the same conditions. The absorption spectra in Figure 4.5(b) show that after 40 min in 8 M urea, the Soret maximum of Cpd I-MbSW at 422 nm did not blue shift, while in 6 M Gdn-HCl the Soret absorption appeared as a broad band at a lower wavelength, indicating solvent-exposed heme.

Time Course of Fe^{III}-Mb, Cpd I-Mb and Cpd II-MbHH Unfolding in 8 M Urea: Fluorescence intensity at 350 nm versus time was measured to determine the time course of Fe^{III}-MbHH, Cpd-I MbHH, Cpd II-MbHH [Figure 4.7(a)], Fe^{III}-MbSW and Cpd-I MbSW [Figure 4.7(b)] unfolding in 8 M urea. As can be seen from these plots, Fe^{III}-MbHH is significantly more flourescent after 40 min than Fe^{III}-MbSW and the ferryl species. No further increases in fluorescence intensity were observed for Fe^{III}-MbHH, Cpd I-MbHH or Cpd II-MbHH after 40 min in 8 M urea. However, the fluorescence intensities of Fe^{III}-MbSW and Cpd I-MbSW doubled after 24 h in 8 M urea indicating that the MbSW species unfold at a much slower rate than the MbHH species.

SDS-PAGE of Fe^{III}-Mb and Cpd I-Mb: All samples showed a band at 17,000 daltons as expected for Mb (Figures 4.8 & 4.9). However, after incubation

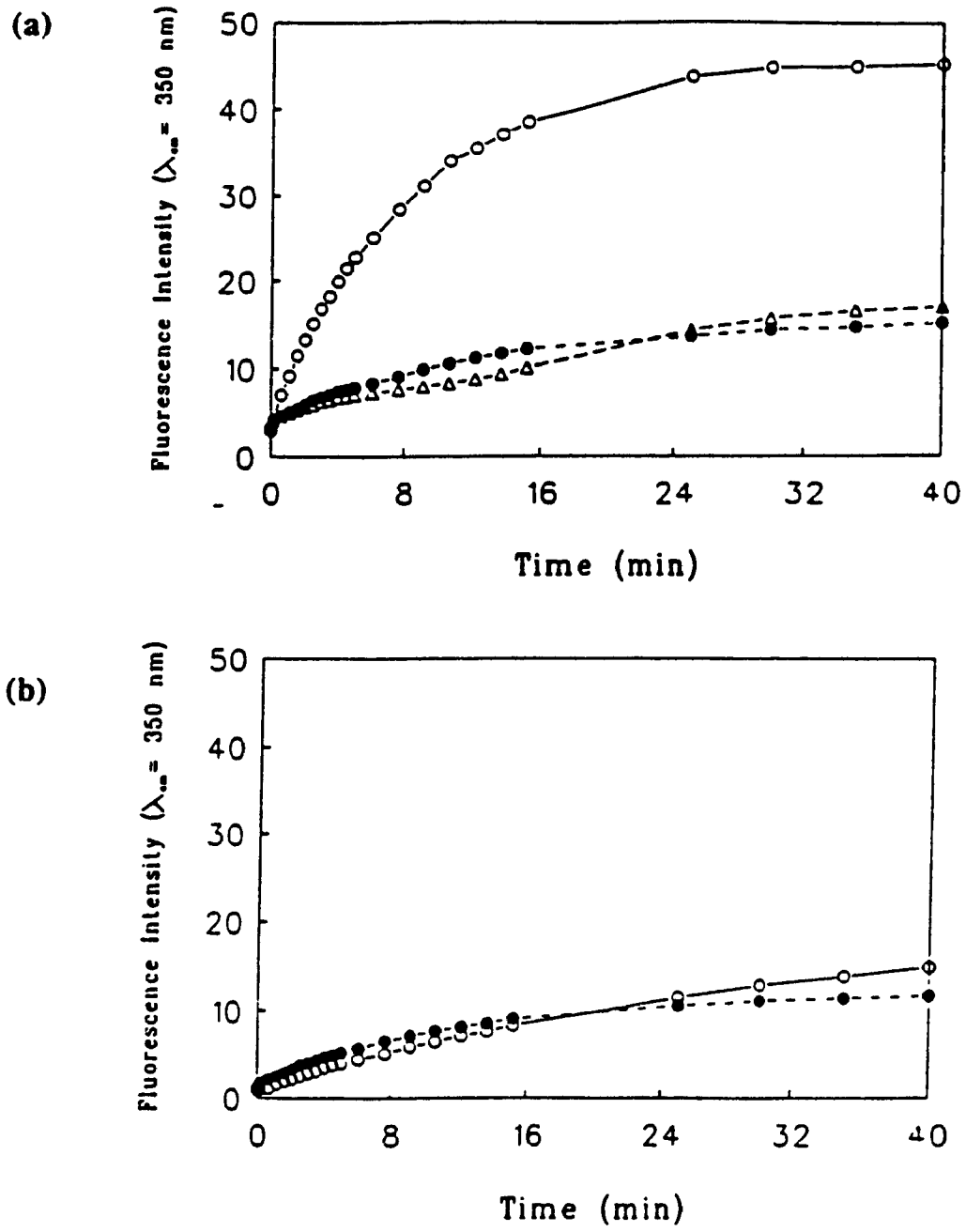

Figure 4.7: Fluorescence intensity at 350 nm vs. time of 1.0 μM (a) Fe^{III}-MbHH (open circles), Cpd I-MbHH (closed circles), Cpd II-MbHH (open triangles) and (b) Fe^{III}-MbSW (open circles), Cpd I-MbSW (closed circles) following the addition of the protein to 8 M urea. The excitation wavelength was 280 nm, and the excitation and emission slits were 5 nm. The ratio of peroxide to Mb was 20:1.

Figure 4.8: SDS-PAGE analysis of Fe^{III}-MbHH, Fe^{III}-MbSW, Cpd I-MbHH and Cpd I-MbSW.

Key: Lane (**a**) and (**j**), molecular weight standards; (**b**) and (**f**), Fe^{III}-MbSW; (**c**) and (**g**), Cpd I-MbSW; (**d**) and (**h**), Fe^{III}-MbHH; (**e**) and (**i**), Cpd I-MbHH. The proteins (5 μM) in lanes (**c**) and (**e**) were incubated with a 20-fold excess peroxide for 3 min in 50 mM sodium borate buffer, pH 8.5. The proteins (5 μM) in lanes (**g**) and (**i**) were incubated with a 20-fold excess peroxide for 60 min in 50 mM sodium borate buffer, pH 8.5. The total amount of each protein sample applied to the gel was 0.85 μg in 25 μl.


45.0
31.0
21.5
14.4
a
b
c
d
e
f
g
h
i
j

Figure 4.9: SDS-PAGE analysis of Fe^{III}-MbHH, Fe^{III}-MbSW, Cpd I-MbHH and Cpd I-MbSW.

Key: Lanes (**a**) and (**f**), molecular weight standards; (**b**) Cpd I-MbHH; (**c**) Fe^{III}-MbHH; (**d**) Cpd I-MbSW ; (**e**) Fe^{III}-MbSW . The proteins (5 μM) in lanes (**b**) and (**d**) were incubated with a 20-fold excess peroxide for 24 h in 50 mM sodium borate buffer, pH 8.5. The total amount of each protein sample applied to the gel was 0.85 μg in 25 μl.


45.0
31.0
21.5
14.4
a
b
c
d
e
f

with 20-fold peroxide for 3 min, 60 min and 24 h, MbSW also showed a dimer band at 34,000 daltons [lanes (c) and (g) Figure 4.8, and lane (d) Figure 4.9]. This indicates that incubating MbSW with 20-fold peroxide results in dimerization of the protein, whereas no dimerization was observed for MbHH under the same conditions.

Removal of the Heme of Fe^{III}-MbHH and Cpd I-MbHH: Figure 4.10(a) shows the absorption spectra of 10 μM Fe^{III}-MbHH and Cpd I-MbHH. Fe^{III}-MbHH (10 μM) was incubated for 3 min with 20-fold excess peroxide prior to acidification to pH 1.5. Figure 4.10(b) shows that the spectrum of the Fe^{III}-MbHH sample has no Soret band after 2 extractions with butanone, while that of the Cpd I-MbHH sample has a broad Soret band at 390 nm. This shows that the heme of Cpd I-MbHH was not removed after acidification and 2 extractions with butanone.

4.4 Discussion

MbSW forms Compound I ($t_{1/2}$ = 10.7 s) more readily than MbHH ($t_{1/2}$ = 37.1 s) in the presence of 20-fold excess peroxide at pH 8.5, at room temperature. The small, but significant differences (16%) in the half-lives of Fe^{III}-Mb decay and Cpd I-Mb formation (Figure 4.3) are due to slow reactions of Cpd I-Mb. To correct for the slow absorbance changes observed following Cpd I-Mb formation, the Guggenheim method of analysis was used to calculate the first-order rate constants.

The data summarized in Table 4.1 reveal the relative stabilities of the various forms of Mb to denaturation at high denaturant concentrations. Fe^{III}-MbHH is considerably more fluorescent after 40 min exposure to 8 M urea than in buffer, which

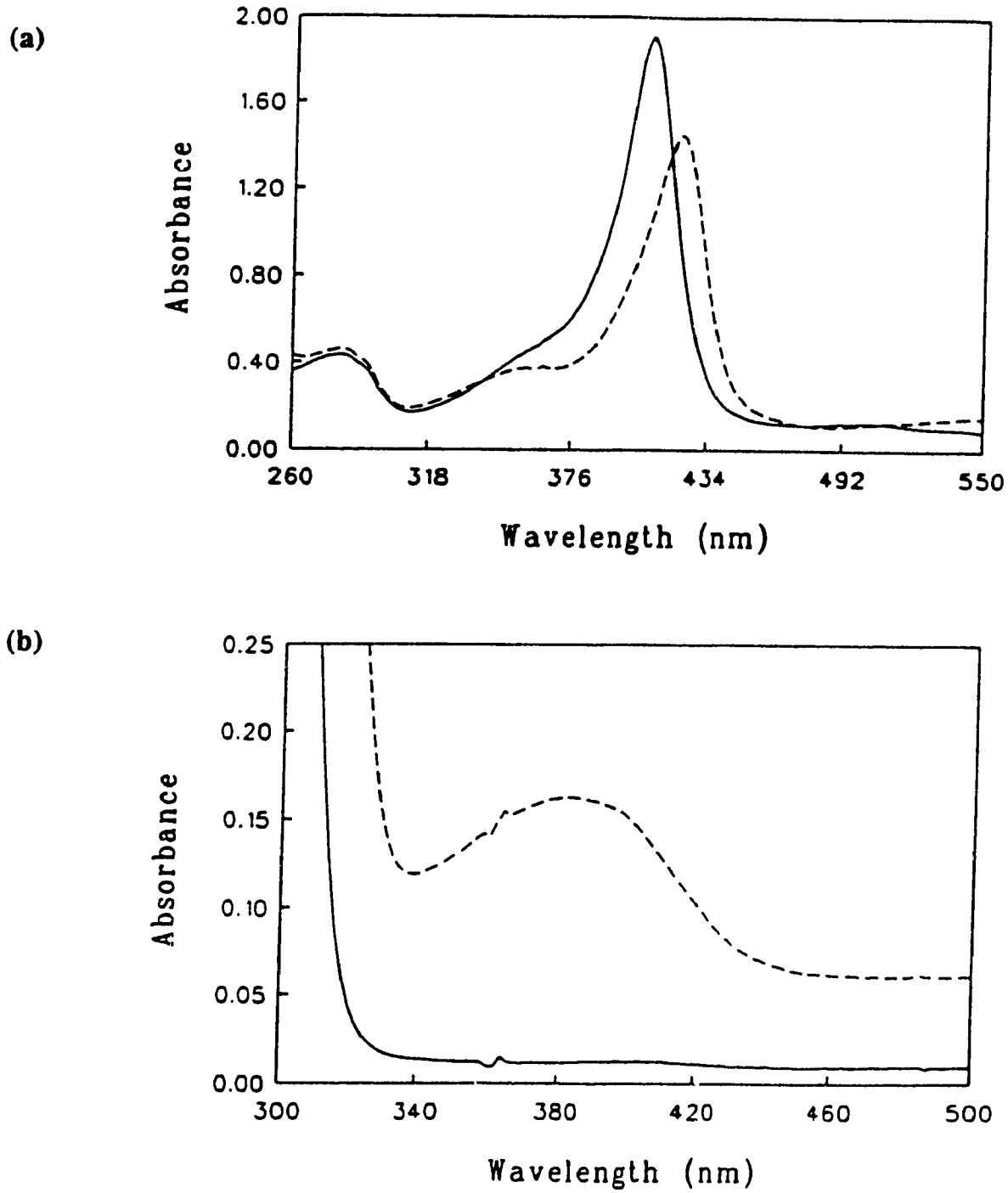

Figure 4.10: **(a)** Absorption spectra of 10.0 μM Fe^{III}-MbHH (solid line) and Cpd I-MbHH (dashed line) in 50 mM sodium borate buffer, pH 8.5. **(b)** Absorption spectra of Fe^{III}-MbHH (solid line) and Cpd I-MbHH (dashed line) after 2 extractions with butanone at pH 1.5.

suggests that the polypeptide is significantly unfolded under these conditions. Unfolding of the protein relieves the highly efficient fluorescence quenching by the heme. However, the addition of Fe^{III}-MbSW and the ferryl forms of Mb (Cpd I-MbHH, Cpd II-MbHH and Cpd I-MbSW) to 8 M urea results in fluorescence intensities that are only 32 (± 3)% relative to Fe^{III}-MbHH in 8 M urea. This suggests that Fe^{III}-MbSW and the ferryl forms of Mb are considerably more stable than Fe^{III}-MbHH in 8 M urea. The relative stabilities of the Mb species are evident from the time course of fluorescence (Figure 4.7), which shows extensive unfolding of Fe^{III}-MbHH at short times.

In the stronger denaturant, 6 M Gdn-HCl, the fluorescence intensity of Fe^{III}-MbHH is similar to its value in 8 M urea, suggesting that the polypeptide is unfolded to a similar extent in both denaturants. However, Fe^{III}-MbSW and the ferryl forms of Mb have significantly higher fluorescence intensities in Gdn-HCl compared to urea, consistent with only partial unfolding of these Mb species in urea.

Solvent exposed heme shows a broad Soret band with a maximum absorbance at 390 nm;[21] thus, the blue shifting and broadening of the Soret maxima of the Mb species in denaturants (Figures 4.4 - 4.6) are also consistent with polypeptide unfolding. In 8 M urea, the Soret spectra reveal that the extent of solvent exposure of the heme varies considerably for the different forms of Mb. For example, Cpd I-MbHH and Cpd I-MbSW show relatively sharp Soret bands at 422 nm which overlap their Soret absorption in buffer, in addition to solvent-exposed heme absorbance at ~ 390 nm. In comparison, the Fe^{III} forms of Mb (Figure 4.4) show significantly more

solvent-exposed heme. In 6 M Gdn-HCl, the extent of solvent-exposed heme appears to be greater for all the Mb samples compared to that in urea. Hence, both the fluorescence and absorption measurements are consistent with greater unfolding of the proteins in 6 M Gdn-HCl.

Although the fluorescence intensities of Cpd I-MbHH and Cpd II-MbHH, which lacks a protein radical (X°), are similar after 40 min in 8 M urea, their absorption spectra are quite different. There is no 422 nm Soret absorbance present in the spectrum of Cpd II-MbHH in urea, unlike Cpd I-MbHH [Figures 4.5(a) and 4.6], indicating that the heme cavity of Cpd I-MbHH remains more intact after 40 min in 8 M urea than that of Cpd II-MbHH. These results suggest that the X° formed in Reaction 4.1 may give rise to the different spectral behaviour of Cpd I-MbHH and Cpd II-MbHH observed here.

SDS-PAGE showed that only MbSW formed a dimer upon mixing with 20-fold excess peroxide. Approximately 50% of the dimer is present in the samples that were exposed to peroxide for 3 and 60 min prior to their addition to SDS (Figure 4.8). However, after 24 h the intensity of the monomer band is greater than that of the dimer (Figure 4.9), suggesting further changes occur in Cpd I-MbSW over 24 h. These results are consistent with those reported in that Cpd I-MbSW dimerizes, but Cpd I-MbHH shows only monomeric species after exposure to H_2O_2.[11]

Attempts to remove the heme from Fe^{III}-MbHH and Cpd I-MbHH by the acidic butanone method showed that a band was present at 390 nm for Cpd I-MbHH even after two butanone extractions. This reveals that the heme is more tightly bound to

the polypeptide in Cpd I-MbHH than in Fe^{III}-MbHH. The difference in the stability of heme-polypeptide interaction could be due to a covalent crosslink between the heme and a residue in Cpd I-MbHH. Following peroxide binding, Fe^{III}-Mb undergoes a two-electron oxidation (Reaction 4.1).[2,3] One of the oxidizing equivalents is retained in the Fe^{IV} of Cpd I-Mb, and the other oxidizing equivalent is associated with a protein radical. For MbHH, Tyr103 has been proposed as the site of X° formation[10,23] and is reported to be crosslinked to the heme.[10] Such intramolecular crosslinking is consistent with the results found here since both heme removal and unfolding of Cpd I-MbHH would be inhibited on covalent binding of the heme to the polypeptide. However, peptide-mapping studies of Cpd I-MbHH will be necessary to establish the residues altered by X° formation in Cpd I-MbHH at pH 8.5.

4.5 References

1) Suslick, K. S. & Reinert, T. J. *J. Chem. Ed.* **1985**, *62*, 974.

2) George, P. & Irving, D. H. *Biochem. J.* **1952**, *52*, 511.

3) Yonetani, T. & Schleyer, H. *J. Biol. Chem.* **1967**, *242*, 1974.

4) Poulos, T. L. & Kraut, J. *J. Biol. Chem.* **1980**, *255*, 8199.

5) Grisham, M. B. & Everse, J. *Peroxidases in Chemistry and Biology Vol I*, Eds. Everse, J.; Everse, K. E.; Grisham, M. B., CRC Press, Boca Raton, **1991**, Ch. 14.

6) King, N. K.; Looney, F. D.; Winfield, M. E. *Biochim. Biophys. Acta* **1967**, *133*, 65.

7) Takano, T. *J. Mol. Biol.* **1977**, *110*, 537.

8) Evans, S. V. & Brayer, G. D. *J. Mol. Biol.* **1990**, *213*, 885.

9) Ferrin, T. E.; Huang, C. C.; Jarvis, L. E.; Langridge, R. *J. Mol. Graphics* **1988**, *6*, 13.

10) Catalano, C. E.; Choe, Y. S.; Ortiz de Montellano, P. R. *J. Biol. Chem.* **1989**, *264*, 10534.

11) Tew, D. & Ortiz de Montellano, P. R. *J. Biol. Chem.* **1988**, *263*, 17880.

12) Wilks, A. & Ortiz de Montellano, P. R. *J. Biol. Chem.* **1992**, *267*, 8827.

13) Lakowicz, J. R. *Principles of Fluorescence Spectroscopy* Plenum Press, New York, **1983**, Ch. 11.

14) Wills, K. J.; Szabo, A. G.; Zucker, M.; Ridgeway, J. M.; Alpert, B. *Biochem.* **1990**, *29*, 5270.

15) Hochstrasser, R. M. & Negus, D. K. *Proc. Natl. Acad. Sci. U.S.A.* **1984**, *81*, 4399.

16) Beechem, J. M. & Brand, L. *Annu. Rev. Biochem.* **1985**, *54*, 43.

17) Scheler, W.; Schaffa, G.; Jung, F. *Biochem. Z.* **1957**, *329*, 232.

18) Hanania, G. I. H.; Yeghiayan, A.; Cameron, B. F. *Biochem. J.* **1966**, *98* 189.

19) Antonini, E. *Physiol. Rev.* **1965**, *45*, 123.

20) Nielson, T. B. & Reynolds, J. A. *Methods of Enzymology* **1978**, *48*, 3.

21) Rossi Fanelli, A.; Antonini, E.; Caputo, A. *Ad. Protein Chem.* **1964**, *19*, 73.

22) Von Hippel, P. H. & Wong, K.-Y. *J. Biol. Chem.* **1965**, *240*, 3909.

23) Rice, R. H.; Lee, Y. M.; Brown, W. D. *Arch. Biochem. Biophys.* **1983**, *221*, 417.

5.0 General Discussion

The results presented in Chapter 2 of this thesis indicate that three singly-modified derivatives of MbHH with pentaammineruthenium(III) (a_5Ru^{3+}) attached to histidine residues can be readily prepared. These derivatives were isolated from the products of the reaction of MbHH with $a_5Ru^{2+}(H_2O)$ for one hour. The reaction time used is twice as long as that required for MbSW modification, suggesting that the histidine residues in MbHH are less accessible to the ruthenation reagent. The ruthenated products were isolated and separated on a FPLC cation-exchange column into nine distinct peaks. Evidence for the attachment of a_5Ru^{3+} to histidine residues was obtained from the difference spectra of the cyanide complexes of the products and MbHH-CN, following procedures used previously in this laboratory for CCP.[1] Peaks E, F and G (Figure 2.3) were found to contain singly-modified a_5Ru^{3+}(His)MbIII derivatives by this spectroscopic method, while Peak H contained triply-modified derivatives. This work was concerned with the preparation of singly-modified a_5Ru^{3+}(His)MbHH derivatives for use in electron transfer studies, so characterization of the triply-modified a_5Ru^{3+}(His)MbHH derivatives was not carried out. Since the spectroscopic method of analysis used here is specific for ruthenation of histidines, further investigation of the MbHH derivatives in Peaks B, C and D is required to determine if residues other than histidine (e.g. methionine) have been modified. Also, ruthenation of buried histidines (e.g. His82, His113, His119) may alter the

conformation and absorption spectrum of MbHH so that histidine ruthenation may not be detected by difference spectroscopy.

Peptide-mapping, in conjunction with amino acid analysis and mass spectrometry of the peptide fragments (Chapter 3), were used to determine which histidines were modified in two of the singly-modified a_5Ru^{3+}(His)MbHH derivatives. This is one of the first applications of electrospray mass spectrometry in the characterization of covalently-modified proteins.[2] Since mass spectrometry provides rapid confirmation of covalent modification, it should prove to be a useful tool in bioconjugation studies. Both the absorption and mass spectra suggest that the third singly-modified derivative has a_5Ru^{3+} bound to a surface histidine of MbHH. Since computer graphic analysis indicated that His116 is the only remaining surface-exposed histidine, the third singly-modified derivative is predicted to have a_5Ru^{3+} bound to His116. Further investigation of this derivative by peptide-mapping is necessary to conclusively determine its a_5Ru^{3+} attachment site.

The values of reduction potentials of the protein-bound a_5Ru^{3+}(His) groups are important data for electron-transfer studies since electron-transfer rates depend on the driving force. The reported peak potentials of different protein-bound a_5Ru^{3+}(His) groups show considerable variation. For example, a_5Ru^{3+}(His39)cytochrome c has a peak potential of 120 mV,[3] whereas a_5Ru^{3+}(His83)azurin has a peak potential of 50 mV.[4] The peak potentials determined by DPV in this laboratory for the free (Ep = 86 mV) and MbHH-bound a_5Ru^{3+}(His) [Ep = 52 mV (His48), 47 mV (His81) and 76 mV (probably His116)] also showed variation, and are lower than those reported for the

a_5Ru^{3+}(His)MbSW derivatives[5] (Table 3.3). Since the values for MbSW are closer to the value for the free a_5Ru^{3+}(His) complex, this suggests that His48 and His81 may be more buried, or present in a more hydrophobic microenvironment in MbHH compared to MbSW. The former interpretation is consistent with the derivatization reaction results, since a longer time period was required for MbHH modification (1 h) than that reported for MbSW (30 min).[6]

The ultimate goal of the work initiated in this thesis is to investigate the electron-transfer reactivity of the ferryl iron (Fe^{IV}=O) heme in MbHH. The strategy is to generate a ferryl heme species in MbHH and measure rates of electron-transfer from surface a_5Ru^{2+}(His) groups to the ferryl heme, as was carried out before for CCP.[1,7] As discussed previously, the reaction of H_2O_2 with Mb leads to ferryl heme species similar to those observed for heme peroxidases. The results reported in Chapter 4 show that Cpd I of MbSW formed more readily (10.7 s) than Cpd I of MbHH (37.1 s) in the presence of 20-fold excess peroxide at pH 8.5. However, under these same conditions, the formation of Cpd II-MbHH from Fe^{II}-MbHH ($t_{1/2}$ < 2 s) occurs within manual mixing time. These results suggest that oxidation of an amino acid residue may be rate-limiting in the formation of Cpd I-Mb, since *both* electrons come from the ferrous heme in Cpd II-Mb formation.

The results of probing alteration of the Mb polypeptide due to the production of an unstable protein radical in Cpd I-Mb are also presented in Chapter 4. The heme-extraction experiments suggest that a portion of the heme is covalently bound to the polypeptide following incubation of Fe^{III}-MbHH with 20-fold excess peroxide for 3

min. These results agree with tnose reported by Catalano et al.[8] for Cpd I-MbHH. The SDS-PAGE experiments show that ~ 50% dimer was present in the MbSW samples that were incubated for 3 and 60 min with 20-fold peroxide at pH 8.5. Again this is in agreement with the results reported by Tew and Ortiz de Montellano,[9] who observed ~ 30% dimerization of MbSW following 60 min incubation with 15-fold excess peroxide at pH 7.0, indicating that rapid partial dimerization of MbSW occ in the presence of excess peroxide. Also, the SDS-PAGE experiments revealed that, Cpd I-MbHH underwent *no* dimerization in agreement with what had previously been reported.[9]

Using protein tryptophan fluorescence measurements, the ferryl forms of MbHH and MbSW were observed to unfold to a lesser extent in denaturants than their ferric forms. Crosslinked proteins, such as those which contain disulfide bonds, are known to be stable in the presence of denaturants such as urea. High concentrations of denaturants and the addition of reducing agents are required to unfold these proteins. Mb does not contain disulfide bonds, but the heme-extraction and SDS-PAGE experiments indicated possible crosslinking in Cpd I-Mb. However, Cpd II-MbHH, in which no protein radical is formed, was *also* more stable in denaturants than Fe^{III}-MbHH. Hence, the increased stability of the ferryl heme species may be due to the redox and/or coordination state of the heme iron. For instance, it is well established that ferrocytochrome c is more stable than ferricytochrome c.[10] Also, various heme protein adducts are more stable than the unligated form of the protein; the cyanide complex of CCP, for example, is more stable at high pHs and temperatures than native

CCP.[1] Further study is required to establish the reason for the greater stability observed here of the ferryl Mb species to denaturants; however, the fluorescence results clearly indicate that Cpd I-Mb formation does not lead to tryptophan loss as was observed for CCP.[1] Peptide mapping of Cpd I-Mb and Cpd II-Mb will hopefully reveal the sites of amino acid oxidation, or of crosslinking, in these species. Such information will be necessary to establish the nature of electron-transfer pathways between the a_5Ru^{3+} and heme centres.[11]

5.1 References

1) Fox, T. "Studies on Enzyme Intermediates of Yeast Cytochrome *c* Peroxidase", Ph.D. Thesis, Concordia University, **1991**.

2) Conrad, D. W. & Scott, R. A. *J. Am. Chem. Soc.* **1989**, *111*, 3461.

3) Selman, M. "Preparation and Characterization of an Intramolecular Electron Transfer in a Pentaammineruthenium Derivative of *Candida Krusei* Cytochrome *C*.", Ph.D. Thesis, California Institute of Technology, **1989**.

4) Margalit, R.; Kostić, N. M.; Che, C-M.; Blair, D. F.; Chaing, H-J.; Pecht, I.; Shelton, J. B.; Shelton, J. R.; Schroeder, W. A.; Gray, H. B. *Proc. Natl. Acad. Sci. USA* **1984**, *81*, 6554.

5) Cowan, J. A.; Upmacis, R. K.; Beratan, D. N.; Onuchic, J. N.; Gray, H. B. *Ann. New York Acad. Sci.* **1988**, *550*, 68.

6) Axup, A. W.; Albin, M.; Mayo, S. L.; Crutchley, R. J.; Gray, H. B. *J. Am. Chem. Soc.* **1988**, *110*, 435.

7) Fox, T.; Hazzard, J. T.; Edwards, S. L.; English, A. M.; Poulos, T. L.; Tollin, G. *J. Am. Chem. Soc.* **1990**, *112*, 7426.

8) Catalano, C. E.; Choe, Y. S.; Ortiz de Montellano, P. R. *J. Biol. Chem.* **1989**, *264*, 10534.

9) Tew, D. & Ortiz de Montellano, P. R. *J. Biol. Chem.* **1988**, *263*, 17880.

10) McLendon, G. & Smith, M. *J. Biol. Chem.* **1978**, *253*, 4004.

11) Beratan, D. N.; Onuchic, J. N.; Betts, J. N.; Bowler, B. E.; Gray, H. B. *J. Am. Chem. Soc.* **1990**, *112*, 7915.

6.0 Conclusions

1) a_5Ru^{3+} is attached to His48 and His81 in two derivatives of MbHH isolated from its reaction with $a_5Ru^{2+}(H_2O)$.

2) A third derivative has a single a_5Ru^{3+} bound to an unidentified histidine residue of MbHH.

3) DPV showed that the peak potentials of the a_5Ru^{3+}(His) centres in the singly-modified MbHH derivatives vary by ~ 30 mV, suggesting the microenvironments of the ruthenium complexes is different in each case.

4) Fluorescence and absorbance studies in denaturants (urea and Gdn-HCl) indicate that the ferryl forms of MbHH and MbSW are more stable to denaturation than the ferric forms.

5) The spectroscopic studies also indicate possible alteration of the polypeptide in Cpd I-MbHH and Cpd I-MbSW. This should be investigated further by peptide mapping of these species.

6) SDS-PAGE revealed ~ 50% dimerization of Cpd I-MbSW but *no* dimerization of Cpd I-MbHH.

7) Acidic butanone extraction of the heme showed that *not* all the heme can be extracted from Cpd I-MbHH unlike Fe^{III}-MbHH. This suggests possible crosslinking between the heme and the polypeptide in Cpd I-MbHH.